REFERENCE:	TASI-SD-SBSP-ORP-0292
DATE:	20/12/2023
ISSUE:	4

Final Report

Written by	
Di Tommaso Umberto	Written on 20/12/2023 18:32
Verified By	
Massobrio Federico	Verified on 20/12/2023 18:46
Cavaglia' Rosetta	Verified on 21/12/2023 08:22
Di Tommaso Umberto	Verified on 20/12/2023 18:53
Approved By	
Musso Giorgio	Approved on 21/12/2023 10:19
Released By	
Cavaglia' Rosetta	Released on 21/12/2023 12:01

Approval evidence is kept within the documentation management system.

SBSP Pre-Phase A System Study

Final Report

DRL: FR

Written by	***Responsibility*** + handwritten signature if no electronic workflow tool
U. Di Tommaso	Author
Verified by	
F. Massobrio	Checker
R. Cavaglià	Configuration Manager
U. Di Tommaso	Systems Engineer
Approved by	
G. Musso	Program Manager
Documentation Manager	
R. Cavaglià	Configuration Administrator

Approval evidence is kept within the document management system

Change Records

ISSUE	DATE	§ CHANGE RECORDS	AUTHOR
01	05/12/2023	Issue 1	SBSP Team
02	12/12/2023	Updated §2, §4.4, §6.4.4, §9, §13.3, §13.6 and §14.1	SBSP Team
03	19/12/2023	Updated §4.4, §6.2, chapter 9, §13.6 and §14.3 Added chapter 16	SBSP Team
04	20/12/2023	Updated §2	SBSP Team

Table of contents

1 Introduction

1.1 Scope and purpose

This document concludes the “Pre-Phase A System Study of a Commercial-Scale Space-Based Solar Power (SBSP) System for Terrestrial Needs” and summarizes the work performed during the 5 tasks of the study. All the detailed technical information is reported in the specific study documents.

1.2 Applicable documents

Internal code / DRL	Reference	Issue	Title	Location of record
[AD1]			Orbit Analyses for Commercial-Scale Space-Based Solar Power Systems	
[AD2]			ESSB-HB-U-005 Space system Life Cycle Assessment (LCA) Guidelines iss.1.0	
[AD3]			ESA LCA Database	
[AD4]			ECSS-U-AS-10C Rev.1 – Adoption Notice of ISO 24113: Space systems – Space debris mitigation requirements (3 December 2019)	
[AD5]			Study Report(s) from ESA Future Launchers Preparatory Pro-gramme activity titled “euroPean Reusable and cOsT Effective heavy lIft transport investigation” (PROTEIN)	
[AD6]			ESA-TECSF-SOW-2022-003590 - Statement of Work Pre-Phase A System Study of a Commercial-Scale Space-Based Solar Power (SBSP) System for Terrestrial Needs	

1.3 Reference documents

Internal code / DRL	Reference	Issue	Title	Location of record
[RD1]			Final Deliverables from Frazer-Nash Consultancy for ESA-funded study titled “Cost-Benefit Analysis of Space-Based Solar Power Generation for Terrestrial Energy Needs” https://ec.europa.eu/eurostat/cache/infographs/energy/bloc-2a.html https://esamultimedia.esa.int/docs/technology/frazer-nash-consultancy-SBSP-cost-benefit-study-full-deliverables.zip	
[RD2]			Final Deliverables from Roland Berger for ESA-funded study titled “Cost-Benefit Analysis of Space-Based Solar Power Generation for	

Internal code / DRL	Reference	Issue	Title	Location of record
			Terrestrial Energy Needs" https://esamultimedia.esa.int/docs/technology/roland-berger-SBSP-cost-benefit-study-full-deliverables.zip	
[RD3]			SPS-ALPHA: The First Practical Solar Power Satellite via Arbitrarily Large Phased Array (A 2011-2012 NASA NIAC Phase 1 Project)	
[RD4]			Mankins, John C. "New Developments in Space Solar Power." NSS Space Settlement Journal (2017): 1-30.	
[RD5]			Space Solar Power: An Overview – John C. Mankins (Presentation at ISDC 2022)	
[RD6]			Cash, Ian. "CASSIOPeiA–A new paradigm for space solar power." Acta Astronautica 159 (2019): 170-178. https://doi.org/10.1016/j.actaastro.2019.03.063	
[RD7]			Cash, Ian. "CASSIOPeiA solar power satellite." 2017 IEEE International Conference on Wireless for Space and Extreme Environments (WiSEE). IEEE, 2017. 10.1109/WiSEE.2017.8124908	
[RD8]			UK Patent: GB2571383 - Solar concentrator: https://www.ipo.gov.uk/p-ipsum/Case/PublicationNumber/GB2571383	
[RD9]			UK Patent: GB2563574 - A phased array antenna and apparatus incorporating the same https://www.ipo.gov.uk/p-ipsum/Case/PublicationNumber/GB2563574	
[RD10]			CASSIOPEIA SPS: Advantages for Commercial Power, I Cash (Presentation at ISDC 2022)	
[RD11]			Space Solar Power development in China and MR-SPS, 4th SPS Symposium 2018, Kyoto, Japan https://www.sspss.jp/MR-SPS4.pdf	
[RD12]			Fraas, Lewis M. "Mirrors in space for low-cost terrestrial solar electric power at night." 2012 38th IEEE Photovoltaic Specialists Conference. IEEE, 2012.	
[RD13]			Fraas, Lewis M., Geoffrey A. Landis, and Arthur Palisoc. "Mirror satellites in polar orbit beaming sunlight to terrestrial solar fields at dawn and dusk." 2013 IEEE 39th Photovoltaic Specialists Conference (PVSC). IEEE, 2013.	
[RD14]			Çelik, Onur, et al. "Enhancing terrestrial solar power using orbiting solar reflectors." Acta Astronautica 195 (2022): 276-286.	
[RD15]			Çelik, Onur, and Colin R. McInnes. "An analytical model for solar energy reflected from space with selected applications." Advances in Space Research 69.1 (2022): 647-663.	
[RD16]			ESSB-ST-U-004 ESA Re-entry Safety Requirements iss.1.0	
[RD17]			FNC 011337 53514R Space Based Solar Power End of Life Study Final Report (Frazer-Nash Consultancy) Issue 1	
[RD18]			FNC 011337 53615R Space Based Solar Power End of Life Study	

Internal code / DRL	Reference	Issue	Title	Location of record
			Summary Report (Frazer-Nash Consultancy) Issue 1	
[RD19]			Sala, Serenella, et al. "Global normalisation factors for the environmental footprint and life cycle assessment." Publications Office of the European Union: Luxembourg (2017): 1-16	

1.4 Definitions and Acronyms

Acronym/Abbreviation	Definition
AC	Alternating Current
ARCADIA	Architecture Analysis & Design Integrated Approach
CAPEX	Capital Expenditure
CER	Cost Estimation Relationships
CFRP	Carbon Fiber Reinforced Polymer
CSI	Current Source Inverter
DLR	Deutsches Zentrum für Luft- und Raumfahrt
DC	Direct Current
EES	Electrical Energy Storage
EESS	Electrical Energy Storage Systems
EHLL	European Heavy Lift Launcher
EPBT	Energy PayBack Time
ERoEI	Energy Return on Energy Investment
ESA	European Space Agency
FOAK	First Of A Kind
GCPC	Grid-Connected Power Converters
GEO	Geostationary Orbit
GHG	GreenHouse Gas
GPS	Ground Power Station
GWP	Global Warming Potential
HMI	Human Machine Interface
HV	High Voltage
IEC	International Electrotechnical Commission
IED	Inter-Activity Exchange Document
ISS	International Space Station
LCA	Life Cycle Assessment
LCE	Life Cycle Emissions
LCOE	Levelized Cost Of Energy
LV	Low Voltage
MBSE	Model Based Systems Engineering
MC	Main Controller
MV	Medium Voltage
NOAK	N-Of A Kind
OM	Operations & Maintenance
OPEX	Operational Expenditure
PCU	Power Control Unit
POC	Point Of Connection
PV	Photovoltaic
PVA	Photovoltaic Assembly
RF	Radio Frequency
RTLS	Return To Launch Site
SARJ	Solar Alpha Rotary Joint
SBSP	Space-Based Solar Power
S/C	Spacecraft
SPS	Solar Power Satellite
SSSD	Strathclyde Space Systems Database
TAS	Thales Alenia Space
TSTO	Two Stage To Orbit
VSI	Voltage Source Inverter

2 Reference use-case

Between 17 and 20 April 2023, just after the study technical kick-off meeting, ESA has organized consultation meetings with the following relevant energy sector players: Schellhas Engineering, Microsoft, EDF, TransnetBW, EirGrid Group / ENTSO-E and Shell. These stakeholders were interviewed by our Consortium to establish a consistent set of stakeholder needs and expectations for a prospective future SBSP service.

Based on the analyses of the stakeholder survey an *On-Grid power use case* is considered more interesting to be pursued further as:

- responds to the needs of a larger community of users
- provides more flexibility in terms of utilisation
- it is less driven by specific application requirements (e.g. ICT, water desalinisation, etc…)

In terms of preferred GPS installed power the stakeholder interviews outcome are summarized in Figure 2-1.

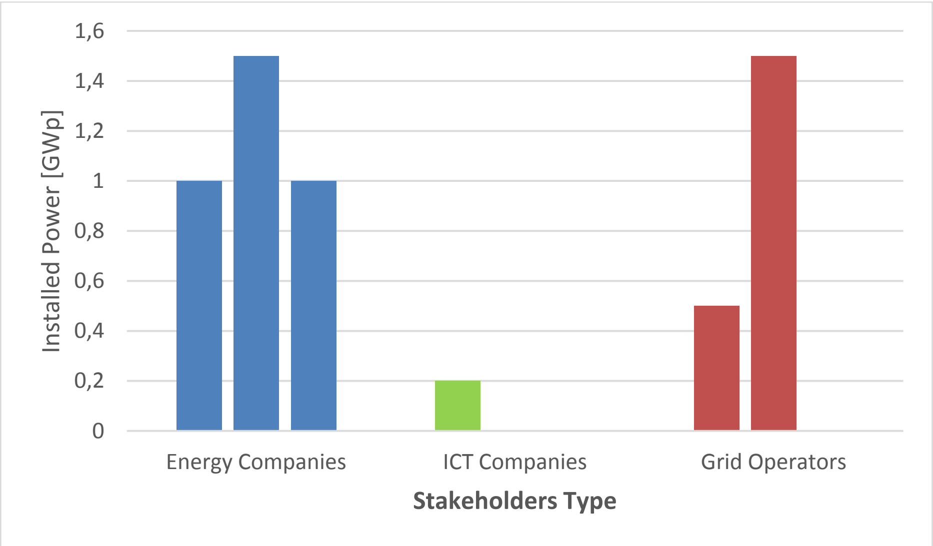

Figure 2-1 Preferred GPS Installed Power [GWp]

In particular the reference use case selected by the Consortium has the following characteristics:

Up to 1GW ± TBD % constant baseload power available 24/7 to be provided from one or several SPS to one GPS in Europe

3 Architecture Trade-offs & Selection

This section contains the trade-offs executed and the relevant justifications leading to the reference architecture. At this stage we have purposely focused on simple solutions that meet the mission requirements, avoiding complexity, as much as possible.

These solutions, mainly based on existing real-world scenarios (e.g., ISS), are expected to include any advantageous improvement deriving from technology evolution in the upcoming years.

3.1 Scoring guideline and weight factors

The following scoring guideline is used for the trade-offs execution:

Criteria	Input value					Description
	1	2	3	4	5	
Cost	Very Bad	Bad	Medium	Good	Very Good	Relative cost of the proposed solution, LCOE
Energy expediture	Very Bad	Bad	Medium	Good	Very Good	Energy Returned on Energy Invested across the system lifetime
Social acceptance	Very Bad	Bad	Medium	Good	Very Good	People acceptance of the proposed solutions
Carbon footprint	Very Bad	Bad	Medium	Good	Very Good	Carbon footprint of the proposed solutions
Mass / Area / Volume	Very Bad	Bad	Medium	Good	Very Good	Physical dimensions of the analysed solutions will be assessed and quoted
Design Complexity	Very Bad	Bad	Medium	Good	Very Good	Streamline of proposed design
Deployment complexity	Very Bad	Bad	Medium	Good	Very Good	How difficult would it be to launch and assemble the SBSP system
Operational complexity	Very Bad	Bad	Medium	Good	Very Good	How difficult would it be to operate, maintain and de-commission the SBSP system
Failure Tolerance	Very Bad	Bad	Medium	Good	Very Good	Capability of the solution to withstand to failure and performance degradation
Capacity factor	Very Bad	Bad	Medium	Good	Very Good	How much power can be provided by the solution
Modularity	Very Bad	Bad	Medium	Good	Very Good	Capability of the analyzed solution to be realized with separate parts that, when combined, form a complete whole
Scalability	Very Bad	Bad	Medium	Good	Very Good	Capability of the analyzed solution to be scalable in performance
TRL / Heritage	Very Bad	Bad	Medium	Good	Very Good	Technology maturity of the proposed solution
Lifetime	Very Bad	Bad	Medium	Good	Very Good	Capability of the analyzed solution to comply with the speficified functionalities for the entire lifetime minimizing the maintainability
Industrial capabil-ity/scalability	Very Bad	Bad	Medium	Good	Very Good	In terms of logistic (technological reasons vs. geopoliti-cal location) and industrial supply

Table 3-1 Trade-offs scoring guideline

The following weight factors are used for the trade-offs execution:

Weight factors		
Criteria	**Weight factor value**	**Justification**
Cost	5	Cost are considered critical for mission feasibility
Energy expediture	3	The Energy Returned on Energy Invested across the system lifetime has been considered less critical than the relative cost of the proposed solution
Social acceptance	5	This criterion was indicated by all the stakeholders as the most critical for SBSP applications

Weight factors		
Criteria	**Weight factor value**	**Justification**
Carbon footprint	5	High criticality has been assigned to carbon footprint considering the size of the system. Environmental impact importance has been highlighted both by ESA SoW and by the stakeholders
Mass / Area / Volume	5	The SBSP mission feasibility is strongly dependend on this criterion which depends on the architecture and technologies selected
Design Complexity	3	All the SBSP concepts exhibit considerable design complexity. This complexity need to be minimized but has been considered of medium criticality, provided that the feasibility is granted
Deployment complexity	3	The SBSP system deployment is considered of medium criticality for mission feasibility. There is a strong impact in terms of launcher performances
Operational complexity	3	The operational complexity has been considered of medium criticality in particular for safety reasons
Failure Tolerance	2	The failure tolerance has not been considered particularly critical since an highly reliable and efficient support IOS system is foreseen
Capacity factor	4	The power provided by the solution has been considered important by the stakeholders and for economical feasibility
Modularity	4	The modularity has been considered quite critical considering the size of the system and the need of assembling it in-orbit
Scalability	4	The scalability of the performance has been considered quite critical considering the need to develop a demonstrator
TRL / Heritage	1	Considering only the scalability required of already existing technologies and the timeframe available for technology improvements the TRL has been considered not critical
Lifetime	4	Lifetime has been considered critical for the required operations of 30 years and the competition with alternative energy solutions
Industrial capability and scalability	3	The industrial capability and scalability have been considered of medium criticality

Table 3-2 Weight factors

3.2 Space Segment trade-offs

For the solar power satellite itself a functional level trade-off is proposed, looking at trading of the various top level architectural functions of the system (e.g. collect function, convert function, distribute function etc).

Feature	Examples of Options	
Collect	Direct – Conversion system pointed at the sun	Monolithic (1 or few large elements)
		Multiple (many smaller elements)
	Reflect - Reflectors used to illuminate ground conversion system with the sun	Monolithic
		Multiple
Point	Separate Sun and Earth Pointing	Rotating across electrical Interface
		Rotating across optical interface
		Rotating across transmission interface
	Solid State	Geometric – Beam steering

Feature	Examples of Options	
		Non-constant Illumination
		Redundant elements (collection or transmission)
Convert	Solar Array	Direct sun exposure of the on-orbit PVA
		Reflector and Concentrator used to reflect sun flux on a fixed Solar Array located on orbit
	Thermal (e.g. a Stirling engine, or even a steam generator)	
Distribute (among on-orbit elements)	High Voltage	
	Low Voltage	
	Wireless (RF)	
Transmit	Microwave	
	Laser	

Table 3-3 SPS functional level trade-offs

This could be illustrated with the trade-off tree in Figure 3-1.

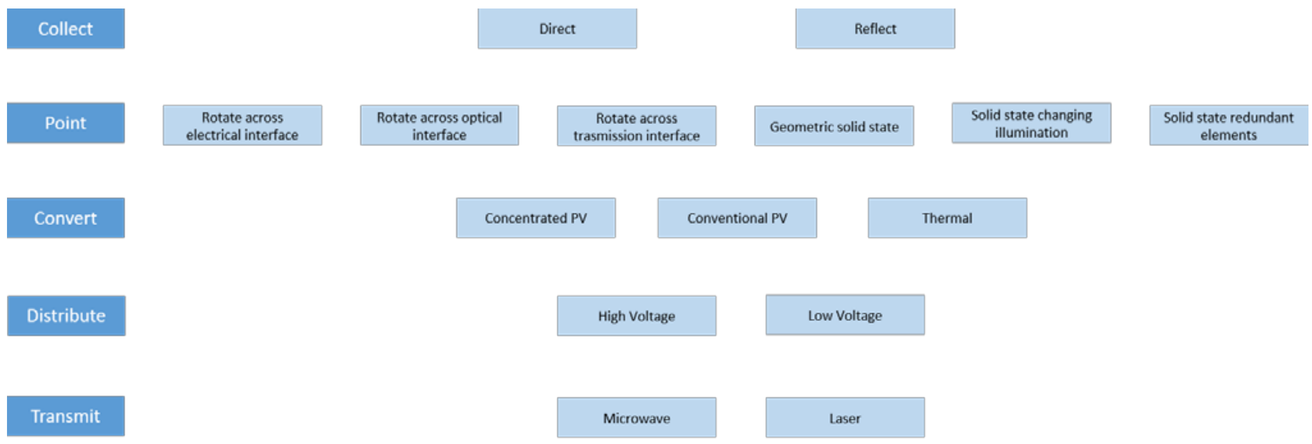

Figure 3-1 SPS trade-off tree

The trade-off tree presented (derived from a first functional analysis) serves as an excellent initial framework for outlining the trade-space. However, it was necessary to carry out a preliminary pruning to facilitate subsequent development work on possible design paths.

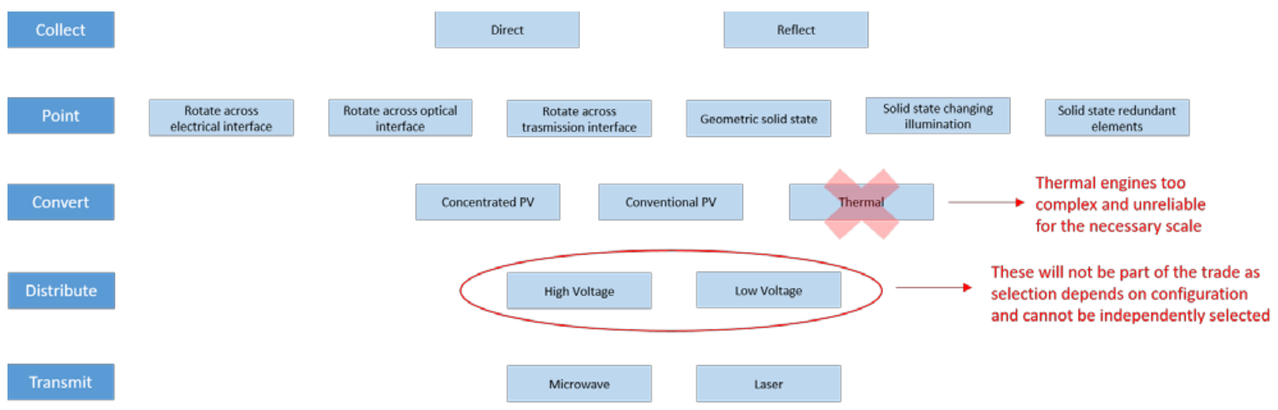

Figure 3-2 Trade tree preliminary pruning

For the selection of the transmission function, the following considerations hold. Two options are essentially possible for the wireless power transmission, i.e., either microwave or laser. The laser option is discarded for the following well-known disadvantages that affect laser power beaming:

- The laser option is affected by climatic conditions, like rain and clouds, and hence it is unable to deliver continuous electricity thus violating the SBSP system requirement UR-REQ-0110 (constant power provision);
- The laser option has a limited conversion efficiency and requires massive battery storage systems;
- If not properly treated the laser presents high risks, in terms of skin and eye damage.

Moreover the trade-offs performed lead to the selection of the “Direct” option for the collect function and the “Rotate across electrical interface” option for the pointing function.

3.2.1 SPS convert

Although the potential benefits in terms of mass and PVA costs when implementing CPV are acknowledged (albeit uncertain in terms of scalability due to secondary impacts from higher overall complexity), factors such as operational and design complexities lean towards favouring the implementation of conventional PV cells, which are selected as baseline.

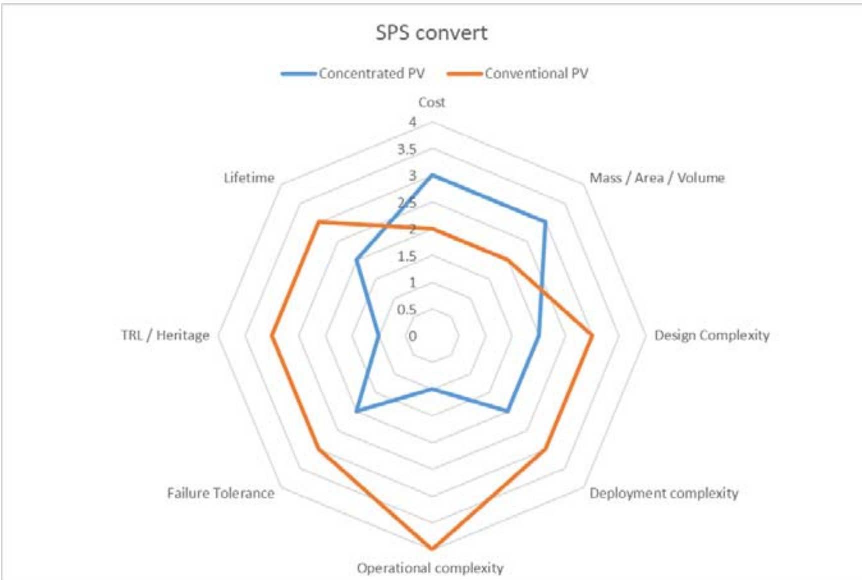

Figure 3-3 SPS convert trade-off summary graph

3.2.2 Orbit selection

For the orbit selection, the following configuration are evaluated: Low Earth Orbits, Medium Earth Orbits, Molniya orbits and Geosynchronous Earth Orbit. Each option is analysed and pros and cons derived in order to perform a preliminary orbit pruning.

The trade-off analysis clearly shows that GEO is the most suitable orbit for the scope of the mission, mainly for the possibility of using only one satellite and for having a fixed beam towards Earth, at the cost of a bigger GPS due to the slant range.

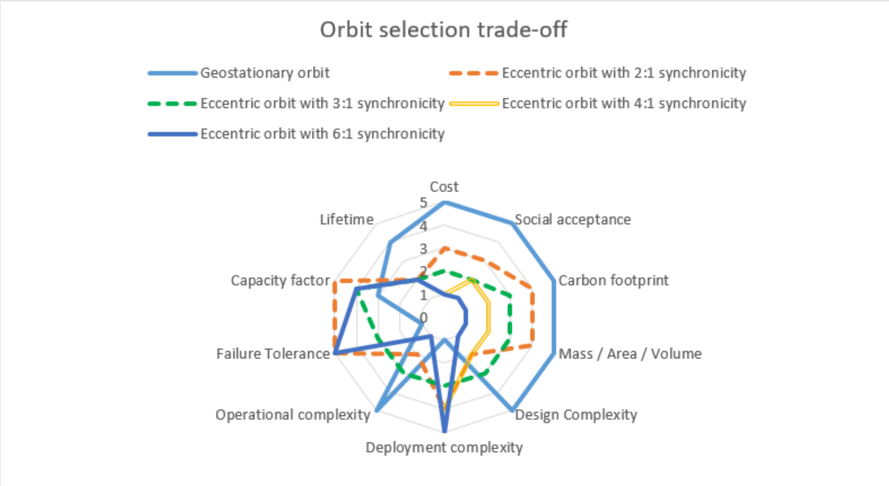

Figure 3-4 Orbit selection trade-off summary graph

3.2.3 Operating frequency

Frequency choice is one of the critical points of SBSP system concept. It is plausible to consider a range of operative frequencies between 1 and 24 GHz (in particular considering the ISM frequencies available).

However, frequencies from 10 GHz onwards are strongly affected by the atmosphere. Consequently the availability of the power link and its power capacity (losses) will depend on weather conditions (rain, snow, fog, etc.) above the GPS so this is not compliant with the 24/7 baseload use case considered.

For this reason, and considering the available ranges of ISM band, the two remaining alternatives are 2.45 GHz and 5.8 GHz.

The decision depends mainly on the Mass/Area/Volume attribute for this trade-off. In fact, the majority of other applicable criteria result to be direct consequences of this (for example, at least for this trade off, cost is only a direct consequence of the 3 main project areas we are considering such as deployment and operational complexity too).

For this reason we notice how for 5.8 GHz we obtain a reduction of the on board antenna area of 1/3 with respect to 2.45 GHz solution, while having only a small arise of the solar panels area. Since reducing the antenna area could be a great advantage not only for mass/volume criteria, but also for cost and design complexity reasons, the choice is an operative frequency of 5.8 GHz.

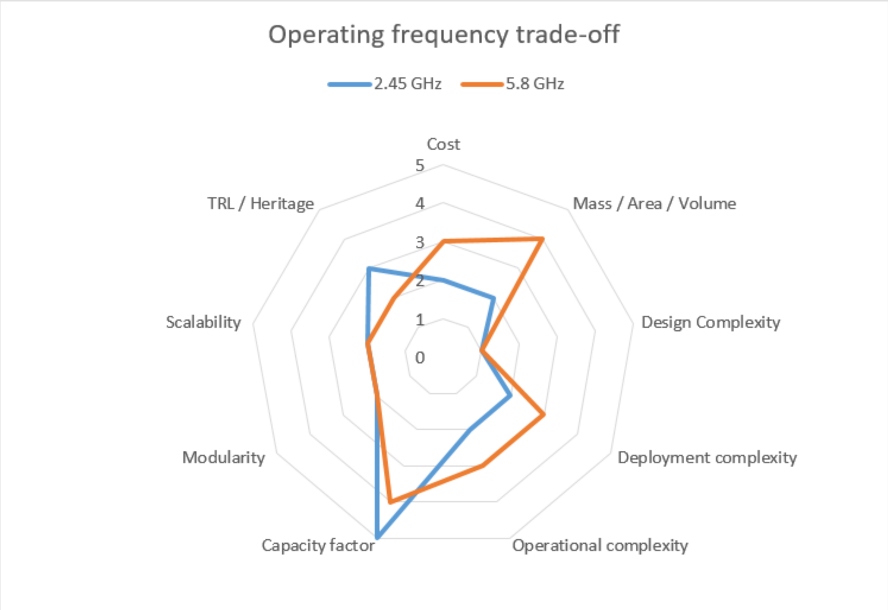

Figure 3-5 Operating frequency trade-off summary graph

3.2.4 Cell technology selection

A precise selection of cell technologies applicable to SPS, considering up-to-date PV cells data are reported in Table 3-4:

	Conventional Multijunction 3j/4j (e.g., XTG)	Thin film InGaP/GaAs/Ge (e.g., 3G30-C)	Thin film single junction GaAs	Thin film CIGS	Perovskite cells
Module efficiency (proved in space applications)	32%	29%	/	/	/
Max lab proved efficiency	/	/	29%	23.4%	26%
Expected module efficiency (2050) with adequate funding	40%	36%	32%	29%	29%
Technology TRL	9	9	5-6	4 -5	3-4
Specific power density [W/g]	0.47	0.8	3	3	23
Mass/area [kg/m2] under 1 Sun	2.9	2.05	0.5	0.5	0.07
Manufacturing cost (expected)	High	High	Medium	Low	Low

	Conventional Multijunction 3j/4j (e.g., XTG)	Thin film InGaP/GaAs/Ge (e.g., 3G30-C)	Thin film single junction GaAs	Thin film CIGS	Perovskite cells
Degradation rate (expected in future applications)	0.5-1.5 %/year	0.5-1.5 %/year	0.5-1 %/year	0.1-0.5 %/year	0.1-0.5 %/year

Table 3-4 Possible cell technologies that could be implemented in a SPS

Among the selected options, thin film InGaP/GaAs/Ge cells (e.g., 3G30-C) and Perovskite cells stand out as the two most promising choices, each offering distinct advantages.

While thin film InGaP/GaAs/Ge cells hold their own in terms of efficiency and TRL, Perovskite cells prove to be a compelling option due to their cost-effectiveness and impressive specific power density, even considering their current lower TRL status (which is an attribute with low value in the project decisional logic). Moreover this technology shows an incredible rise in efficiencies in the last 10 years, from 14% in 2013 to 26% in 2023 (lab tested). For this reason (with adequate funding needed for further research to increase lifetime, crystal stability and overall TRL) Perovskite cells result as the most promising option for future SPS applications. Therefore, Perovskite PV cells is selected as baseline.

3.2.5 DC to RF power conversion

The choice of the technology for the conversion of DC into RF depends on many design elements of the WPT: frequency, type and size of the antenna, power to be transmitted. The SSPA are chosen for the proposed range of frequencies.

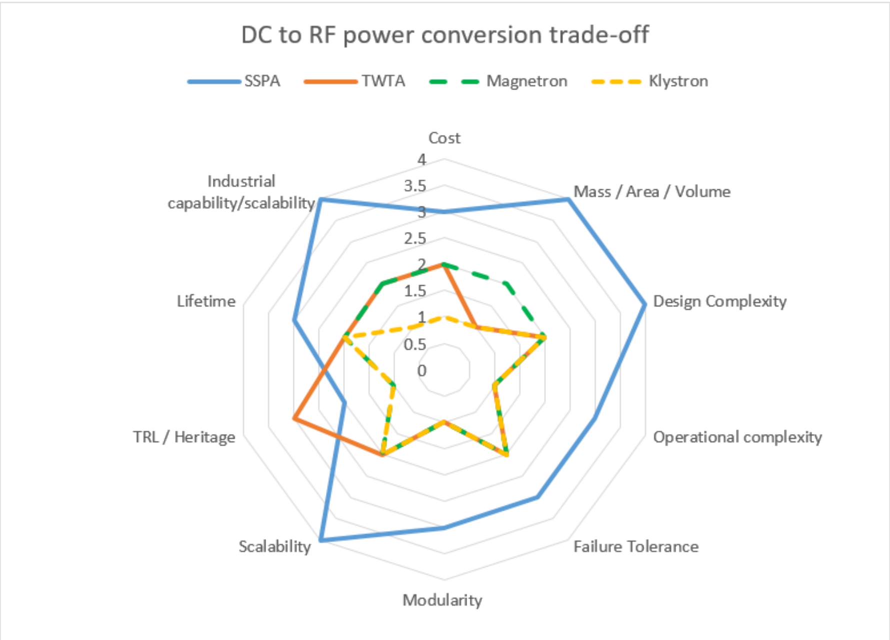

Figure 3-6 DC to RF power conversion trade-off summary graph

3.2.6 Structure and materials

This trade-off is focused on 3 options concerning structures with the relevant materials for the solar array modules concurring to the SPS assembly as here after summarized:

OPTION 1	OPTION 2	OPTION 3
Flexible Roll-out Structures	**Rigid Structures**	**Inflatable Structures**
		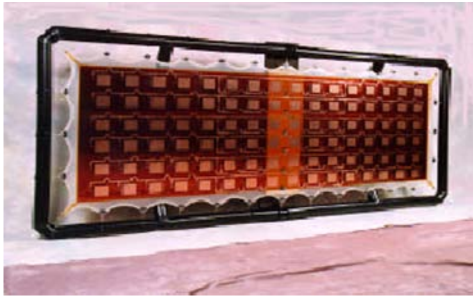

Figure 3-7 Options for Structures for Trade-off

The Option 1 based on Flexible Roll-out Structures for the SPS solar arrays results the most suitable for this application.

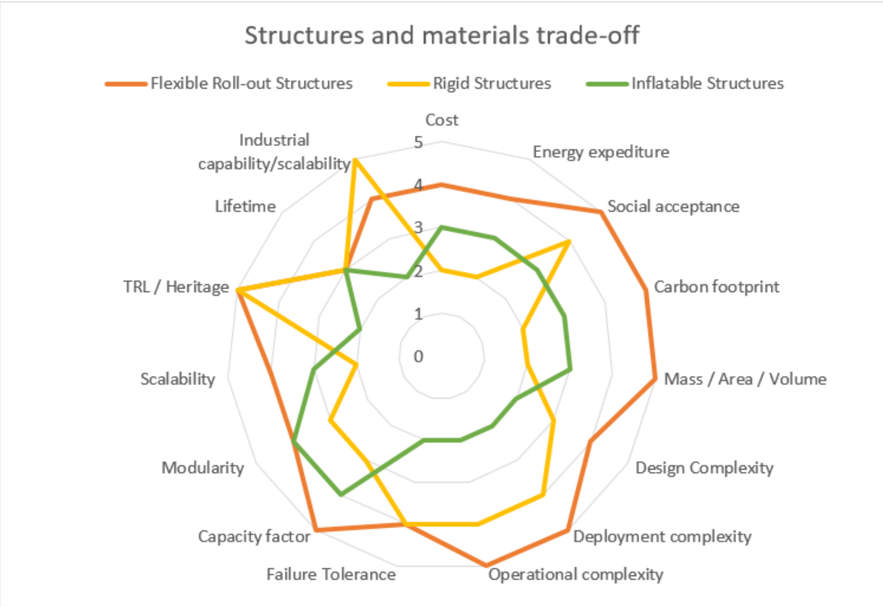

Figure 3-8 Structures and material trade-off summary graph

3.2.7 In-space transportation and infrastructure

The trade-offs shows that using a LEO as injection orbit brings the most advantages compared to other configurations, especially considering the propellant required.

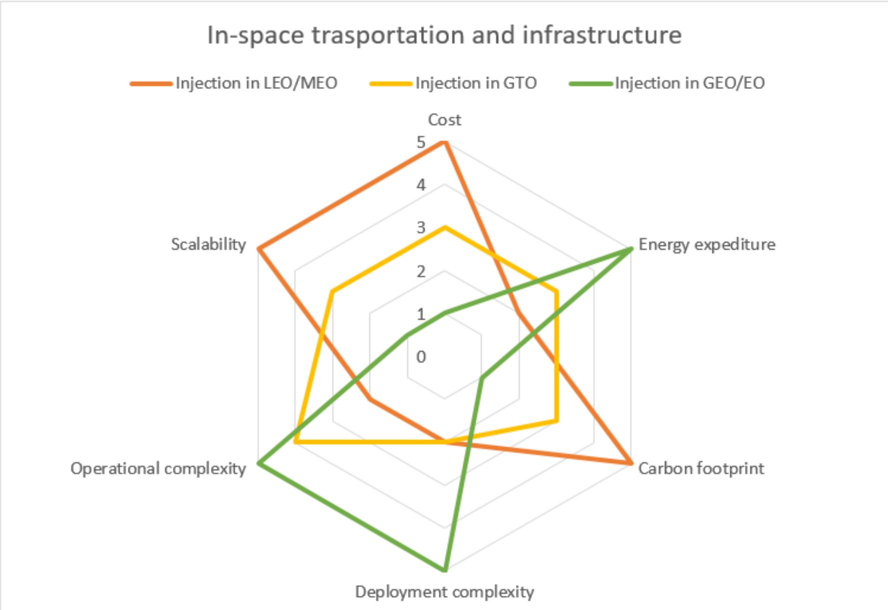

Figure 3-9 In-space transportation and infrastructure trade-off summary graph

3.3 Ground Segment trade-offs

3.3.1 GPS location

The on-shore installation, considering the high level of power that the station must handle is the best compromise among all the parameters. This installation, especially as a first big plant of this kind, will probably require a continuous control and continuous improvement approach to be optimized. The added complexity due to an off-shore installation will probably introduce several other potential failure modes and difficulties in O&M operation that cannot be considered in principle as the first plant of its kind. In a second phase, once the plant will be optimized and all the technical issue solved, we can think to move on an off-shore installation.

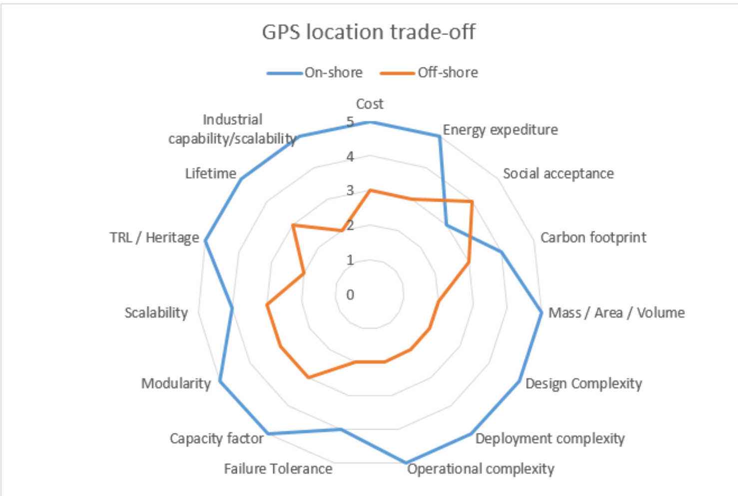

Figure 3-10 GPS location trade-off summary graph

Considering the location among all the parameters the main driving input is related to cost and to the connection to European energy distribution network. We need also to take into account the social acceptance of the receiving antenna and, since the trade-off between on-shore and off-shore is in favor of an on-shore installation, the human factor can be quite important. All the 3 countries considered are actually quite open to installing this kind of technological platforms especially if related to renewable energy. The labor cost can do the difference among these 3 countries. With the actual inputs Spain seems to be among all the countries the best solution.

Figure 3-11 GPS location (country) trade-off summary graph

3.3.2 Energy storage system

In the last years, SuperCap have emerged as a promising alternative for Li-ion as they exhibit high power densities, excellent and fast cycling stability and longevity. New materials for SuperCap are now providing ultra-high theoretical energy density (300 Wh/kg), elemental abundance in the earth's crust, and environmental friendliness. Without sacrificing power density and reliability the cost per kWh is getting close to Li-ion. Therefore, supercapacitors are selected as baseline.

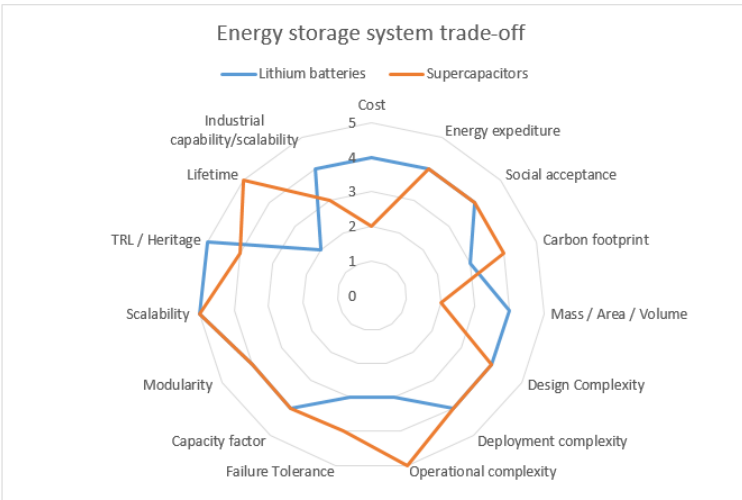

Figure 3-12 Energy storage system trade-off summary graph

3.4 SBSP selected architecture

Based on the trade-offs, summarized in Table 3-5, the following architecture is selected for the SPS:

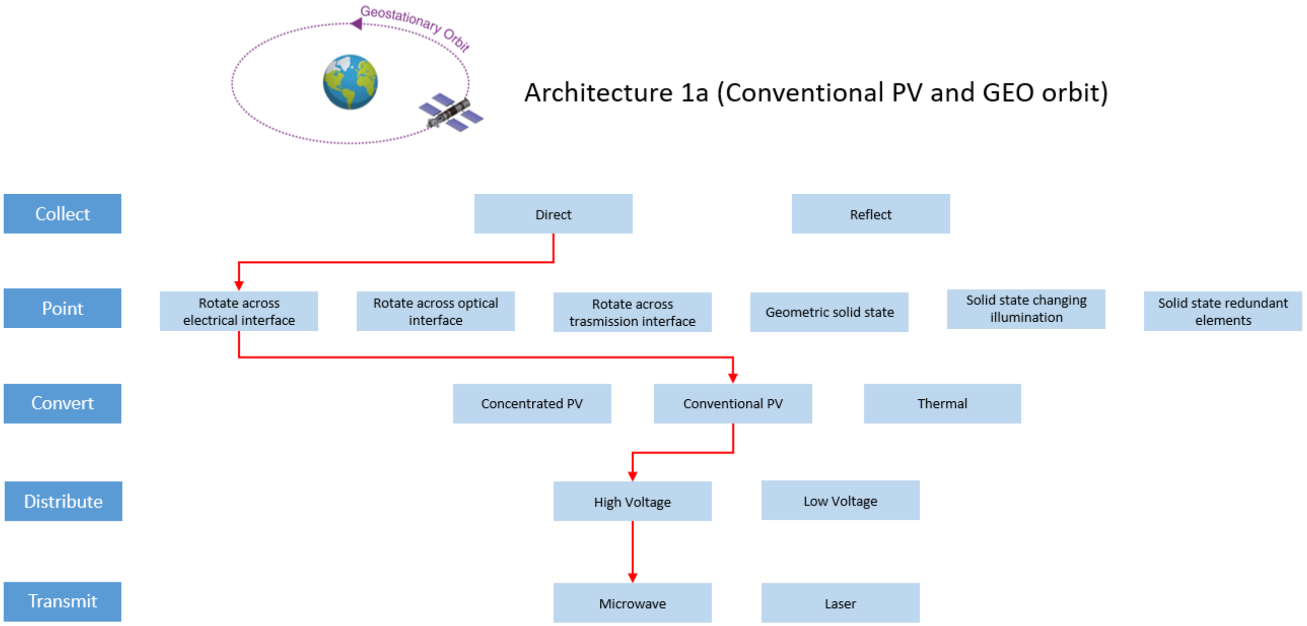

Figure 3-13 SPS Architecture 1a (Conventional PV and GEO orbit)

	Performed Trade-off	Selected option
Space Segment	Orbit trade-off	Geostationary orbit
	Operating frequency trade-off	5.8GHz
	Cells technology selection	Perovskite cells
	DC to RF power conversion trade-off	SSPA
	Structures and materials for solar array modules trade-off	Flexible Roll-out Structures
	In-space transportation and infrastructure trade-off	Injection in LEO
Ground Segment	GPS location trade-off	On-shore
	GPS location (country) trade-off	Spain
	Energy storage system trade-off	Supercapacitors

Table 3-5 Trade-offs summary

4 Concept of Operations

4.1 Mission Phases

The mission phases are summarized below:

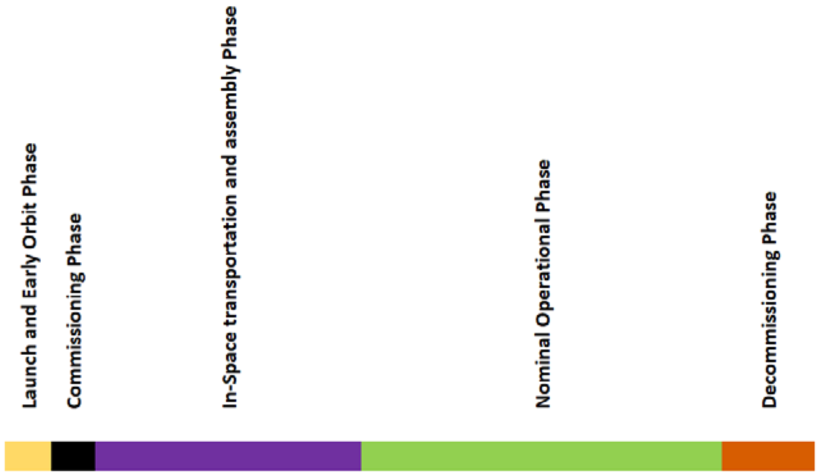

Figure 4-1 Mission phases

and a pictorial overview is provided in Figure 4-2.

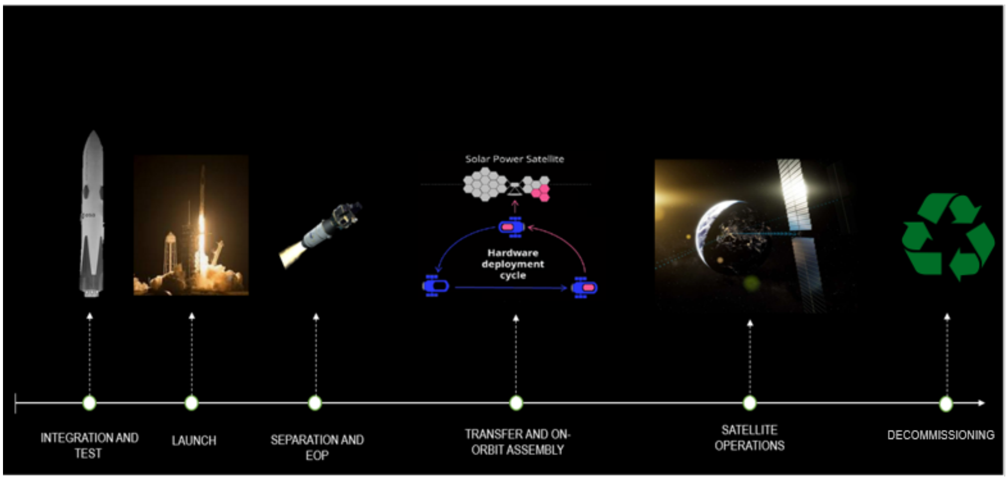

Figure 4-2 Mission phases overview

4.2 Launch, Deployment & Assembly

For SPS launch, deployment and assembly the selected option is shown in Figure 4-3.

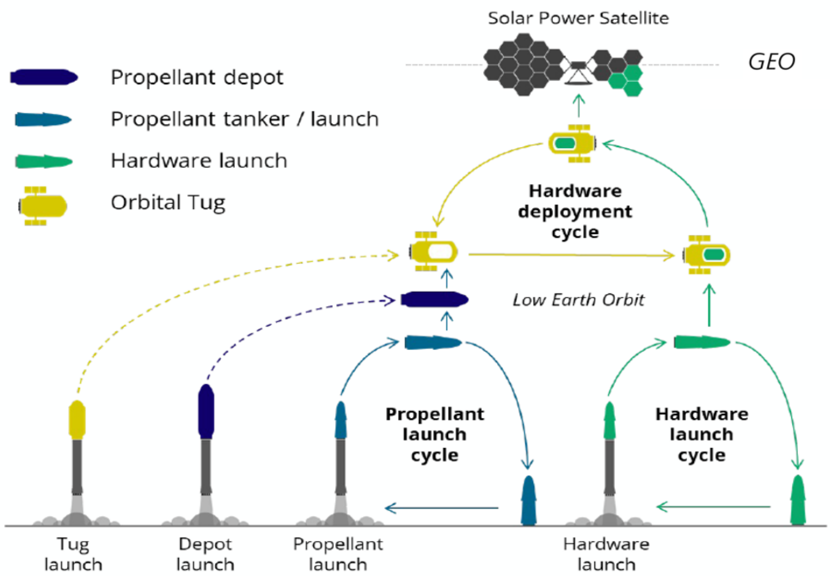

Figure 4-3 SPS launch, deployment and assembly

The concept foresees a modular in-orbit assembly for the antenna and the solar arrays, with several launches to LEO with cargos. Once in LEO, an orbital tug is used to move the hardware from LEO to GEO. A propellant depot is needed to refuel the tug during the mission.

Once in GEO, the hardware is assembled thanks to the contribution of automated devices called In-Orbit Services. The concept foresees the capability to operate the SPS in a <u>reduced power mode</u> before the complete assembly take place. This will grant solar power beaming from early stage of the mission allowing in orbit test and refinements.

4.3 Communications Strategy

The Communications strategy, similar to the standard GEO satellites, is summarized in Figure 4-4.

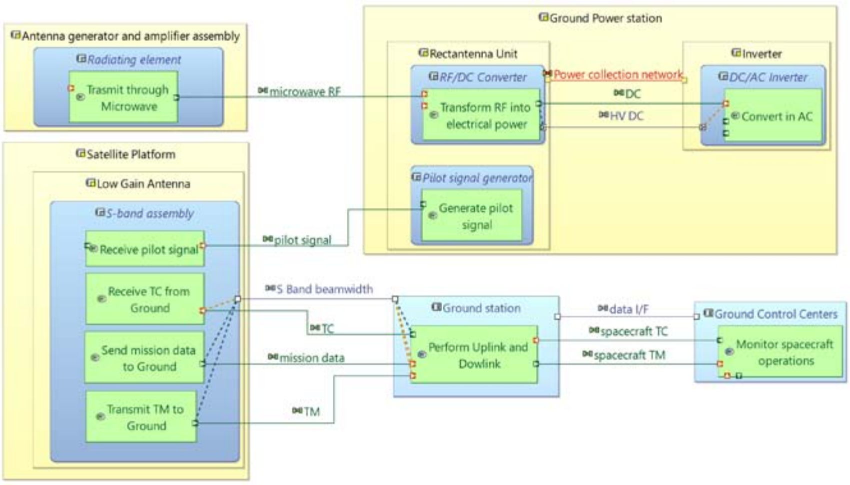

Figure 4-4 Communications strategy

The SPS is equipped with an S-band low gain antenna to communicate with ground and to receive the retrodirective beaming signal, essential for a precise pointing of the power beam.

4.4 Decommissioning Strategy

As the graveyard orbit is not compliant with the Zero Debris policy the SPS will be disassembled with the help of the robotic systems and then recycled. Two options are proposed:

- *Lunar recycling* (Figure 4-5): the robotic systems disassemble a small hardware part from the SPS and the orbital tug, after being refueled, transfers it to the Moon. This hardware decommissioning cycle is then repeated. The Orbital Tug is capable to perform GEO to Moon orbit and back trip as the Delta V required is similar to the LEO to GEO transfer;
- *In-situ recycling*: the SPS will be disassembled and then recycled in GEO via in-orbit manufacturing.

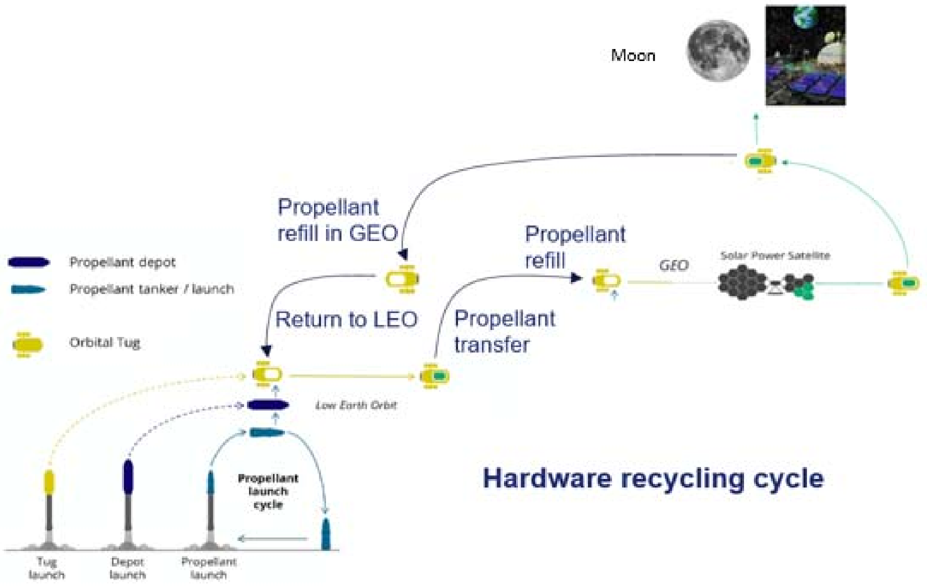

Figure 4-5 SPS Moon disassembly and decommissioning

5 System Size Optimization

5.1 Optimization Approach & System Driving Parameters

A main mathematical model containing the efficiency chain parameters, is implemented in an SBSP digital framework (for details refer to chapter 11) following a methodology similar to the one adopted to make decisions for frequency trade-offs. This integration aims to shed light on the potential impact of variations in key design parameters related to the three principal SBSP domains: GPS area, solar panels area and on-board antenna area.

Each of these values is inserted in an objective function to be minimized by the optimization model with the correspondent weight factors, which could be changed arbitrarily to observe the possible impact on the optimized solutions.

Optimization Weights List

Pameter Name	Parameter Value
WGoundStation	1
WAntenna	50
WSolarPanel	50

Figure 5-1 Possible combination of weight factors for the optimization model

The main parameters affecting the system (in terms of the three areas), with the corresponding possible options and implications, are implemented inside the tool and listed below (considering GEO orbit and 1GW power provision as baseline for the solution).

Parameter	Options	Main impact on the SBSP System
Cell technology	Thin Film 3 Junctions (Expected cell efficiency: 36 %)	Cell technology and the associated cell efficiency significantly influence the size of PVA (though factors like cost and weight remain equally relevant).
	CIGS (Expected cell efficiency: 29 %)	
	Perovskite (Expected cell efficiency: 29%)	
Frequency	2.45 GHz	Considering the GEO orbit as baseline and a fixed GPS location, the frequency remains the only parameter affecting the product of the GPS area and the on-orbit antenna area (higher frequencies lead to lower product values)
	5.8 GHz	
GPS location	Spain (Latitude: 40.2°)	Considering the GEO orbit as baseline and a fixed value of frequency, an higher GPS area is needed when considering higher latitudes (because of the power footprint stretching)
	Germany (Latitude: 51.1°)	
	Sweden (Latitude: 60.1°)	

Table 5-1 Main mathematical model implementation: parameters and possible options

5.2 Main Mathematical Model Results

Three analyses are conducted to examine the variations in results stemming from various weight factor combinations (1-1-1, 1-30-30, 1-50-50, 1-200-200). Furthermore, for each individual analysis, all viable option combinations are assessed.
In addition to the summary results table two graphical representations are added for each simulation:

- A scatter plot for a visual representation of optimized area values corresponding to the given weight factor combination.
- A bivariate histogram illustrating the multiplicity of solutions that involve precise couplings between on-board antenna area and GPS area. This graph provides insights into the multiplicity of couplings between the antenna area and the GPS area in the simulations. A higher occurrence of coupling with a specific solution multiplicity indicates that, for the corresponding weight factor combinations, that solution emerges as the most credible and well-optimized choice across a wide range of parameter options.

In particular, for the 1-200-200 weight factor combination, the baseline solution highlighted presents the following values:

System area	Area value [km^2]
GPS area	34
PVA area	6.2
On-board antenna area	0.44

Table 5-2 Optimized area values for the selected architecture

The simulation results are displayed below.

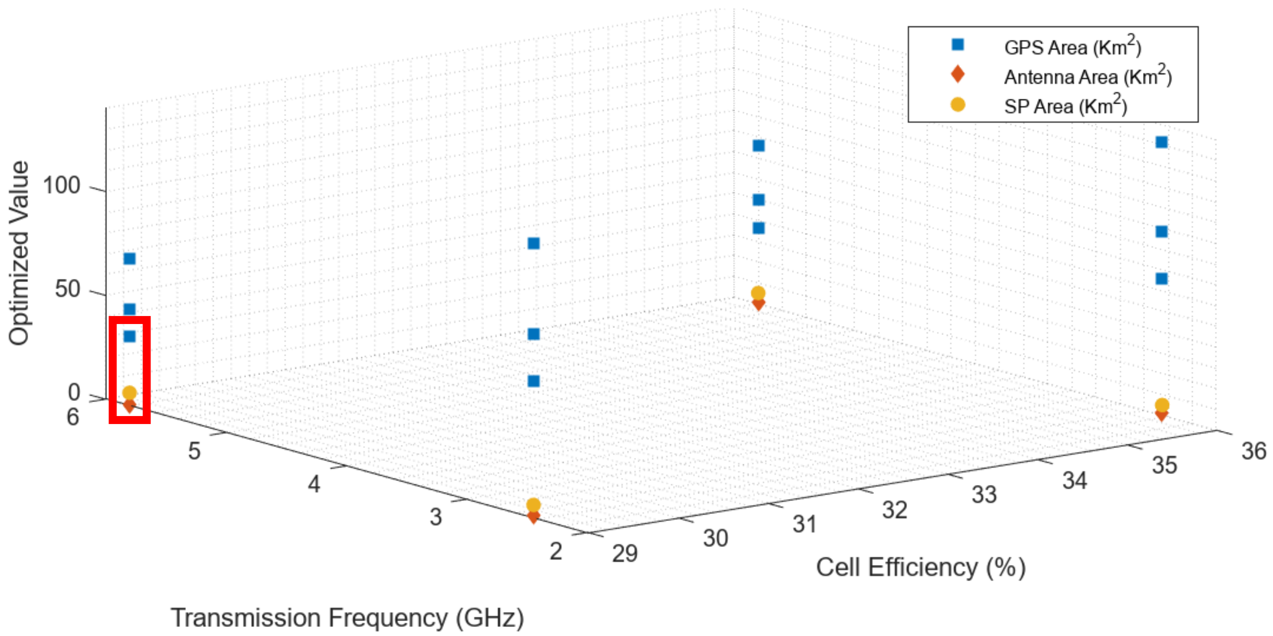

Figure 5-2 Optimized area values for 1-200-200 weight factors combination (with the baseline solution selected)

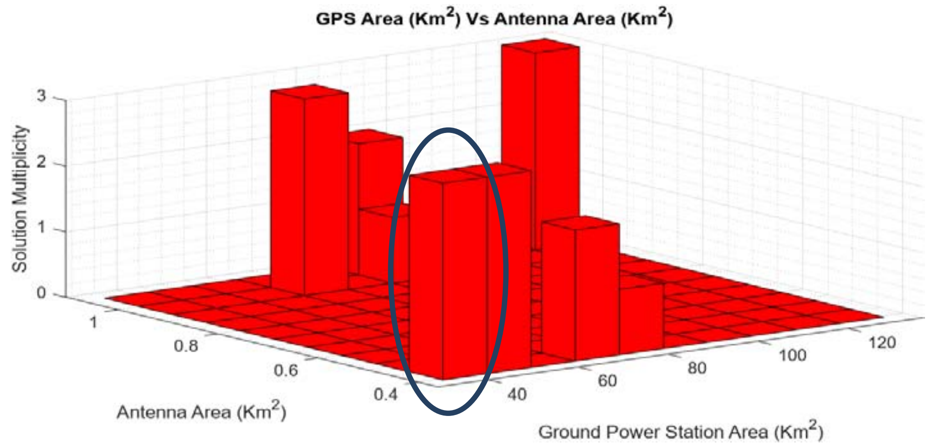

Figure 5-3 Solutions multiplicity for the GPS-antenna area coupling for 1-200-200 weight factors combination

6 System Definition

This chapter describes the SBSP System, starting from mission analysis considerations. The following topics are subsequently addressed:

- Space Segment;
- Ground Segment;
- Launch Segment.

6.1 Mission Analyses

The Geostationary orbit is chosen as operative orbit due to its advantages in terms of amount of required satellites (only one), GPS area and ease of operations. In the following sections the effects of the chosen orbit in terms of perturbations are analyzed.

6.1.1 Effect of the ecliptic plane

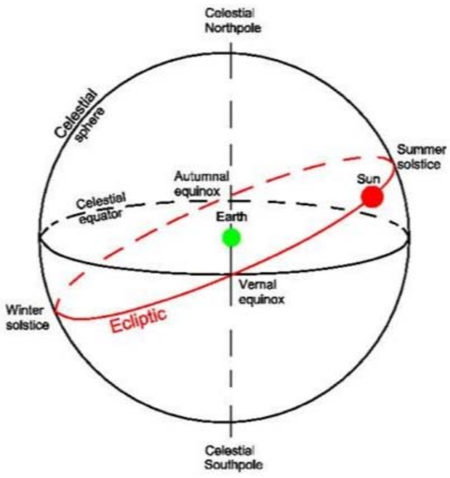

Figure 6-1 Ecliptic and equator relative position

Due to the inclination between the ecliptic and the equator plane, the inclination of the Sun vector w.r.t. the solar arrays changes over time, from a minimum of 0 deg during the equinoxes to a maximum of 23.44 deg during the solstices, resulting in a small decrease of performances of around 8%. During equinoxes there are eclipses of a duration of up to 71 minutes, which causes a loss of energy delivered during the eclipses. The effect on the system of both these events are shown in chapter 11.

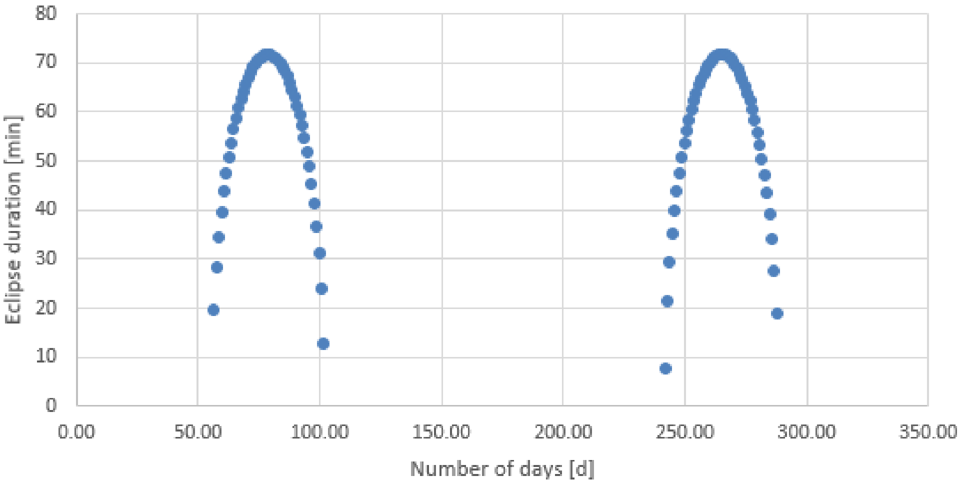

Figure 6-2 Eclipse duration during a year

6.1.2 Station-keeping considerations

Considering the GEO orbit baseline, preliminary station-keeping considerations are needed to perform the sizing of the thrusters for AOCS.

Amongst the perturbations suffered by the SPS in GEO orbit, the solar pressure is prominent due to the high area of the SPS. For a conservative approach, a cannonball model is utilized to evaluate the solar radiation force with the considered values reported below:

Solar panels	6.2 km^2
Scaling coefficient C_R	2

Table 6-1 Input values for the Solar Radiation Force

The output values for the SPS in GEO with a propagation time of one year is shown in the following figure:

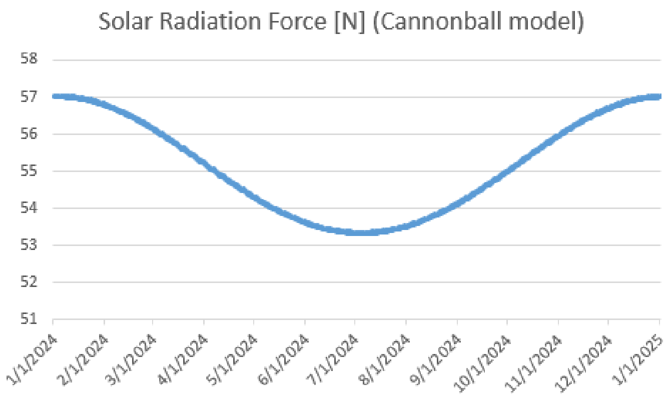

Figure 6-3 Solar Radiation Force in a year

So the dimensioning value is of 57N. As the effect is continuous during the year, the proposed station-keeping approach to contrast this perturbation is to have thrusters that continuously burn in the opposite direction of the solar radiation force with the same force to even out the forces. Due to the inclination of the ecliptic a force along the satellite x-axis is required to contrast the solar radiation pressure when getting nearer the solstice.

Another perturbation to consider is the luni-solar effects, mainly affecting the orbit's inclination. The station-keeping for this disturbance is called North-South stationkeeping as the thrust shall be applied in the out-of-plane direction, along the satellite x-axis. The DeltaV tipically required to compensate for this disturbance is of 50 m/s per year. The time required to perform this DeltaV change based on the total thrust is shown:

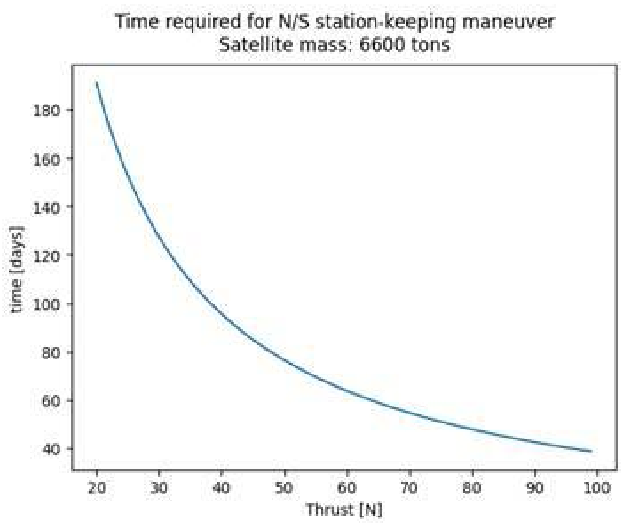

Figure 6-4 Continuous burn time for N/S station-keeping based on total thrust

To maximise the thruster usage this effect shall be contrasted when the satellite is near the equinoxes, as the effect of the solar radiation pressure is lower along the x-axis thus there are more thrusters available.

The last considered perturbation is the Earth triaxiality which affect the satellite's longitude. The station-keeping for this disturbance is called East-West station-keeping as the thrust shall be applied in the in-plane direction. The DeltaV tipically required to compensate for this disturbance is of 2 m/s per year. As before, the time required to obtain this DeltaV is shown:

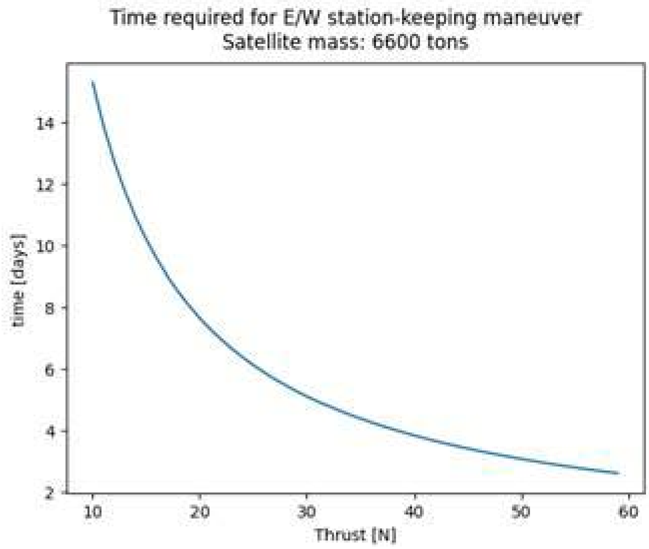

Figure 6-5 Continuous burn time for E/W station-keeping based on total thrust

During nominal operation, the spacecraft absorbs solar photons but re-emits microwave photons towards Earth. This megawatt microwave beam could also produce a propulsive force in the opposite direction (i.e. towards zenith) due to the photon pressure.

The force emitted can be evaluated as:

$$F_{emitted} = P_{emitted} * Area = \frac{Transmitted\ Power}{speed\ of\ light\ in\ vacuum} = 2.058\ GW * 3.34\ \left(\frac{N}{GW}\right) = 6.87\ N$$

This effect cannot be neglected and is tackled in the AOCS section.

6.2 MMOD Preliminary Assessment

The SPS features extremely large solar panel and antenna surfaces, in order to accomplish the mission objectives. Consequently, micrometeoroids and orbital debris (MMOD) impacts on these item surfaces represent an element of criticality to be addressed. For instance, impacts on solar arrays may cause not only mechanical damage but also electrical damage due to high density plasma induced by impact energy, which can lead to arcing between solar cells and substrate on the solar array. These may cause a degradation of performances up to a failure of the item, with the need of on-orbit replacement.

A preliminary and simplified evaluation of the MMOD fluxes that the SPS solar panels and antenna would face in the GEO orbit has been carried out with ESA tool MASTER 8.0.3. The MASTER and the Grun (with Taylor velocity distribution) environment models have been respectively used for debris and meteoroids flux assessment. The time range is limited by the available MASTER population files to 2036, which was then used as reference epoch.

Figure 6-6 to Figure 6-9 show the impact flux on each surface as a function of the impactor diameter.

The *oriented surface* functionality of the tool has been used to represent the envisaged orientation of the critical surfaces along the orbit. Frontal and back impacts have been considered. Spectrum between 1.0E-4 and 100 m have been considered.

Surface	MASTER surface orientation	Total flux in spectrum [1/m^2/year]
Antenna surface, frontal impacts	Earth-oriented (azimuth = 0°. Inclination = -90°)	0.2189E+1
Antenna surface, back impacts	Earth-oriented (azimuth = 0°. Inclination = 90°)	0.2228E+1
Solar panels, frontal impacts	Sun-oriented (right ascension = 0°, declination = 0°)	0.1859E+1
Solar panels, back impacts	Sun-oriented (right ascension = 180°, declination = 0°)	0.1907E+1

Table 6-2 MASTER oriented surface and related flux in GEO

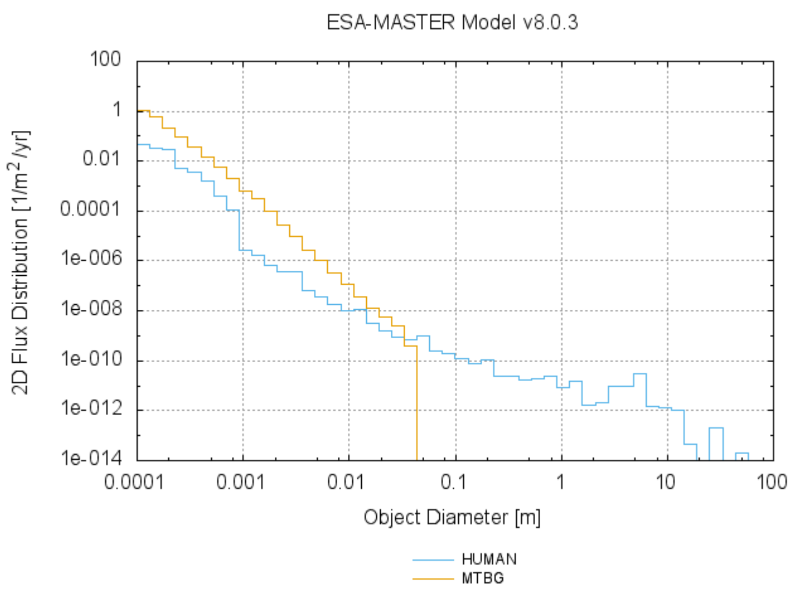

Figure 6-6 Frontal flux on antenna as a function of the impactor diameter

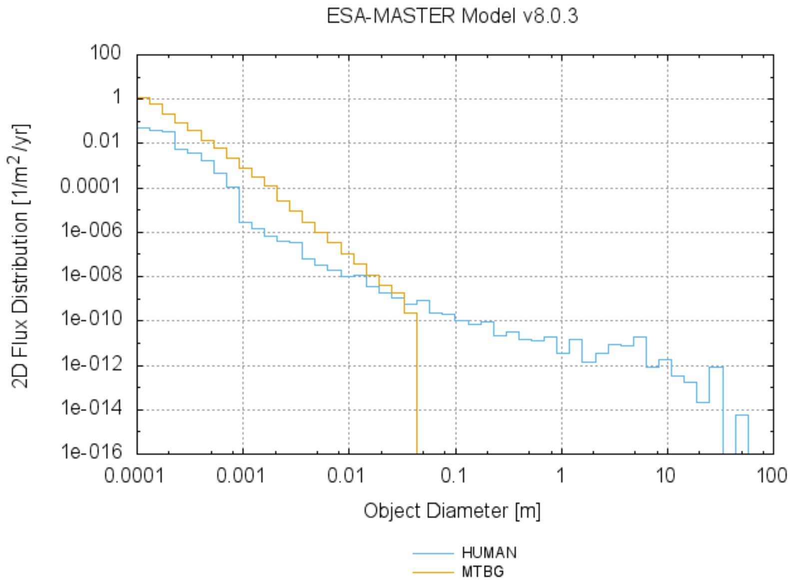

Figure 6-7 Back flux on antenna as a function of the impactor diameter

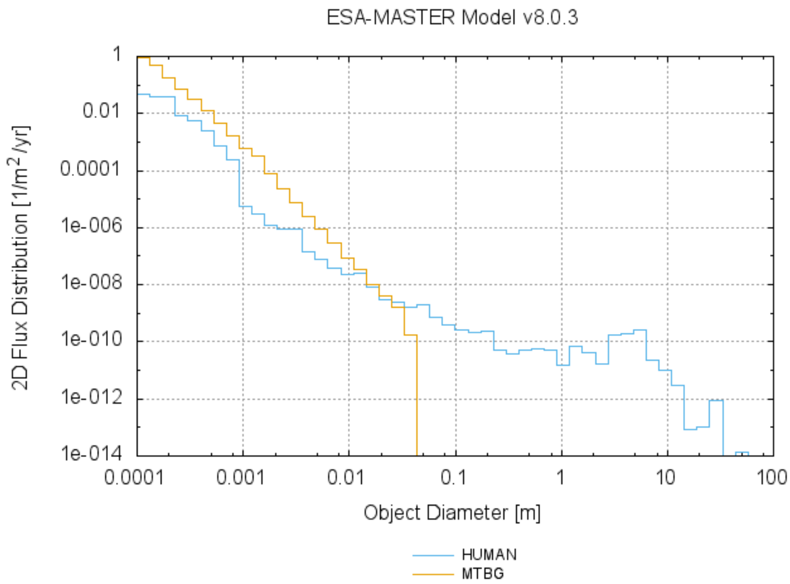

Figure 6-8 Frontal flux on solar panels as a function of the impactor diameter

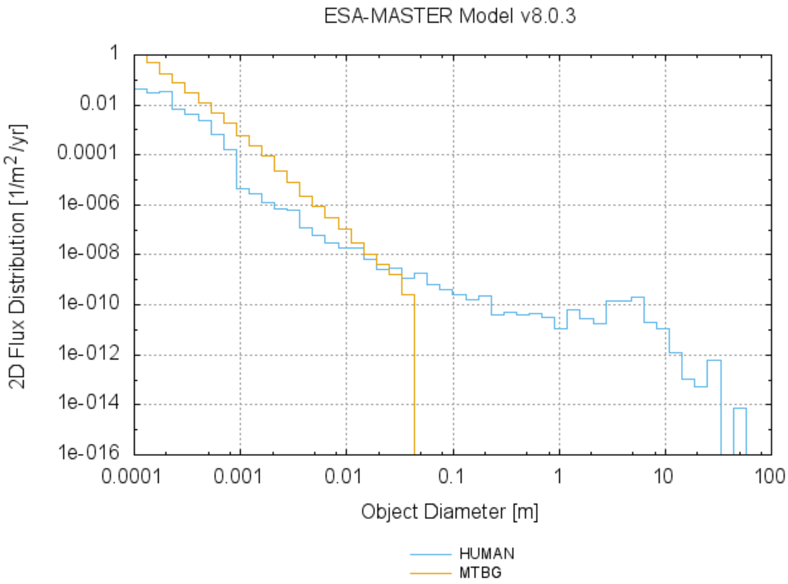

Figure 6-9 Back flux on solar panels as a function of the impactor diameter

Note that the meteoroid flux overcomes the debris flux in GEO in the range up to 1 cm.

Debris with diameter higher than 1 m are generally trackable in GEO. As an impact with a large piece of debris can cause severe or catastrophic damages to the spacecraft, impact risk shall be mitigated by performing collision avoidance manoeuvres, which could be coupled with station-keeping manoeuvres in order to optimize fuel consumption.

For smaller non-trackable particles, only passive mitigation measures can be adopted. In order to carry out an assessment of the probability of failure due to MMOD impacts, more detailed information not available at this stage are needed, i.e. physical and design properties of solar panels / antenna (thickness, material composition, …), to preliminarily characterize them from a ballistical point of view and determine:

- the impactor critical diameter causing a penetration (i.e. select suitable Ballistic Limit Equations). Nonetheless, penetration of a solar array or antenna does not necessarily result in loss of functionality and depends significantly on the design of the array / antenna.
- the cratered area due an impact. This parameter allows to tank into account the degradation in performance caused by the accumulation of MMOD damage. Moreover, it allows to estimate the amount of secondary ejecta by MMOD impacts.

Measures to reduce the risk of failure and generation of additional debris from an impact include:

- using thin arrays so that a particle may pass through causing less damage, i.e. they should be thin enough so that the MMOD pass through without creating a hole much larger than the diameter of the particle.
- adding MLI layers to the rear of the panel / antenna structure. MLI layers could also contain portion of the ejected materials.
- incorporating robust wiring architecture with redundant electrical connections.
- protecting the antenna feed and mechanisms with dedicated shielding.
- scrutinize materials used for the large solar panels and antenna surfaces to evaluate the amount of shattered material ejected by the impact of a small MMOD in orbit. Either a modification of the used materials

or the adoption of a finishing surface treatment could be envisaged to reduce the amount of ejecta generated by a primary impact.

6.3 Space Segment

6.3.1 SPS Configuration

The SPS is composed of 4 main elements:

1. Roll-out Module;
2. Truss and Active Truss Modules;
3. Node Module.

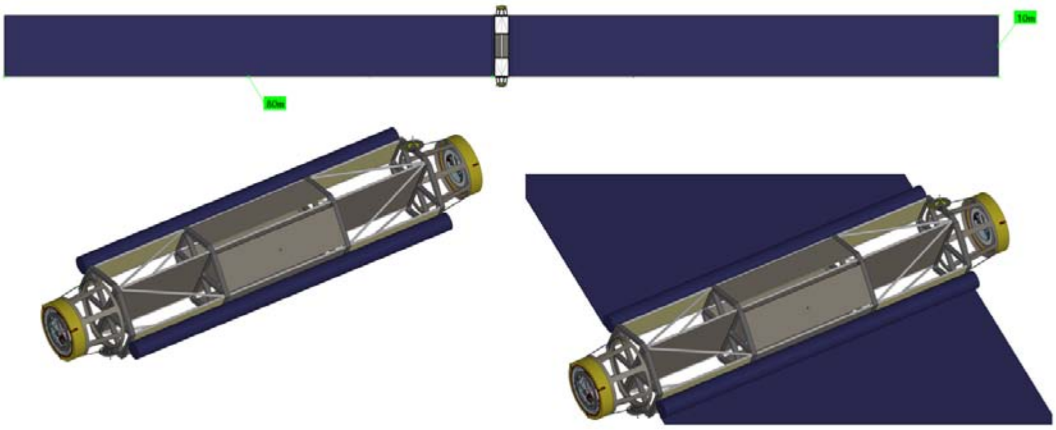

Figure 6-10 Roll-out Module

Figure 6-11 Truss & Active Truss Modules

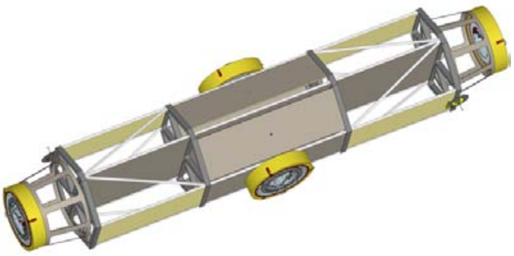

Figure 6-12 Node Module

An SPS overview is provided in Figure 6-13.

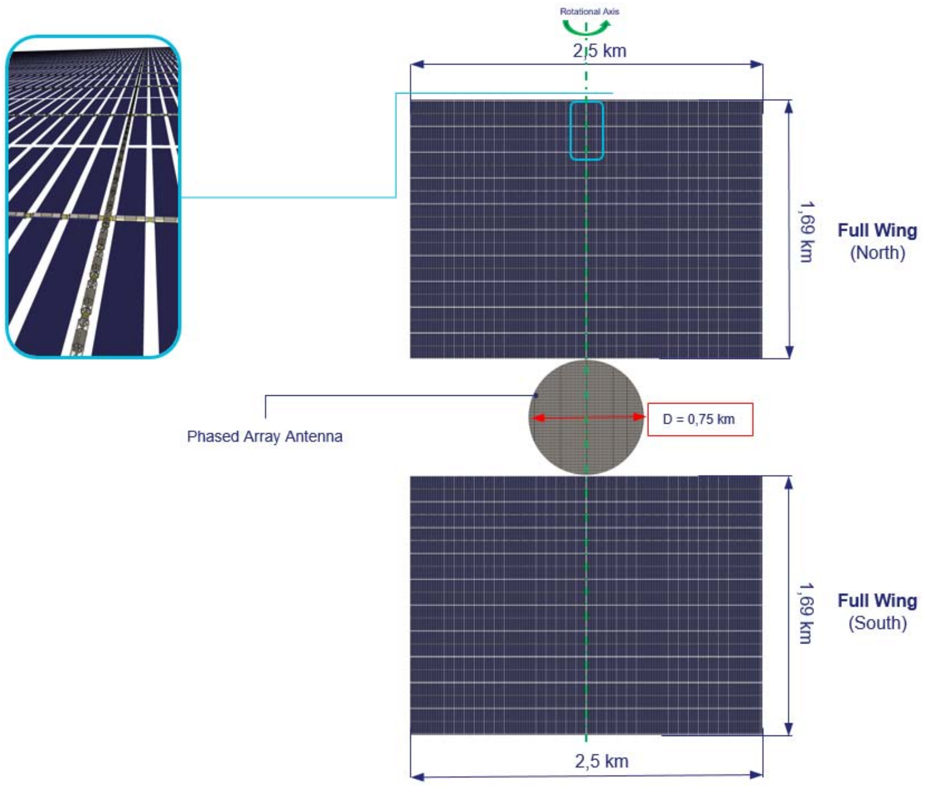

Figure 6-13 SPS overview

Each Full Wing (North & South) is composed of 10 Single Wing of (97+97) Roll-out Module as shown in Figure 6-14.

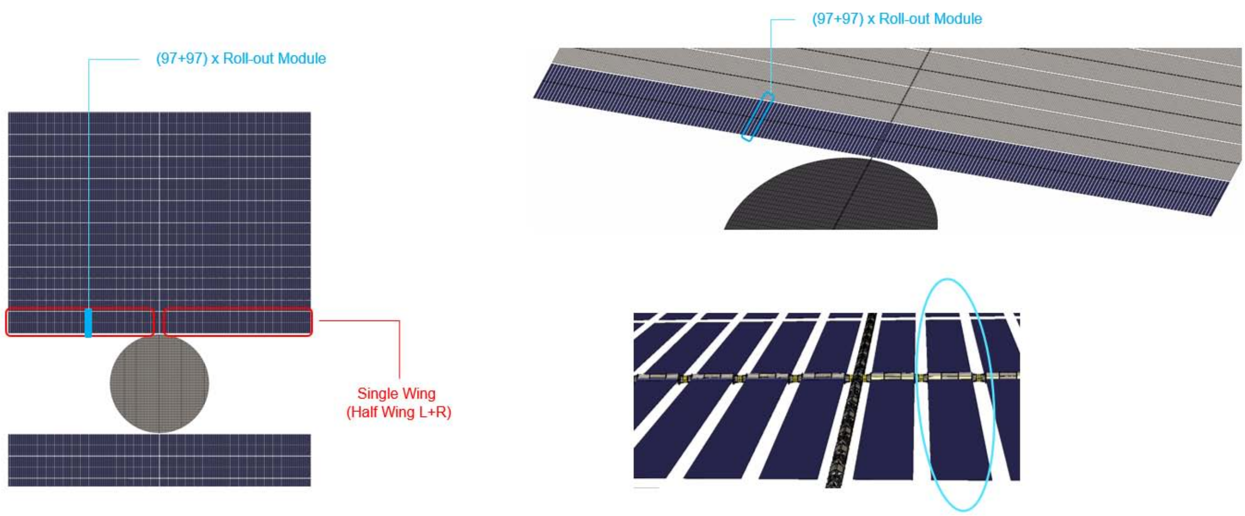

Figure 6-14 Single Wing details

Details of the Central Truss composed, for each Full Wing, of 120 Truss Module + 10 Node Module, are shown in Figure 6-15.

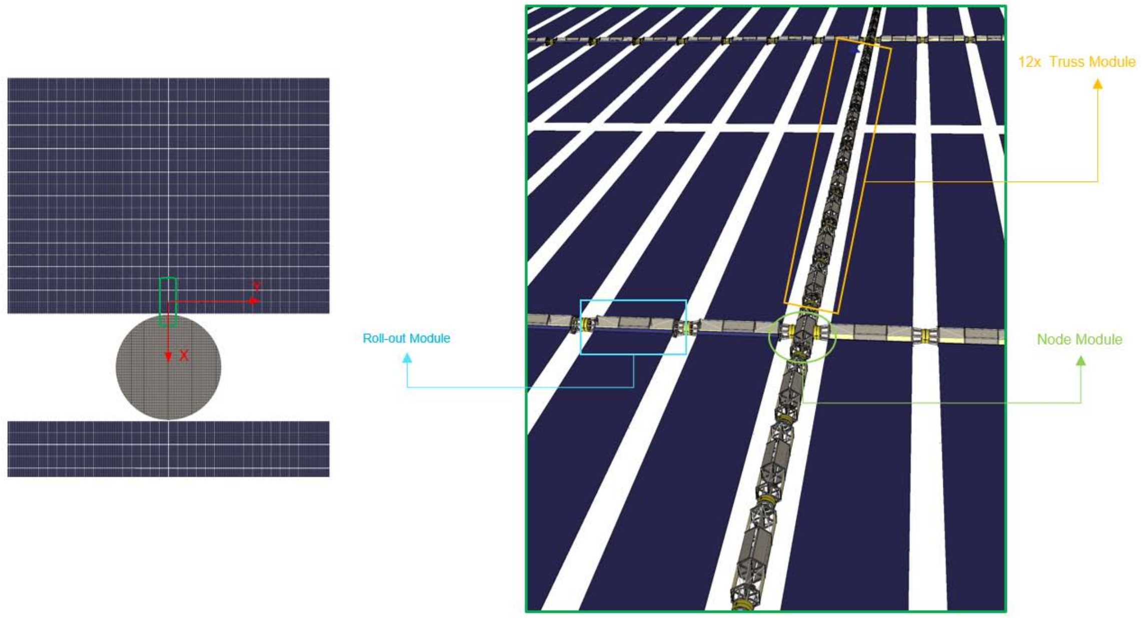

Figure 6-15 Central Truss details

The Phased Array Antenna Structure composed of 59 Active Truss Modules is shown in Figure 6-16.

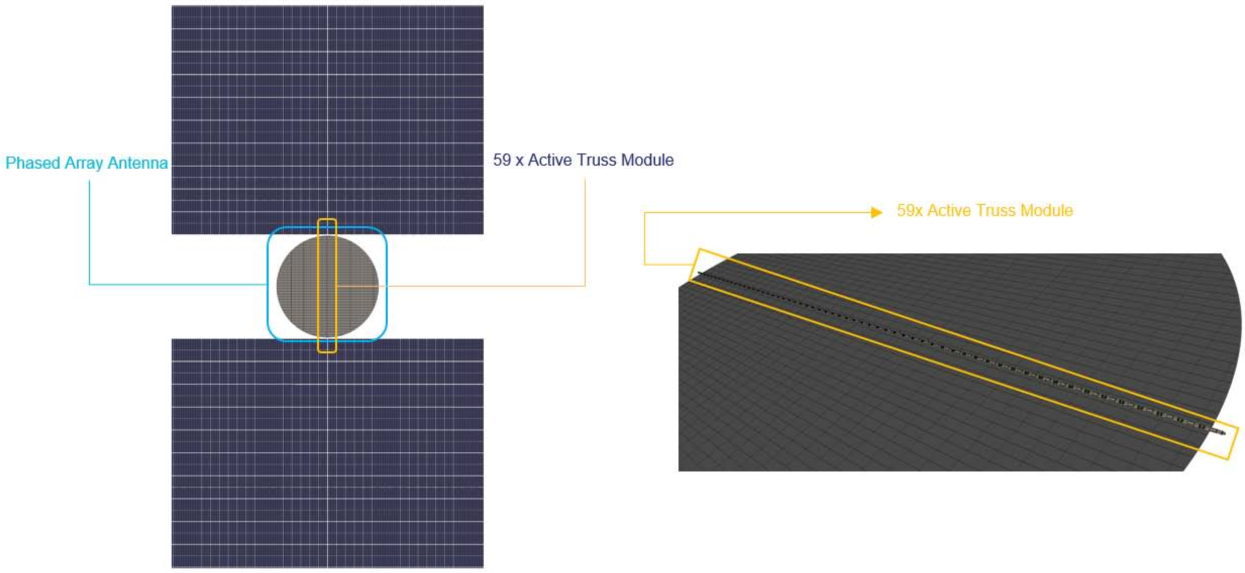

Figure 6-16 Phased Array Antenna Structure

6.3.2 Full Wings & Phased Array Antenna Rotation Strategy

Due to the size of the solar arrays system, the body axes are considered fixed w.r.t. the two solar array full wings. In this reference frame, the antenna rotates along the x-axis to follow the Earth's relative movement.

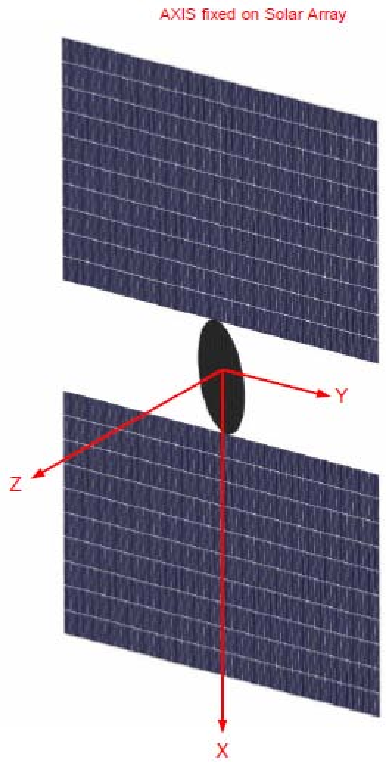

Figure 6-17 Satellite axis reference frame

In terms of attitude, the antenna shall be nadir pointing, while the solar array z-axis shall be parallel to the Sun vector as much as possible. This means that the antenna shall be nadir pointing for the whole duration of the mission, thus the body plane y-z is considered to be on the same plane of the equator. The rotation of the Phased antenna structure (0.75km diameter, 250tons mass) is one of the main technological challenges of this project. Although the speed is very limited (360°/24h, i.e. 15°/h), there is no space heritage for similar bulky solutions. The use of thrusters coupled with a free joint is excluded (for fuel consumption reasons) so only motorized rotary joints can be baselined.

The closest TRL9 mechanism is the Solar Alpha Rotary Joint (SARJ), a single-axis pointing mechanism used to orient the solar power generating arrays relative to the sun for the International Space Station (ISS). The ISS has a backbone or set of trusses that house several ISS systems. These trusses are joined to a set of pressurized modules that house the crewmembers living and working aboard the ISS. The figure below shows the ISS after assembly mission 17A by the Space Shuttle. The pressurized modules are located along the center of the truss structure, extending forward and aft. The power generating solar arrays are located on the port and starboard sides of the truss structure outboard of the SARJs. The location of each Solar Alpha Rotary Joint (SARJ) is indicated in Figure below (outdated w.r.t. current ISS configuration, but applicable w.r.t. the heritage discussion).

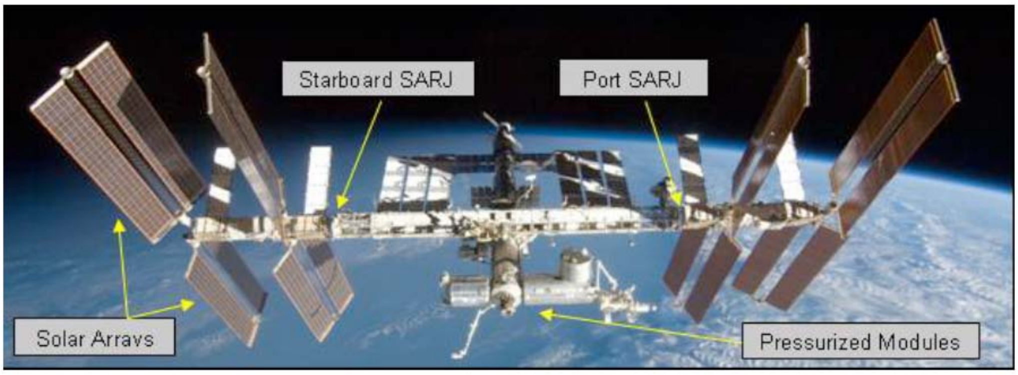

Figure 6-18 ISS after assembly mission 17A

The SARJ completes one full rotation per orbit of the ISS, approximately every 90 minutes. The figure below shows a drawing of the SARJ with the major components labeled. The SARJ is capable of transferring 60 kW of electrical power, spare low power (300 W), and data channels across the rotary joint. The total weight of the SARJ is 1161 kg. Two SARJ mechanisms are installed onboard the ISS - Port (activated December 2006) and Starboard (activated June 2007). The SARJ serves as the structural joint between the ISS inboard and outboard truss elements via twelve Trundle Bearing Assemblies (TBA). The trundle bearings straddle between an inboard and outboard triangular cross-section race rings. The race rings are approximately 3.2 meters in diameter.

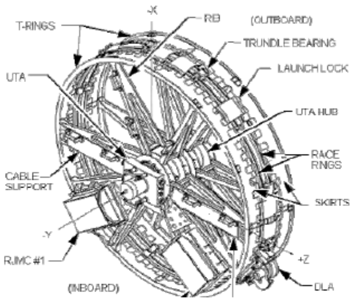

Figure 6-19 SARJ drawing

Considering to readapt such heritage, the concept proposed for the SPS is to equip the Phased Array Antenna truss modules (59x) with a motorized rotary joint, that can be disengaged in case of failure (to avoid single failures on the pointing function). The motorized rotary joint is preliminary specified as follows:

- 500 kg mass
- 100 W power consumption (rotating @ 15°/h)

6.3.3 Structure

The structure is preliminary designed based on individual modules some of them acting as nodes, a more accurate sizing is demanded to the next program phases although a preliminary assessment is performed hereafter based on the needed inertia of the structural framework to provide the minimum stiffness required by the AOCS.

Starting from literature, the significant control–structure interaction problem, which is a major concern for a very large Abacus platform (3.2 km x 3.2 km) where lowest structural mode frequency of 0.002 Hz is mentioned.

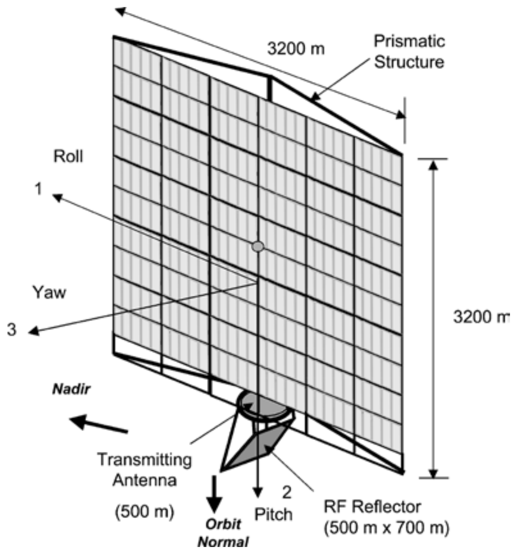

Figure 6-20 Baseline 1.2-GW Abacus satellite configuration

On the other hand the very same ISS, after the first 6 modes which are associated to rigid body motion, the 7th natural frequency mode is the first significant one is in the range of 0.1 Hz and basically relevant to solar arrays:

Table 6.2-1 Mode of Vibration and Natural Frequency of ISS

Modes	Body 1 Frequency (Hz)	Body 2 Frequency (Hz)
1	1.63e-5	2.16e-5
2	9.16e-6	1.80e-5
3	1.95e-6	9.62e-6
4	2.33e-6	1.05e-5
5	9.95e-6	2.06e-5
6	1.53e-5	2.88e-5
7	0.0932	0.115
8	0.0955	0.116
9	0.0965	0.170
10	0.0969	0.172
11	0.0982	0.662
12	0.101	0.662
13	0.102	0.796
14	0.106	0.796
15	0.106	0.931

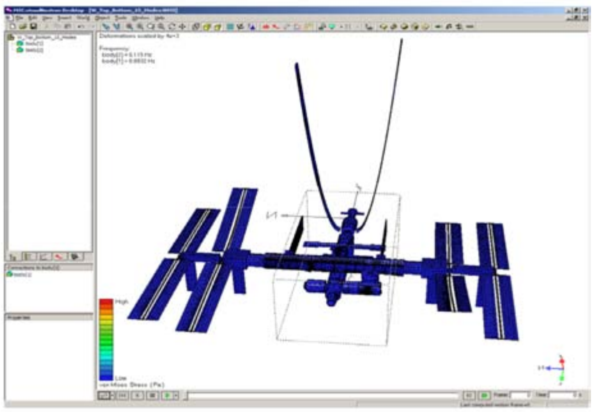

Figure 6.2-17 7th Mode of Vibration of ISS

Figure 6-21 ISS 6 Rigid Body Frequencies & 7th First Mode

A global stiffness requirement in terms of first frequency for the current SPS solution, is established based also on AOCS considerations to **0.005 Hz**.

The SPS components first frequencies leading to the inertia needs for its individual skeleton structure given by the solar array booms, the central and lateral trusses are here evaluated based on the use of formulae from Blevins.

108 FORMULAS FOR NATURAL FREQUENCY AND MODE SHAPE

Table 8-1. Single-Span Beams.

Notation: x = distance along span of beam; m = mass per unit length of beam;
E = modulus of elasticity;
I = area moment of inertia of beam about neutral axis (Table 5-1); L = span of beam;
see Table 3-1 for consistent sets of units

Natural Frequency (hertz): $f_i = \frac{\lambda_i^2}{2\pi L^2}\left(\frac{EI}{m}\right)^{1/2}$; i=1,2,3...

Description[a]	λ_i; i=1,2,3...	Mode Shape, $\tilde{y}_i\left(\frac{x}{L}\right)$	σ_i; i=1,2,3...
1. Free-Free	4.73004074 7.85320462 10.9956078 14.1371655 17.2787597 $(2i+1)\frac{\pi}{2}$; i>5	$\cosh\frac{\lambda_i x}{L}+\cos\frac{\lambda_i x}{L}-\sigma_i\left(\sinh\frac{\lambda_i x}{L}+\sin\frac{\lambda_i x}{L}\right)$	0.982502215 1.000777312 0.999966450 1.000001450 0.999999937 ≈1.0 for i>5 See Ref. 8-2
2. Free-Sliding	2.36502037 5.49780392 8.63937983 11.78097245 14.92256510 $(4i-1)\frac{\pi}{4}$; i>5	$\cosh\frac{\lambda_i x}{L}+\cos\frac{\lambda_i x}{L}-\sigma_i\left(\sinh\frac{\lambda_i x}{L}+\sin\frac{\lambda_i x}{L}\right)$	0.982502207 0.999966450 0.999999933 0.999999993 0.999999993 1.0; i>5
3. Clamped-Free	1.87510407 4.69409113 7.85475744 10.99554073 14.13716839 $(2i-1)\frac{\pi}{2}$; i>5	$\cosh\frac{\lambda_i x}{L}-\cos\frac{\lambda_i x}{L}-\sigma_i\left(\sinh\frac{\lambda_i x}{L}-\sin\frac{\lambda_i x}{L}\right)$	0.734095514 1.018467319 0.999224497 1.000033553 0.999998550 ≈1.0; i>5 See Ref. 8-2
4. Free-Pinned	3.92660231 7.06858275 10.21017612 13.35176878 16.49336143 $(4i+1)\frac{\pi}{4}$; i>5	$\cosh\frac{\lambda_i x}{L}+\cos\frac{\lambda_i x}{L}-\sigma_i\left(\sinh\frac{\lambda_i x}{L}+\sin\frac{\lambda_i x}{L}\right)$	1.000777304 1.000001445 1.000000000 1.000000000 1.000000000 1.0; i>5

Table 6-3 Used Formulae from Blevins

The followed approach for stiffness hand calculation in terms of first natural frequency, is based on 3 STEPS, starting from the individual Solar Array, then to 2 Adjacent Half Wings and finally to the entire SPS (Full Wings & Antenna).

STEP1 - Roll-Out or Extendable Flexible Solar Arrays

The first frequency of the Roll-Out or Extendable Flexible Solar Arrays is preliminary evaluated considering the following dimensions of 80 m x 10 m:

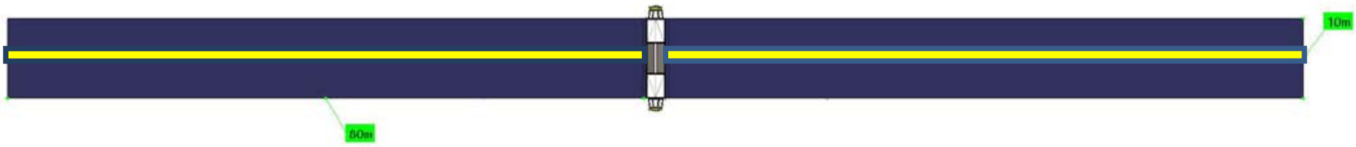

Figure 6-22 Roll-Out or Extendable Flexible Solar Arrays with Central Booms

Due to the 80 m length a coilable boom needs to be thin in order to be “coilable” and limit the drum size, to have a big diameter for sufficient inertia in addition to a high elastic modulus for the required stiffness in terms of first frequency value.

Figure 6-23 Telescoping structure – Credit Northrop Grumman/ASTRO

A rigid central telescopic boom with interior deployment device on the other hand allows more flexibility in terms of use of UHM (Ultra High Modulus) fibers, thickness and size of the section to achieve higher inertia and stiffness properties and is therefore considered more effective: rigid telescopic deployable booms up to 34 m length (see Figure 6-24) have been already manufactured and tested.

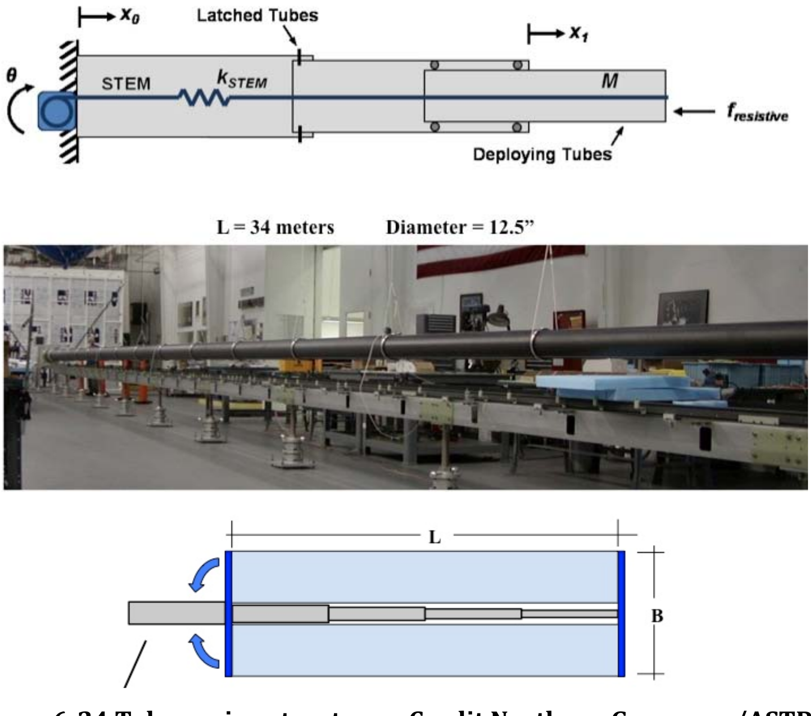

Figure 6-24 Telescoping structure – Credit Northrop Grumman/ASTRO

$$fi = \frac{\lambda i^2}{2 * \pi * L^2} * \sqrt{\frac{E * I}{m}} \quad with\ i = 1,2,3 \ldots.$$

The calculation is performed based on Blevins' formula considering case 3. In Blevins' table considering a clamped-free beam for the first frequency evaluation and assuming in the formula:

- E = 325000 MPa (based on CFRP high elastic modules material e.g. M55J/M18 with a 0 deg lay-up)
- λi = 1.875 (for the first natural frequency in free-clamped condition)
- L = 80 m (span of each Solar Array boom)
- m = 3 kg/m (mass x unit length of the flexible part 0.15 kg/m2 plus the 80 m boom with the inertia and section properties reported in Table 6-4)

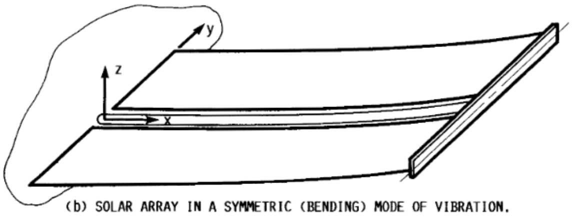

Figure 6-25 First Frequency Flexure Mode Shape (Boom driven)

The iterative calculation, considering a cantilever (clamped-free) solution, leads to the following evaluation having as a preliminary target, a first frequency in the 0.15 Hz range for the single SPS Solar Array which is in any case higher than the one of the current ISS Solar Arrays having considerably lower dimensions.

A frequency of 0.186 Hz is obtained with a CFRP boom of 0.3 m radius and a wall thickness of 0.5 mm.

SOLAR ARRAY - CLAMPED FREE BOOM								
Boom Radius Ext [m]	Boom Radius Int [m]	Boom Inertia [m4]	Boom Section Area [m2]	E [Pa]	rho [kg/m3]	Mass x unit length [kg/m]	Lambda i	fn [Hz]
0.3	0.2995	4.23E-05	9.42E-04	3.25E+11	1600	3.01	1.87	0.186
Thickness [mm]	Mass Boom [kg]	Mass of Flexible Part Solar Array [kg]						
0.5	121	120						

Table 6-4 Solar Array First Frequency

A structural mass of the single Solar Array of 241 kg which considering 388 Solar Arrays for 2 Adjacent Half Wings leads to 93328 kg as reported in the next picture.

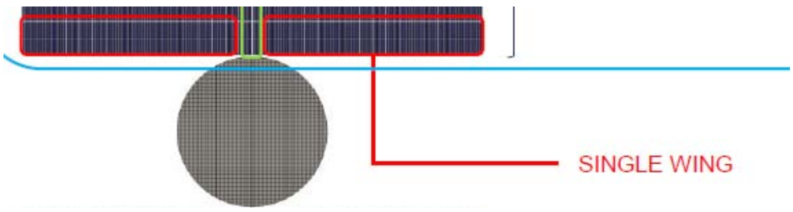

Figure 6-26 2 Adjacent Half Wings

STEP2 - 2 Adjacent Half Wings

The first frequency of 2 Adjacent Half Wings is preliminary evaluated considering the extension of 2500 m and the Roll-out Modules assembly, indicated by the yellow area, as a free-free beam to which its own mass and the masses of the 388 Solar Arrays (flexible parts & booms) are considered in the mass per unit length calculation:

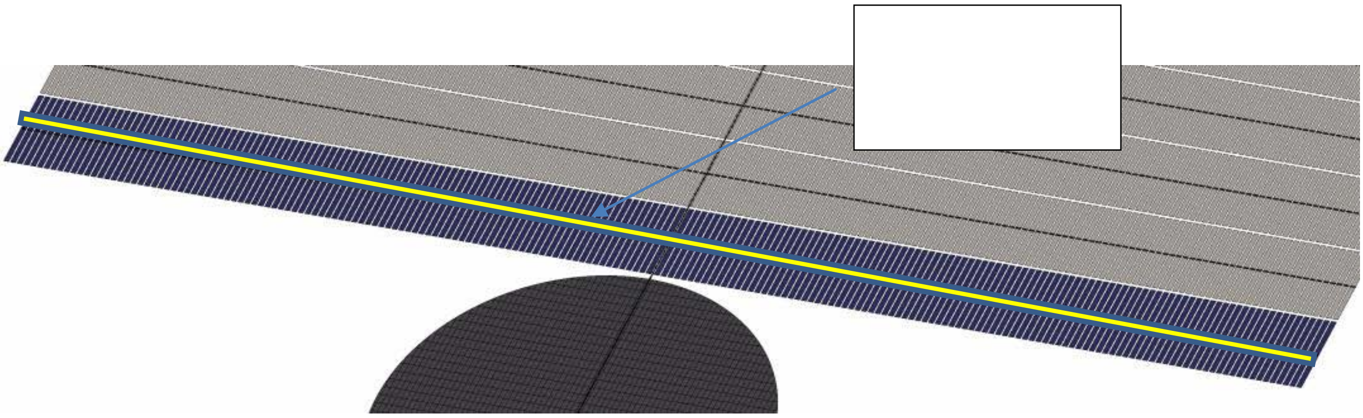

Figure 6-27 2 Adjacent Half Wings with Roll-out Modules

The Roll-out Modules sequence (depicted in yellow) acting as a beam with the 2 Adjacent Half Wings of Solar Arrays as distributed masses, is considered to have a first bending frequency in free-free conditions leading to the following mode shape:

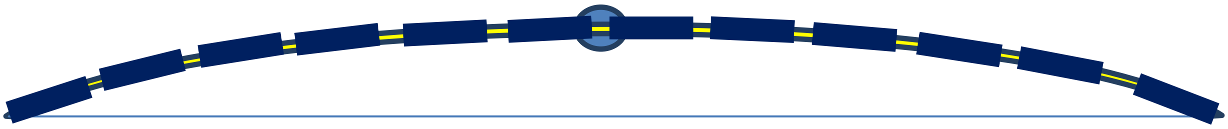

Figure 6-28 2 Adjacent Half Wings with Roll-out Modules Deformed Mode Shape (1 st Frequency)

The calculation is performed based on Blevins' formula considering case 1. and the following values:

- E = 325000 MPa (based on CFRP high elastic modules material e.g. M55J/M18 with a 0 degs unidirectional lay-up)
- λi = 4.73 (for the first natural frequency in free-free condition)
- L = 2500 m (span of the 2 Adjacent Half Wings with Roll-out Modules)
- m = 97.57 kg/m (mass x unit length given by the 388 Solar Arrays with Booms of 2 Adjacent Half Wings (93328 kg) and the mass of the 194 Roll-out Modules over a length of 2500 m (150595 kg) having the inertia and section properties reported in Table 6-5)

The iterative calculation, considering a free-free solution for the 194 Roll-out Modules of 2 Adjacent Half Wings, leads to the following evaluation of a first frequency of 0.007 Hz.

The frequency of 0.007 Hz is obtained with a CFRP equivalent circular module of 1.5 m radius and a wall thickness of 4 mm. This means that, in order to achieve this frequency, the single Roll-out Module shall have inertia properties in line with this equivalent module.

2 ADJACENT WING - FREE FREE ROLL-OUT MODULE SEQUENCE									
Module Radius Ext [m]	Module Radius Int [m]	Module Inertia [m4]	Module Section Area [m2]	E [Pa]	rho [kg/m3]	Mass x unit length [kg/m]	Lambda i	fn [Hz]	L [m]
1.5	1.496	4.22E-02	3.76E-02	3.25E+11	1600	97.57	4.73	0.007	2500
Thickness [mm]	Mass of 2 Adjacent Wings Modules (194) [kg]	Mass of Flexible Solar Arrays per 2 Adjacent Wings [kg]							
4	150595	93328							

Table 6-5 2 Adjacent Half Wings – Roll-out Module Properties & First Frequency

A total structural mass of 243924 kg is so obtained for the 2 Adjacent Half Wings of Figure 6-27.

STEP3 - Entire SPS (2 Full Wings & Antenna)

The first frequency of the entire SPS is preliminary evaluated considering the extension of 4130 m and the Central Truss Modules assembly, indicated by the yellow area, acting as a free-free beam to which its own mass and the masses of the 20 Single Wings with the relevant Truss Modules are considered in the mass per unit length calculation:

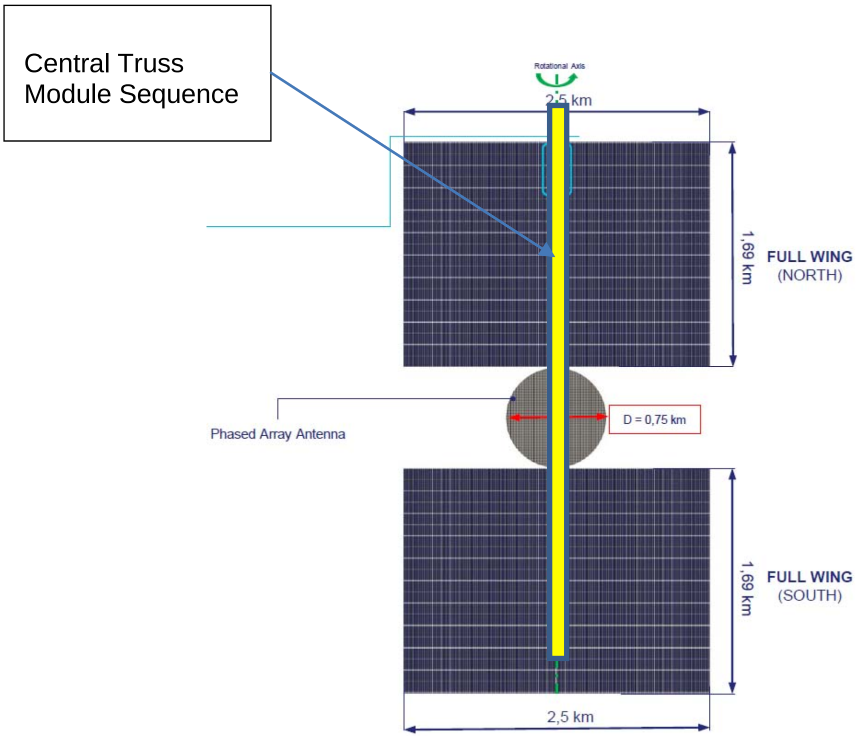

Figure 6-29 Full Wings with Central Truss Modules

The Central Truss Modules sequence (depicted in yellow) of the 2 Full Wings and Antenna is considered to have a free-free first bending frequency leading to the following mode shape:

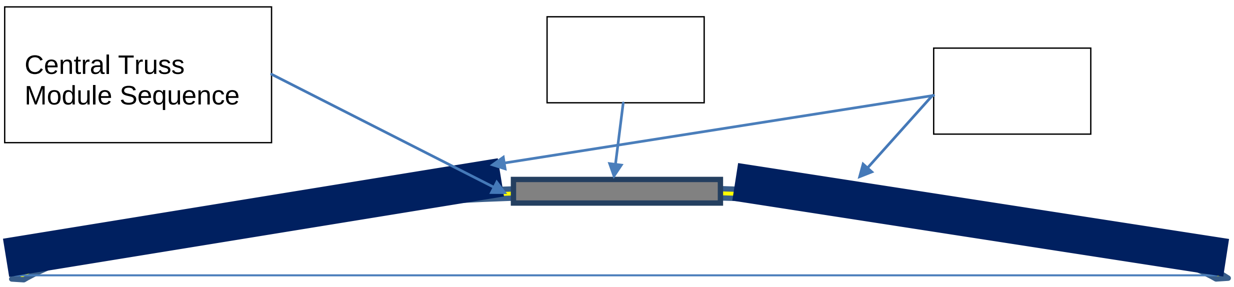

Figure 6-30 Full Wings (North & South) & Antenna with Central Truss Modules Deformed Mode Shape (1 st Frequency)

The calculation is performed based on Blevins' formula considering case 1. and the following values:

- E = 325000 MPa (based on CFRP high elastic modules material e.g. M55J/M18 with a 0 degs unidirectional lay-up)
- λi = 4.73 (for the first natural frequency in free-free condition)
- L = 4130 m (span of the 2 Full Wings with Active Truss Modules)
- m = 1357.27 kg/m (mass x unit length given by the 2 complete Full Wings and Antenna (4879061 kg) and the mass of the Central Truss Modules over a length of 4130 m (726458 kg) having the inertia and section properties reported in Table 6-6)

The iterative calculation, considering a free-free solution for the entire SPS, leads to the following evaluation and by the Central Truss Module assembly of a first frequency of 0.005 Hz.

The frequency of 0.005 Hz is obtained with a CFRP equivalent circular module of 7 m radius and a wall thickness of 2.5 mm. This means that, in order to achieve this final frequency, the single Module of the Central Truss shall have inertia properties in line with this equivalent module.

SBSP - 2 FULL WINGS - FREE FREE									
Module Radius Ext [m]	Module Radius Int [m]	Module Inertia [m4]	Module Section Area [m2]	E [Pa]	rho [kg/m3]	Mass x unit length [kg/m]	Lambda i	fn [Hz]	L [m]
7	6.9975	2.69E+00	1.10E-01	3.25E+11	1600	1357.27	4.73	0.005	4130
Thickness [mm]	Mass of Central Truss [kg]	Mass of Wings [kg]							
2.5	726458	4879061							

Table 6-6 SPS Central Truss Properties & First Frequency

A total basic structural mass of 5605519 kg is so obtained for the SPS structure under the assumptions used for the calculations of Figure 6-29.

6.3.4 AOCS

The analysis of the expected disturbances is used to select the type of actuators to be used and to estimate the required torque and force levels.

Based on this analysis, an architecture for the actuators is proposed.

6.3.4.1 Disturbance Analysis

The disturbance acting on the S/C are estimated based on the following assumptions:

- Rotational axis (x) perpendicular to orbit plane
- Z axis pointed toward the Sun
- Diagonal inertia matrix with the following values:
  - $I_{xx} = 2.78e12$ kgm^2
  - $I_{yy} = 9.19e12$ kgm^2
  - $I_{zz} = 11.96e12$ kgm^2

6.3.4.1.1 Gravity gradient

Under the analysis assumptions, the gravity gradient torque is a periodic torque around the X axis with periodicity twice the orbital period and peak depending on the difference between the inertias I_{yy} and I_{zz}.

The following figure shows the behavior during an orbit of the gravity gradient torque and of the accumulated angular momentum.

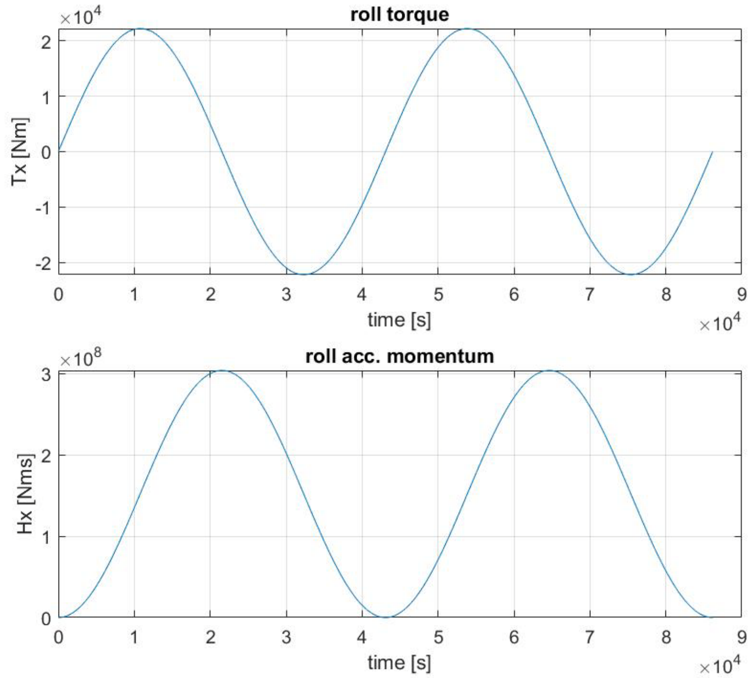

Figure 6-31 Gravity gradient torque and accumulated momentum

The peak torque is approximately 22000 Nm, while the peak accumulated angular momentum is 300e6 Nms.

Regarding the estimation of the torques around Y and Z axis, associated to pointing errors and non-diagonal inertia matrix, we assume here a maximum value of 10% of the torque around X axis.

If this disturbance has to be controlled by means of angular momentum exchange devices, such as control momentum gyros (CMGs), this would require:

- 85 CMGs to produce the peak torque
- 64000 CMGs to store the angular momentum

This estimation is based on the properties of the CMGs used on the ISS, with the following characteristics:

- torque: 258 Nm
- momentum capacity: 4760 Nms
- mass: 272 kg

Since the mass of 64000 CMGs is approximately 17400 tons, this makes clearly unfeasible the options of using this type of devices to control the gravity gradient torque, even considering future and more performing units, with a much larger and more favorable ratio between mass and momentum storage capacity.

6.3.4.1.2 Solar pressure force and torque

The analysis of the force produced by the solar pressure is shown in section 6.1.2.

The maximum solar pressure force is approximately 57 N, parallel to the Z axis.

A preliminary estimation of the solar pressure torque is made considering a shift of 10 m along each axis between the center of mass and the center of pressure, resulting in a torque of approximately 600 Nm around X and Y.

6.3.4.2 Actuator sizing and proposed accommodation

Based on the analysis of the previous paragraphs, the required forces and torques to be produced by the control system are:

- Torque X: 22000 Nm (gravity gradient) + 600 Nm (solar pressure) + 600 Nm (other, added as a margin) = 23200 Nm
- Torque Y: 2200 Nm (gravity gradient) + 600 Nm (solar pressure) + 600 Nm (other, added as a margin) = 3400 Nm
- Torque Z: 2200 Nm (gravity gradient) + 600 Nm (other, added as a margin) = 2800 Nm
- Force X = 20 N (in both directions), for station-keeping maneuvers
- Force Y = 6 N (in both directions), for station-keeping maneuvers
- Force Z = 60 N for solar pressure removal + 6 N in opposite direction
- Force along beaming vector = 7 N for antenna photon pressure removal

The force along X is computed in order to implement the station-keeping maneuvers described in section 6.1.2 (i.e. 90-days continuous firings around the equinoxes for north-south corrections). For the force along Y (east-west corrections) and along Z opposite to solar pressure (other corrections), a value of 10% of the solar pressure is assumed.

It is proposed a simplified and fully decoupled architecture, i.e. the accommodation of the thrusters is selected in order to have a set that produces a pure torque around X, a second set that produces a pure Y torque and so on, for a total of six independent sets.

In order to minimize structural stress, a distributed mounting is preferred.

The thrusters are supposed to be mounted close to the border of the wings, in order to maximize the arm (maximum 1250 m available for X torque, 375+1690 available for Y and Z torque).

The accommodation concept is shown in the following figure.

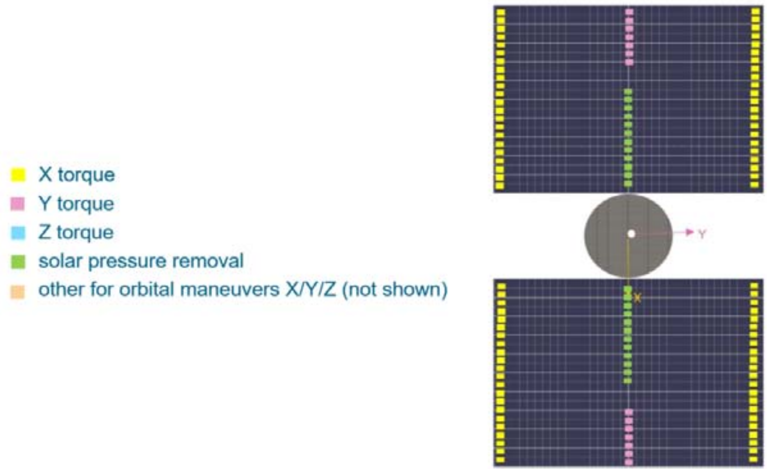

Figure 6-32 RCS accommodation

The number of thrusters depends on the thrust level of the selected thruster.

In order to maximize the possibility of a distributed accommodation, we consider Hall thrusters with a force level of 0.1 N. If the force level increases, the number of actuators will decrease approximately in a proportional way.

- Torque X. Required force = 23200/1250 ≈ 19 N → 190 thrusters for negative torque, 190 thrusters for positive torque. They can be divided in 8 groups, 4 firing along +Z, 4 firing along –Z
- Torque Y. Required force = 3400/(375+1690) ≈ 1.65 N → 17 thrusters for negative torque, 17 thrusters for positive torque
- Torque Z. Required force = 2800/(375+1690) ≈ 1.4 N → 14 thrusters for negative torque, 14 thrusters for positive torque
- Force X: 20 N along +X, 20 N along –X → total of 400 thrusters
- Force Y: 6 N along +Y, 6 N along –Y → total of 120 thrusters
- Force Z: 60 N along +Z, 6 N along –Z → total of 660 thrusters
- Force along beaming vector: 7 N along +beaming vector → total of 70 thrusters

The total number of thrusters is therefore 1692.

6.3.4.3 Yearly propellant consumption

Finally, we propose here an estimation of the amount of propellant needed during one year of operations.

The estimation is based on the following assumptions:

- Total mass: 6600 tons
- Solar pressure 60 N
- Force for disturbance removal: 20 N

The assumption for the force needed for disturbance removal is associated with the peak value of the gravity gradient torque, therefore this estimation can be considered very conservative.

The following figure shows the propellant consumption as a function of the specific impulse of the thrusters. Two components are considered: station-keeping maneuvers and disturbance control (assuming a continuous removal of solar pressure, gravity gradient and other disturbances).

The propellant associated to station-keeping maneuvers assumes a yearly ΔV of 50 m/s and is computed from the Tsiolkovsky rocket equation.

With a specific impulse of 5000 s, considered as baseline, the consumption is approximately 63 tons/year. Considering that the typical Hall thrusters propellant is Xenon, the required amount poses a challenge in terms of scale-up global production, as in 2015 the global production was in the order of 53 tons. Many alternative propellants are available that can overcome the Xenon shortage, but a dedicated study shall be conducted to compare the efficiencies and availability of such materials.

A sensitivity analysis is proposed in Figure 6-33 to show the required propellant amount based on the thruster's specific impulse, which can be a key element to choose alternative propellants or thruster types. The analysis shows how high Isp are extremely valuable to save propellant but even with an Isp of 1000 s a total of 4 launches per year are sufficient to refuel the AOCS subsystem, an amount that does not compromise the mission in terms of overall costs.

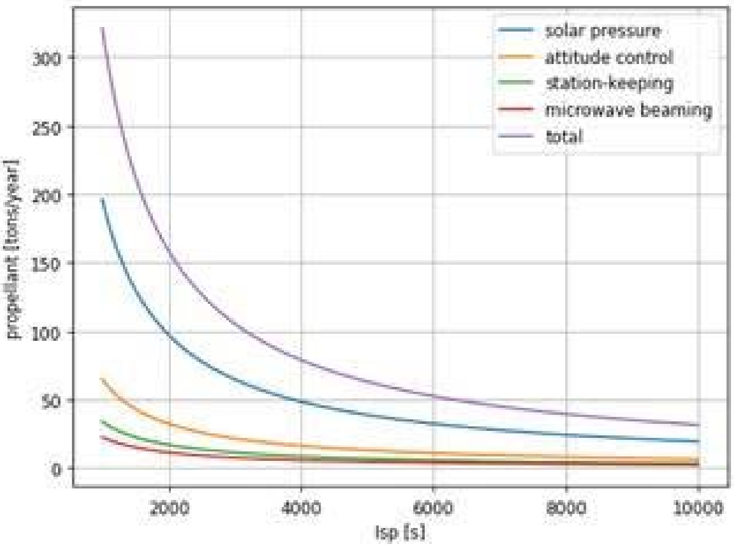

Figure 6-33 Yearly propellant consumption

6.3.4.4 Control concept

One of the major concerns in the design of the AOCS is the potential control–structure interaction, due to the expected low frequency of the structure.

The simplest way of dealing with this concern is to design a controller with sufficiently low bandwidth, such that the interaction with the structure frequencies is avoided by design. As shown in the paragraph that describes the structure, in our case the lowest structural frequency is 0.005 Hz. This value allows the design of a simple control law with a bandwidth in the order of $5 \cdot 10^{-5} \div 10^{-4}$ Hz, that is sufficiently apart from the structural frequency, but is expected to ensure a sufficiently prompt removal of the disturbances.

The AOCS is in charge of pointing the solar panels toward the Sun, while the pointing of the transmitting antenna toward the Earth is performed by the motorized rotary joints as described in the paragraph about the Antenna rotation strategy.

A pointing accuracy requirement of 0.5 deg (angle between Sun direction and Z axis) is assumed. It can be preliminary expected that a simplified control law, such as a classical PID controller, can be sufficient to ensure this level of accuracy. Independent control laws for each axis can be implemented, including a feedforward term to describe the expected disturbances, in particular the gravity gradient torque.

It has been shown that a low-bandwidth attitude control system of this type, with a bandwidth in the order of 1e-5 Hz, is able (for a 3.2 km x 3.2 km planar SPS with a structural frequency of 0.002 Hz and equipped with ion thrusters) to provide a pointing accuracy in the order of 0.1 deg, in the presence of large, but slowly varying, external disturbances and dynamic modeling uncertainties.

Although the proposed control concept should avoid excitation of the structural modes, further investigations regarding the interactions between structure and control, requiring models more sophisticated than those available in this phase of the study, are expected to be needed to ensure the robustness of the AOCS design and to identify possible side effects, such as antenna pointing errors and effects associated to structural deformations (e.g. errors on sensor measurements).

For instance, control forces and torques can be affected, through the control algorithms, by signals induced in the sensor measurements by the structural vibrations. Another significant effect of the structural deformation that can be expected is that on the direction of the forces of the thrusters, with consequent generation of spurious disturbance forces and torques around the other axes, and degradation of the pointing performances. Another minor effect of the deformation could be the generation of solar radiation forces also in directions perpendicular to the nominal Sun direction. It has been shown that the aforementioned effects can have a negative impact on the control performances (with respect to the performances obtained considering the system as a rigid body) leading to the need for a more complex control scheme, e.g. a coordinated orbit–attitude–vibration control.

Another issue associated with structural vibrations is the placement of sensors. While the possibility to select the location of the actuators is limited by the need to mount the thrusters as far as possible from the center of gravity in order to reduce the propellant consumption, there are more degrees of freedom for the placement of the attitude sensors. Using distributed attitude sensors (obtaining the attitude information by average processing of multiple sensors) is a way to minimize the influence of the structural flexibility on the attitude motion. It has been shown that it is possible to find optimal locations that reduce the control–structure interaction, employing at the same time a reduced number of sensors (the advantage of using more than 20 sensors for a 3.2 km x 3.2 km plane SPS is minimal).

It must also be pointed out that the control is based on a prolonged and nearly continuous usage of electric propulsion. For instance, the thrusters used for removal of the sun pressure are assumed to be continuously active throughout the operating life of system. This represents a technological challenge for the actuation system, since a sufficiently long lifetime of the thrusters must be ensured.

Another point associated with the thrusters is the improvement of the specific impulse, since this has a direct impact on propellant consumption and refueling needs.

6.3.5 EPS

The Electrical Power Subsystem (EPS) is one of the most critical subsystems in the challenge of collecting and transmitting a huge amount of power from space to Earth, intended as the Space-based solar power system (SBSP) mission goal. The power demand and mission requirements are important driving factors in selecting the most suitable power electronics as well as the ultra-high voltage wires to be installed.

The EPS includes the Solar Array as primary energy source during sunlight, whereas the use of re-chargeable batteries is restricted for eclipse periods, when no power generation from the SA is available. Furthermore, for the regulation, control, and distribution of power, the EPS architecture is equipped with a set of power management, distribution and switching units.

The EPS high level block diagram is reported below (for simplicity only few Single Wings are represent-ed, as the others are identical). It is a purely functional and highly simplified architecture giving a rough overview of typical EPS technical contents.

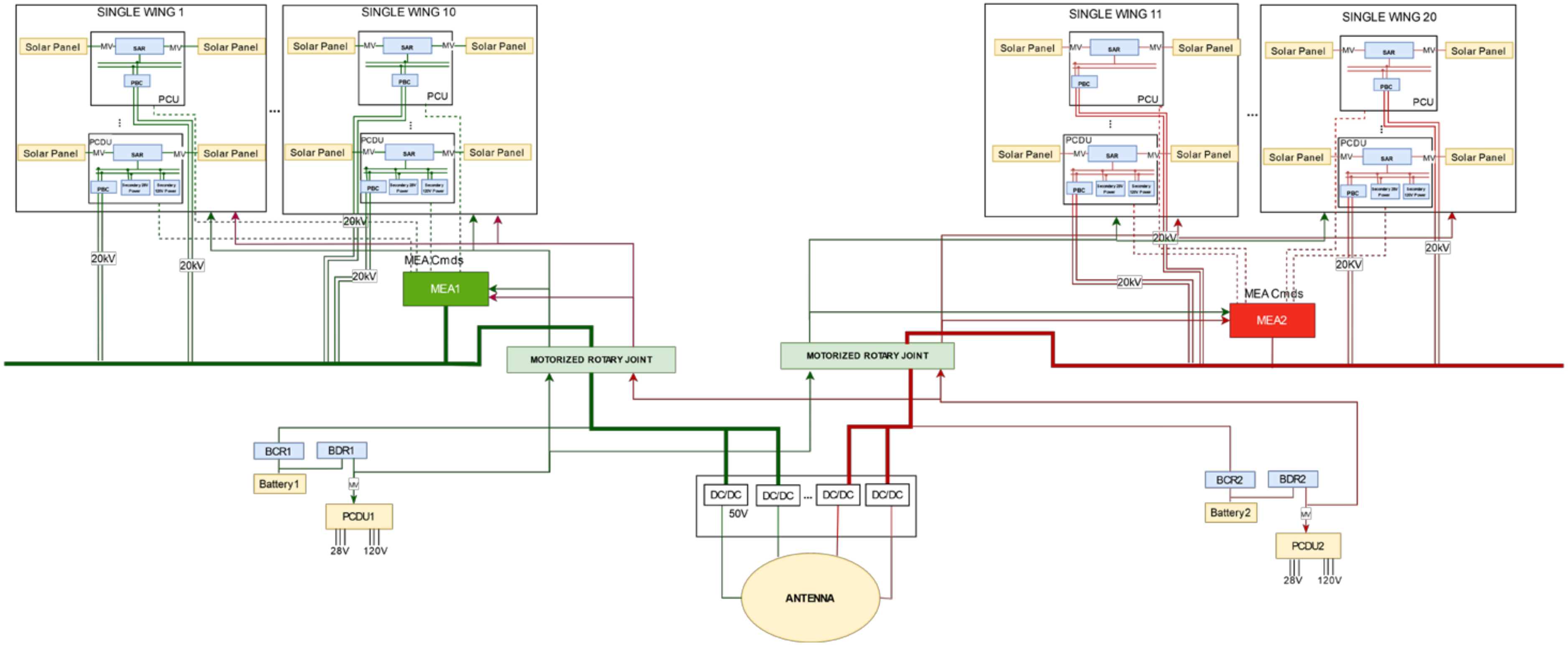

Figure 6-34 EPS block scheme

The SPS EPS shall be able to handle a maximum power capability of 2GW, used for:

- Transferring power to the antenna, for EM power beam transmission toward the Ground Power Station on Earth;
- Satisfying the SPS internal power consumption needs over the sunlight;
- Batteries recharging, needed to supply power for service devices during eclipse periods. At this moment, among the highest capacity qualified cells commercially available there are the 18650MJ1 ABSL cells (252 Wh/kg) which represent a promising candidate for optimizing the power-to-mass ratio and so maximizing the cost and mass saving. No electric thrusters are supposed to be active in eclipse, and thermal control is supposed passive, thus, only the power consumption related to control electronics and TT&C units is intended to be satisfied by batteries. By assuming a power demand of about 500W in eclipse, the battery mass should be negligible (in the order of tens of kg).

The proposed EPS architecture is focused on two independent power domain (green and red in Figure 6-34). In nominal operating scenario (no failure) the total system power is intended to be equally distributed between each power domain. Each domain is managed independently in order to face with a possible double failure scenario that would lead to lose an entire power domain.

The huge amount of power involved and the considerable distances make necessary working at voltage ranges (around 20kV) greater than those commonly used in space. Thus, the power coming from Solar panels is transmitted along the structure by means of ultra-high voltage cables, to decrease electric current, reducing the huge power transmission losses that otherwise there would be to cover the long distances involved. The driving factor for the voltage range assumption is due to the still acceptable power transmission efficiency, i.e about 0.98, computing by considering the worst case of the longest distance from the antenna.

High power electric cables represent a big challenge in space; at this moment there are no space grade high-power technology satisfying the needed voltage requirement, thus, cables used in both military and industrial high voltage applications are considered.

From the datasheets, a good compromise for mass saving and power losses reduction would be the 20kV cables AWG 16, each carrying 6.5A and 130kW. A less voltage value, instead, would lead to a considerable increase of the number of cables for the same section (and thus, at the same current capability), and, consequently, of the mass of the entire system.

The power regulation from the SA is intended at each roll-out module level, by means of a single PCU (Power Conditioning Unit) responsible of controlling the electrical power available from the Solar Array, at medium voltage range (about 400/500 V), via Sequential Switching Shunt regulators (S3R) which regulate the power from the roll-out module to the n buses connected together in the Main bus at central truss level. In some cases, PCDUs (Power Conditioning & Distribution Unit) are necessary for conditioning the SA power to the different voltage levels (120V and 28V) according to the platform equipment.

The power regulation at roll-out module level is assumed to be managed by a Main Error Amplifier (MEA) function based on two different domains, i.e Shunt domain and “Eclipse” one. In the first one, from each roll-out module it is extrapolated as long as sufficient power for power load request (from 0% to 100% of the maximum power capability), in the other no power generation is available.

To increase the voltage range from SA 400-500V up to 20kV, dedicated high power conversion electronics (“PBC” - Primary Bus Converter in the EPS schematic) are necessary so that the power transmission efficiency would increase as well. At this moment, among the best performant space qualified units, it has been developed power electronics for 1,85 kV and able to deliver up to 5kW with a mass of about 47kg. In the overall system about 368 tons are assumed for power conversion electronics.

However, new advanced materials and innovative components are expected to be developed for the high-power electric system in space, abling to satisfy the power and voltage requirements.

Dedicated Battery Control Electronics are also necessary for managing the battery charge and discharge (BCR/BDR) in accordance to the required methodology by regulating the Main Bus power to the battery. In this case the BCE regulates the battery charging through the BCR based on the following three-domain regulation scheme, while the BDR is a simple converter and always provide the required power to the system electronics (computer, RF, etc.):

- *Sunlit domain*: when the power available on the Main bus exceeds the power load consumption and the battery charge demand (the battery will be charged based on constant current/constant voltage (CC/CV) profile)
- *BDR domain*: when the power on the Main bus is not sufficient to satisfy the power requested by the load and for battery charging (the battery will be charged at variable current, smaller than the previous case)
- *Battery domain*: when the power available on the Main bus is not sufficient to satisfy the load demand, the batteries shall provide automatically the missing solar array power

Furthermore, a second stage of power conversion is at truss module level, before being transmitted to the antenna for the microwave generation.

6.3.6 Phased Array Antenna

We propose in this chapter to define the antenna of the WPT with a technical solution based on coherent phase array. It is a large planar phase array of hundreds of meters in diameter (750m in our case). It is made up of rigid sub-panels of few meters in side. Each sub-panel is made up of hundreds of bricks of few centimetres in side. Each brick includes few radiating elements (RE).

The sub-panels shall be rigid and preferably launched in one piece. Each sub-panel contains a local power distribution network to feed the EPC of the RF power generators. It will also be able to transmit electric current to its neighbours. For reasons of symmetry, it has roughly a square shape. It is equipped with assembly locks and hinges and electrical connectors to allow assembly in orbit.

The radiating element (RE) is the basic element of the antenna; it ensures the emission of RF power. In planar array it is slim and is sometimes called patch. Several RE constitute the aerial of a brick. The brick is equipped with a RF power generator, a phase and amplitude control device (for electronically steering) and supporting and ancillary electronics.

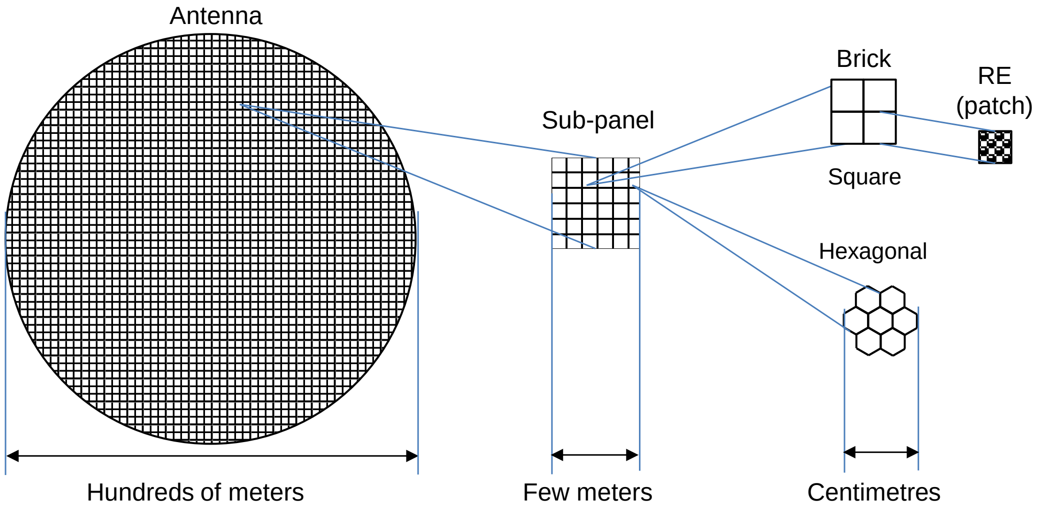

Figure 6-35 WPT antenna mechanical architecture

6.3.6.1 Radiating element (RE) definition

The RE are arranged in a lattice whose shape and spacing are constrained by the rejection requirement of the grating lobes and the scanning loss. There are typically two lattice patterns: the square lattice where the RE are equally spaced in the two directions and the equilateral triangle lattice (hexagonal). Equilateral triangle based lattice requires hexagonal RE. Hexagonal lattice requires less radiating elements than the square lattice for the same area.

There is a third configuration: an isosceles triangle based lattice, close to the hexagonal one, which is composed by rows of square radiating elements with half a step shift from one row to the next. We will consider the two first configurations: square and hexagonal.

The spacing is constrained by two conditions: to minimize the scanning loss and to control the grating lobes, so that they are out of the earth. The following figure is used to assess the RE spacing.

θ_{earth} is the angle at which the earth is seen from GEO: $\sin(\theta_{earth}) = R_{earth}/R_{GEO}$, R_{earth} is the earth radius (6378km), R_{GEO} is the radius of the GEO (42164km).

θ_{beam} is the half beamwidth of the power beam (1.22λ/Dtx), Dtx is the antenna diameter.

θ_{scan} is the scanning range. This corresponds here to the uncertainty of the mechanical pointing of the antenna

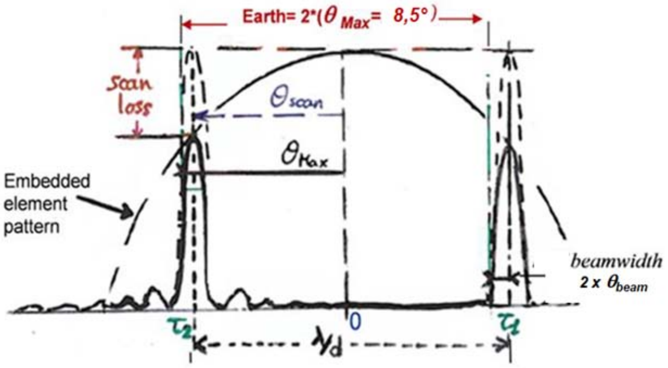

Figure 6-36 Grating lobe configuration

The condition to have grating lobes without a significant radiating power on earth is:

$d/\lambda < 1/(\tau 1 + \tau 2)$, where d is the RE spacing, $\tau 1 = \sin(\theta_{earth} + \theta_{beam})$ and $\tau 2 = \sin(\theta_{scan})$.

The RE gain is given by $G = 10.\log(\eta.4\pi.S / \lambda^2)$, η is the aperture efficiency (0.9) and S is the radiating surface.

The scanning loss at the edge of the scanning range is given by:

$$L = 3/\left(\frac{2}{\sqrt{3}} \times \frac{50.8}{\theta_{scan}.d}\right)^2$$

In the frame of Solaris WPT antenna, θ_{scan} corresponds to the uncertainty of the mechanical pointing of the antenna. This uncertainty should be in the order of 1 to 2 deg. accordingly the scanning loss it is completely negligible.

6.3.6.2 Brick definition

A brick is the assembly of several RE. The arrangement of the RE must respect the lattice pattern (rectangular, triangular) and the maximum spacing ($d/\lambda < 1/(\tau 1 + \tau 2)$). Note also that RE with a side exceeding 3λ is very difficult to design with a good aperture efficiency.

The brick includes the aerial (patches), a polarizer (we assume circular polarization), a distribution network which feeds the patches, a RF generator and a phase setting device.

We give two examples of brick designs.

Square lattice

In the square lattice with a 6λ spacing, the brick could have a square surface of 6λ on each side.

Achieving a flat radiating surface of 6λ on a side with good aperture efficiency requires using smaller patch, for example: a sub-array of 4 patches of 3λ side.

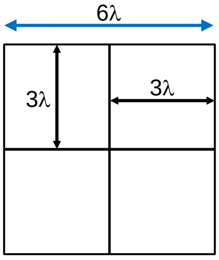

Sub-array 2x2

Example : sub-array made of horns

Hexagonal lattice

In the hexagonal lattice, the brick has a hexagonal area included in a rectangle.

To achieve a flat radiating surface of 6λ on a side with good aperture efficiency, it is necessary to use a sub-array of smaller radiating elements: here a sub-array of 7 patches.

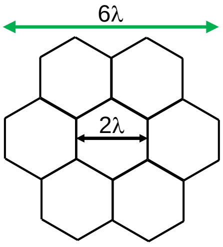

Sub-array 7

Example

6.3.6.3 Sub-panels definition

The sub-panel is a rigid infrastructure which houses the bricks. In the two cases of lattice, the sub-panel is roughly a square. The side of the panel will measure a few meters so that it can be launched in one piece and fit into the launcher fairing.

Radiofrequency wise, the sub-panel is a complete and autonomous phased array that is able to emit a continuous wave (CW) in a given direction. It includes a set of bricks, one or several synchronised frequency generators associated with a distribution network, possibly a beam forming network and control electronics. It includes also an electrical power distribution network to feed the RF generator within the brick.

There are at least two possible RF architectures:

- a centralized architecture where all the phase control devices (phase shifters) are centralized in a beam forming network fed by a frequency oscillator and providing CW to each brick. The beam forming network is controlled by electronics responsible for defining the required phases of all phase shifters to form and point the beam. Each brick shall include in its back: a RF power generator with its EPC and an input for the external oscillator.
- a distributed architecture where each brick has its own phase and amplitude control device. The brick has a local oscillator or it receives a CW from a centralizer oscillator. The required phase of its phase shifter is provided the control electronics at sub-panel level. Each brick shall include in its back: a RF power generator with its EPC, a phase shifter with its controller and a local oscillator or an input for an external oscillator.

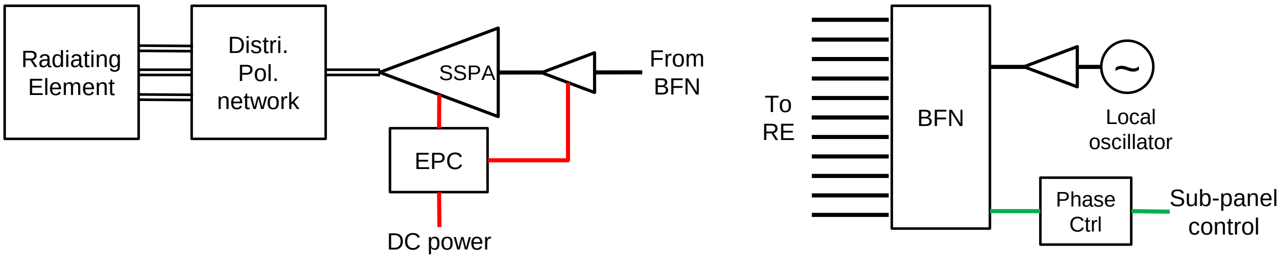

Brick definition (centralized configuration) **Centralized BFN**

Figure 6-37 Centralized architecture

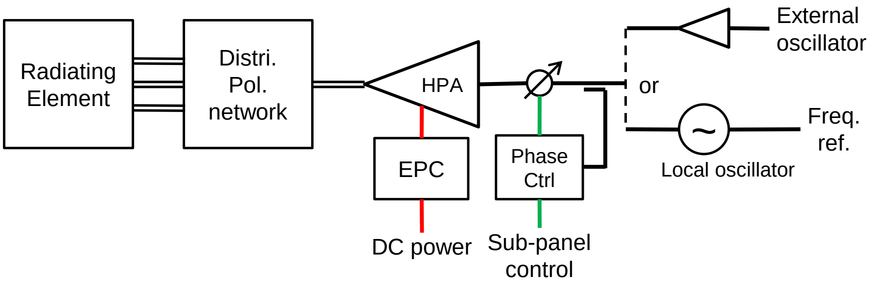

Figure 6-38 Brick definition (distributed configuration)

6.3.6.4 Consideration on brick failure

The antenna includes several hundreds of thousands of bricks. Each brick participates in the creation of the illumination law and it contributes to the transmission of RF power in proportion to the nominal power of its RF power generator (HPA).

Let's consider the most probable failure, the stopping of power transmission by a brick. In the event of a brick failure of this type, there are two impacts:

- a first impact is at the illumination law. The surface of the broken brick no longer participates in illumination and it becomes an obscured or non-radiating surface of the antenna. The aperture efficiency (η_{aper}) is therefore reduced accordingly (ratio between the surface of the brick and the radiating area of the antenna);
- a second impact is at the amount of power that is no more transmitted by the broken brick. Thus the power of the RF generator is no longer transmitted and it reduces the total power transmitted by the antenna in the corresponding ratio.

We therefore see that the breakdown of a brick has a double penalty. For example, a failure rate of 2% of the bricks reduces the overall efficiency of the WTP by 0.96 (0.98x0.98).

Note that it seems inappropriate (too costly) to add redundancies to reduce the failure rate.

6.3.6.5 Consideration on beam pointing

The pointing of the power beam is a very challenging topic.

To point the beam towards the GPS, it is a matter of defining and programming the phase shifts between the hundreds of thousands of radiating elements with a precision better than ten's degrees.

The definition and programming of the phase and amplitude shifts in the RF transmitters of the radiating elements must be done in real time to follow the evolution of the geometry of the system. Indeed, the geometry of the system constantly evolves following deformations of the antenna, dynamic inaccuracies in the mechanical pointing of the antenna, movements in the orbit, etc.

The calculation of each phase shift of each radiating element (or brick) can be done in open loop or closed loop.

In open loop it is necessary to locate very precisely the phase centre of each radiating element (in absolute or in relative to a local phase reference to the antenna), to precisely locate the centre of the Ground Power Station (GPS), then to carry out the calculations of the phase shifts and program the transmitters accordingly.

In a closed loop, it is possible to use the technique of retrodirectivity. A retrodirective antenna transmits the signal in the opposite direction to that of reception of a beacon signal emitted from the centre of the target, here the centre of the GPS. For this, each radiating element measures the received phase ($e^{j\varphi}$) of the beacon, calculates the conjugate ($e^{-j\varphi}$) of this phase and programs the transmitter with this phase. This is called conjugate matching beam-forming. Retrodirectivity can be achieved entirely passively with the use of a Van Atta array.

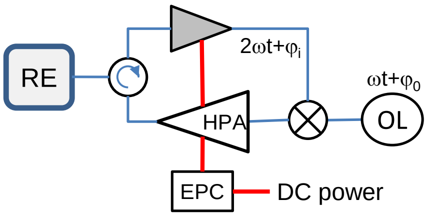

Figure 6-39 Retrodirective radiating element

An active retrodirectional configuration requires a beacon at twice the frequency of the transmitters and the distribution of a local oscillator at the transmission frequency (see on the left). The difficulty is to isolate the receiver from the high power of the transmitter and the distribution of the local oscillator to hundreds of thousands of radiating element with the same phase (as a phase reference).

The precision of calculation and material realization of phase shifts and also the precision of the power level setting of the transmitter have an impact on:

- beam pointing accuracy: This point can be critical if the beam does not point very precisely to the centre of the GPS. We are looking here for pointing accuracy of the order of a hundred meters on ground (1.6E-4 deg.).
- beam shape: When the actual illumination law deviates from the ideal uniform illumination law of the aperture, the shape of the main beam flattens and the level of the secondary lobes increases (loss of power).

Beam pointing accuracy: The RMS Beam Pointing Error due to the RMS phase error of the phase shifters is very negligible in case of very substantial number of phased shifters are involved for electronic beam steering. This is intuitively explained by the fact that the contribution of the error of each phase shifter to the total error is divided by the number of phase shifters, which in our case is hundreds of thousands.

Beam pattern: The impact of inaccuracies in the phase and amplitude (power level) setting of the radiating elements of a phase array antenna could be very important on the radiating pattern. In the telecommunication and radar antennas, the degradation of the gain (the ability to focus energy in the main lobe) due to amplitude and phase uncertainties can reach 5% to 15% loss. Without adequate simulation means, it is difficult to estimate the losses for phase arrays with hundreds of thousands of radiating elements.

6.3.6.6 Consideration on power handling

Two options are possible in the design of the very large antenna of GEO WPT.

- The first consists of having the bricks with the largest possible surface to minimize their number and therefore the number of amplifiers, phase shifters, local oscillator distribution subscribers, etc... But this leads to extreme power levels for amplifiers.

- The second consists of having the smallest brick to minimize the amplifier power level. Of course this leads to maximizing the number of amplifiers, phase shifters, local oscillator distribution subscribers, etc...

Let's take our example: a WPT antenna of 750 m in diameter, an RF power to transmit of 1.63 GW and operating at 5.8GHz (see next table).

Spacing	Brick type	Number	HPA power (W)
3,2 λ	Square 1RE	16 035 958	100
9,6 λ	Square 3x3RE	1 781 773	915
16 λ	Hexagonal 19RE	806 820	2020

Table 6-7 HPA power vs. number of bricks

6.3.6.7 Beacon link budget for retrodirective pointing

The next table gives the link budget of the beacon to be received by each brick to be able to perform conjugate matching beam forming (retrodirective).

The received power of the beacon depends on the brick size and RE spacing & lattice. The example is given with the hexagonal mesh with 7RE brick and 3.2λ spacing.

Frequency	11,60	GHz	
GPS antenna diameter	32	m	
GPS antenna gain	69,6	dB	
Half power Beamwidth	0,11	deg.	GEO arc of 70 km
GPS transmit power	2000	W	
GPS EIRP	100,1	dBW	
Distance	37323	km	
Free Space Loss	-205,2	dB	
Atmospheric loss	-0,54	dB	Europe average at 98% availability
Brick type	Hexa 7RE		
RE spacing	3,2	λ/d	
Brick Gain	28,5	dB	
Received power (brick ouput)	-47,1	dBm	0,03 mV
Reception gain	30,0	dB	
Achieved input level	-17,14	dBm	0,98 mV

Table 6-8 Beacon link budget

The GPS requires an antenna of 32 meter in diameter and a power amplifier of 25 kW. The operating frequency is twice the frequency of the WPT.

6.3.6.8 Phased Array Antenna Definition

Let's take our case of a WPT operating at 5.8 GHz, which WPT antenna has a diameter of 750 meters and emitting 1.6GW.

6.3.6.9 RE design

First let find the RE spacing. In our case:

- θ_{beam} is 4.8 millidegres (84 µrad)

- θ_{scan} is 2 deg. which corresponds to an mechanical pointing uncertainty of +/- 1 deg.

The resulting maximum spacing is ~5.4λ and so ~28cm (wavelength at 5.8GHz is 5.2cm).

In order to have a good aperture efficient for the RE, we will limit the RE spacing to less than 3.2λ. Larger spacing will lead to lower aperture efficiency.

WPT antenna diameter (Dtx)	750	m	5,8 GHz
Half Beam Width	0,0046	deg.	1,22 λ / Dtx
Scanning range	2	deg.	mechanical pointing inaccuracy
Required RE spacing	5,4	λ/d	

Table 6-9 Antenna characteristics

For a 750 m diameter the total number of RE can reach tens of millions of RE depending on spacing (see next figure).

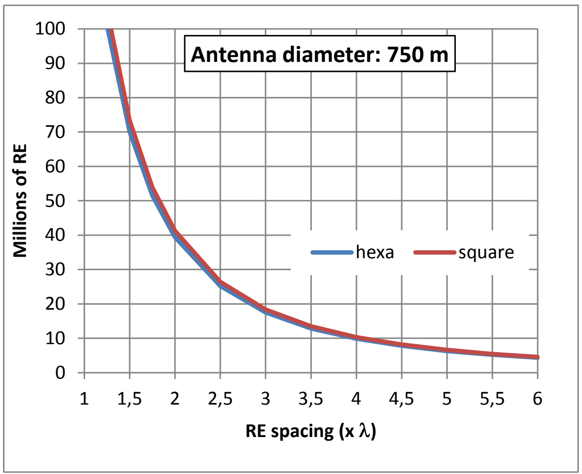

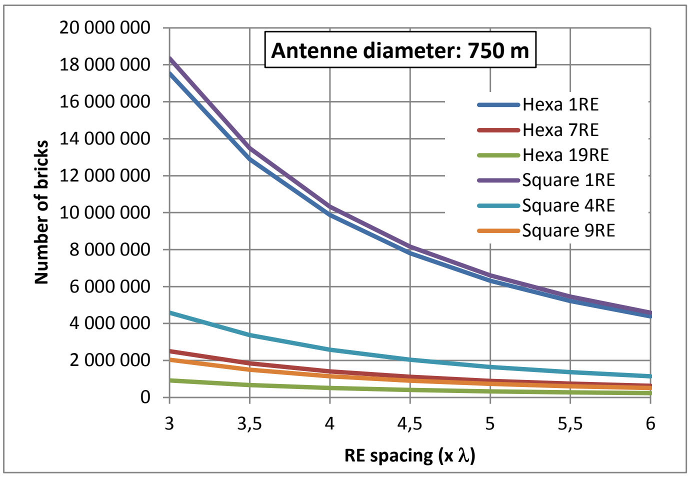

Figure 6-10 Number of RE and brick vs. spacing

6.3.6.10 Brick design

We consider six types of lattice, three square lattices and three hexagonal or triangular lattices (see next figure).

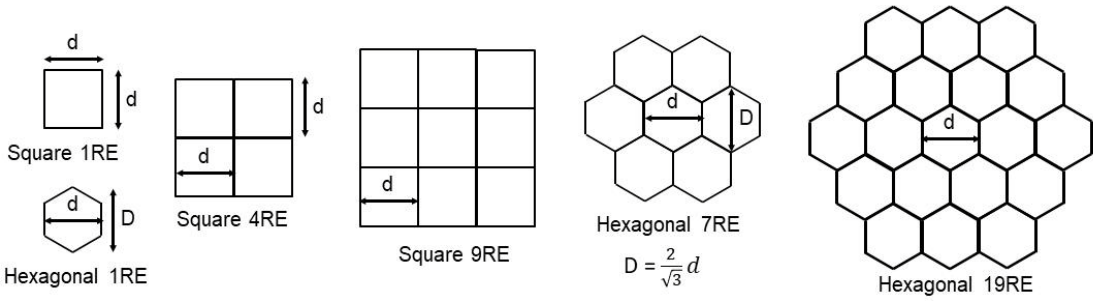

Figure 6-40 Brick designs

We have selected two RE spacings, 3.2λ which corresponds to a RE whose main beam covers the earth (~16 deg) and 5.4λ which corresponds to the largest spacing without grating lobes on the earth. We consider two lattices: a square lattice with 4 RE and a triangular lattice with 7 RE.

We choose a sub-panel side of about 8 meters which could allow a launch in one piece which will avoid deployment in orbit before assembly.

Spacing	3,2λ		5,4λ	
Lattice	Squa 4RE	Hexa 7RE	Squa 4RE	Hexa 7RE
Number of RE	16 121 245	15 411 067	5 660 364	5 414 977
Number of brick	4 030 311	2 201 581	1 415 091	773 568
Sub-panel size (m x m)	8,3 x 8,3	8,5 x 8,1	8,4 x 8,4	8,4 x 8,1
Number of sub-panel	6415	7578	6309	7759

Table 6-11 Example of antenna design (RE, brick, panel)

Consequently, in our case of an antenna of 750 meter in diameter, the total number of RE ranges from 16 million for 3.2 spacing to 5 and a half millions for the 5.2 spacing.

With a choice of sub-panel side about 8 meter (what would be compatible with a one-piece launch), the number of sub-panel to launch, assemble and wire is around 7000.

In the case of the SBSP Pre-Phase A, we recommend taking the conservative solution which maximizes aperture efficiency and eases thermal management: a spacing of 3.2λ and bricks of 4 X 4 RE (see orange column in above table).

6.3.7 TCS

6.3.7.1 Introduction of thermal design

In the context of this Pre-Phase A study of Space Based Solar Power, the thermal aspects are critical to understand if the material and equipment can withstand the harsh scenario and be operative during the mission. The SBSP project is particularly challenging from the thermal point of view, due both to the huge dimension of elements which constitute it, and hence the heat power received, and also to the modularity of the system. These constraints practically prevent the implementation of typical active thermal control solutions for high-dissipation equipment, such as cooling loops and external radiators, to manage the heat power received from the Sun and generated by avionics. As a consequence, the thermal design can only be based on fully passive thermal control solutions. The design proposed in the earlier phases of this study, in line with the outcome of the literature review, capitalizes the spacecraft substantial size, exploiting the large inactive surfaces of the modules that can act as radiators, and is based on a careful selection of coating materials and paints in order to optimize the thermo-optical properties on the active surfaces.

The thermal design of the spacecraft bus, including avionic units and propulsion system, will be addressed when the detailed design of these elements is defined. In particular, thrusters are supposed to have dedicated thermal control systems which allow the compliance of thermal requirements at element level (not assembly element). Nevertheless, the low maturity level of the design of these elements is acceptable at the current stage, and it is not critical from the thermal point of view. Indeed, the contribution to the overall thermal budget of the spacecraft bus is negligible, compared to those given by the antenna and the solar panels, and do not significantly affect the radiating exchange of the larger modules.

In this section, a thermal analysis will be described, performed with ESATAN software, on a simplified model; the aim of this analysis is to evaluate heat power received and rejected by the S/C and compute the temperature achieved during the mission.

This first analysis is focused only on the main, large elements (antenna and solar panels). As anticipated, avionics and thrusters are considered negligible for the purpose of the analysis and are currently omitted from the thermal model. Nevertheless, they can be addressed in future phases, once their design will be consolidated, and the results of the analysis will drive the decision about the most suitable techniques to be implemented for the thermal control.

The results reported in the next paragraphs will consider only the “equinoxes scenario” where the Sun is on the nodes in his apparent path around the Earth. In facts, this scenario has been found to represent for the solar panels and the antenna both the worst hot case, as in this position the Sun is normal to all S/C surfaces (and so the heat fluxes from the Star is maximum) and the worst cold case, as the S/C experiences the longest eclipse period during which temperature drops considerably.

6.3.7.2 Assumptions and Thermal Model

This section presents all assumptions made to carry out the analysis. Considering the current low maturity of the configuration, the implementation of a detailed model of the SPS is neither practicable nor significant in this phase. Nevertheless, in parallel to analytical calculations, a preliminary simple ESATAN model has been created to support the verification of the feasibility of a passive thermal management of the antenna and the solar arrays. The model is constituted only by three elements: two rectangular wings and one circular antenna. Structures supporting and connecting the modules constituting the antenna and the solar arrays are not modelled, because their temperature requirement are not driving and their contribution to the thermal network can be considered negligible in such a large and modular system characterized by high dissipation and solar input. The shape and the size of elements are quite the same as the real ones defined in this document except for the full wing. As the model simplifies the full wing as a continuous rectangle, while it is formed by several solar panels not united with each other (not a continuous), the sides of full wings are made so that the total area of the rectangle is the same as assumed above. All elements have been considered shells, as the thickness has been assumed to be negligible considering the other dimensions. As already mentioned, avionics, thrusters and relevant propulsion system are not included in the thermal model. Their dissipation is in any case negligible with respect to the other dissipations (e.g. solar panels).

Assumptions made about the materials and thermo-optical properties of solar panels and antenna are listed in Table 6-12. Also in this case, all values are assumed based on available information and heritage. Perovskite thermal properties have been taken from specific papers while thermo-optical properties have been assumed based on common solar panels (values are not too dissimilar). The antenna has been assumed to be in aluminum as bulk material, assuming a rigid supporting structure. Two cases were considered for the analysis: in the first case, we conservatively assumed no specific surface coating on the active side with mediocre optical properties (to account for possible constraints and from impacts from the detailed geometry not known at present), while in the second case we assumed a dedicated paint with low alpha/epsilon ration on the active side, which is probably more realistic.

The rear side of the antenna is assumed to have a radiator-like coating (specifically, the properties of the new First-Flex interferential coating have been used), in order to lower the amount of power received from the Sun and reject the power dissipation, so to remain in the operative temperature range.

Concerning solar panels, with the optical properties of the front side imposed by solar cells and a quite small thermal capacitance per unit area, it will be shown that the critical point is minimum temperature during eclipse, when both the Sun flux and, consequently, the dissipation drop to zero. So, the rear side of the panels shall be characterized by very low emittance: this design driver has been reflected in the assumptions of the thermal model

SOLAR PANEL		ANTENNA	
Parameter	**Assumption**	**Parameter**	**Assumption**
Solar Panels front side Emittance	**0.84** (typical value for solar pan-els)	**Antenna front side Emittance**	**0.5** (no coating case) or **0.81** (coating case)
Solar Panels front side Absorption	**0.75** (typical values for solar panels)	**Antenna front side Absorption**	**0.5** (no coating case) or **0.2** (coating case)
Solar Panels rear side Emittance	**0.1**	**Antenna rear side Emittance**	**0.81** (First-Flex)
Solar Panels rear side Absorption	**0.5** (First-Flex)	**Antenna rear side Absorption**	**0.1** (First-Flex)
Density **Specific Heat** **Thermal Conductivity of Perovskite**	**Rho=3190 kg/m3** **Cp= about 500 J/(kg*K)** **K= 0.19 (W/(m*K)**	**Density** **Specific Heat** **Thermal Conductivity Antenna of Aluminum (aluminum only for reference)**	**Rho=2700 kg/m3** **Cp= about 870 J/(kg*K)** **K= 237 (W/(m*K)**
Solar Panels Thickness	**1E-3m (1mm)**	**Antenna Thickness**	**1E-2 m (1cm)**

Table 6-12 Assumptions made on thermal model

Concerning the requirements, as said before, in this pre-phase-A of project, constraints and temperature limits can not be defined in a precise and consolidated way. For this reason, the requirements listed in Table 6-13 shall be considered preliminary reference temperature ranges, based on the current maturity of the overall design and related available information and on literature values when solid heritage is missing on the candidate materials/components. They are, however, suitable enough for this first assessment on the mission, in terms of thermal management, and to indicate the critical areas where design/technological efforts shall be done. Of course, the considered temperatures depend strongly on the specific design (of both the solar panels and the antenna) and they could evolve in future.

	MAXIMUM TEMPERATURE	MINIMUM TEMPERATURE
SOLAR PANELS	+150°C	-140°C
ANTENNA	70°C	-50°C

Table 6-13 Reference requirements

6.3.7.3 Thermal Analysis: Solar Panels

In the following section, the front side of solar panels is defined as the one exposed directly to the Sun, while the rear side is the one never exposed. Figure 6-41 and Figure 6-42 show the heat fluxes (solar, IR and albedo) received by the front and rear sides of solar panels.

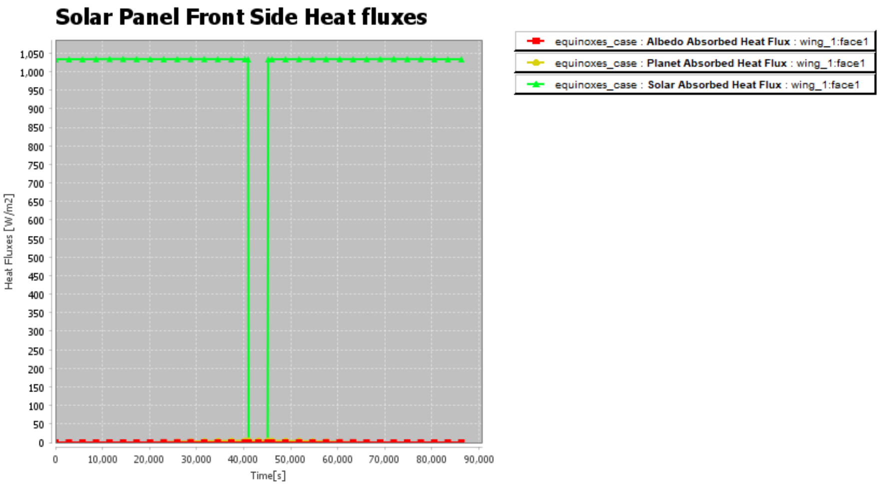

Figure 6-41 Heat Flow received by front side of Solar Panels

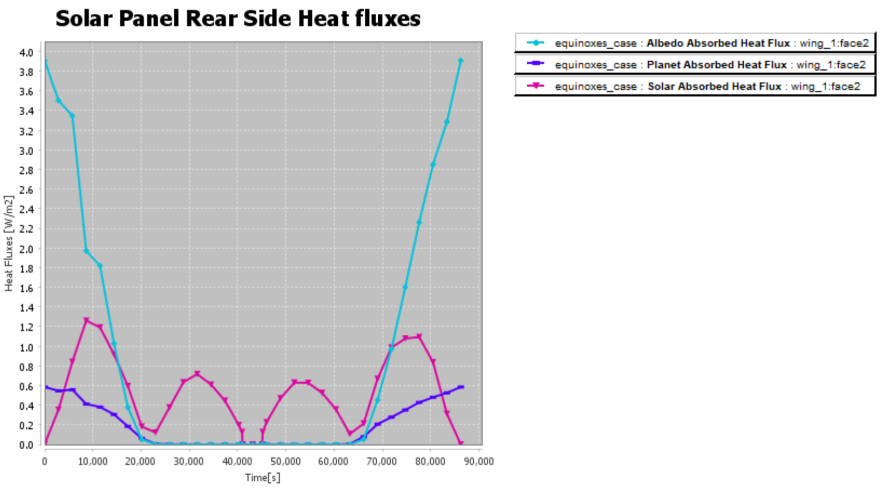

Figure 6-42 Heat Flow received by rear side of Solar Panels

As shown in Figure 6-41, the most relevant contribute to the heat flow received by the solar panels is the solar one (about 1000/1025 W/m2); this value is constant because the solar panels always point the Sun and receive the same amount of power around the whole orbit. The contributions of IR planet radiation and albedo are negligible due to the distance of spacecraft from the Earth in a GEO orbit (about 36000 km).It is possible also to see the eclipse period (between 40000 and 45000 s) where solar flux drops to zero. Figure 6-42 shows the heat flow received by the rear side of solar panels. The main contributors, in this case, are the IR planet radiation and the albedo (as the side does not see directly the Sun); the maximum value occurs when the Sun is " behind" the spacecraft and so the back side of solar panels is directly exposed to the Earth. The heat flow values are, anyway, very low (maximum 4 W/m2) due to the distance from the Earth, and negligible compared to the Sun power received by the front side. In conclusion, the most relevant contributor to the whole solar panels is the solar power received by the front side and it is about constant along the orbit, whereas the back side of the panels can reject the power received about constantly (mostly exposed to deep space). During eclipse, the amount of heat power received is negligible. The result of this heat balance is shown in Figure 6-43, reporting the temperature of solar panels.

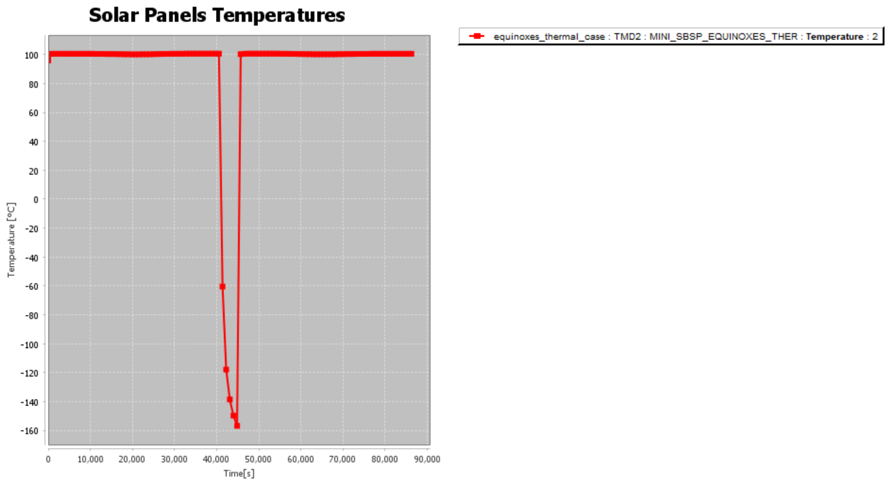

Figure 6-43 Temperatures of Solar Panels

The temperature is constant along the orbit, at about 100 °C, except in the eclipse period where it drops noticeably (down to -156°C, slightly exceeding the reference requirement of Table 6-13). This behavior can be explained by the fact that the solar panels have very small thermal capacity, due to the small mass. Indeed, the information about the minimum temperature requirements of the solar panels materials and components currently available is not consolidated. Either the hardware can accommodate the calculated temperatures or design solutions to increase the thermal capacitance of the deployable substrate shall be put in place, to limit the temperature drop in eclipse.

6.3.7.4 Thermal Analysis: Antenna

The thermal analysis of the antenna involved two cases. The first analysis considers a worst case where coating is not implemented on the front side of the antenna, and so the thermo-optical properties are not optimal (intermediate alpha and epsilon values). The second analysis assumes it is allowed to implement proper surface finish, to get radiator-like properties on the antenna, namely standard white paint.

6.3.7.4.1 Case 1: No coating on Front side of Antenna

In this first analysis we assume the front side of antenna has no coating, this means that the thermo-optical values used are:

- α=0.5
- ε=0.5

These values are not optimal, but are evaluated to assess the impact of optical properties in case of future constraints from the supplier of the antenna.

The rear side of the antenna receives only the Sun power radiation, as the front side always point to Earth. As shown in Figure 6-44, the highest value of power received by Sun occurs when the Sun hits perpendicularly the back of the spacecraft (heat power per area is about 135 W/m2).

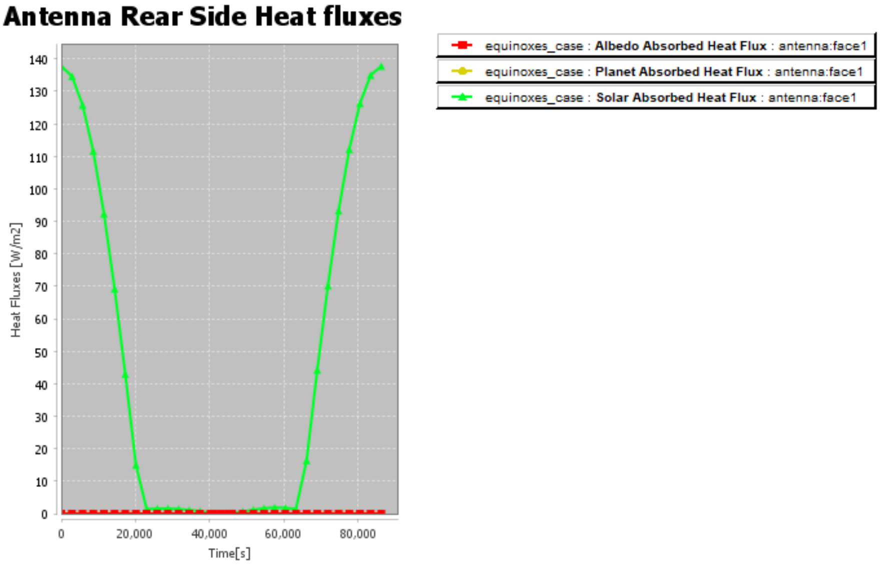

Figure 6-44 Heat power per area surface received by rear side of antenna

The front side of antenna receives always the planet IR and albedo radiation and also the Sun power which represents, also in this case, the most relevant contribute. In particular, the highest values of solar power received occurs when the Sun is "in front" of the antenna (opposite side to the respect of the Earth); also in this case it can be seen the eclipse period during which the solar flux in the front side drops to zero. The lowest value, occurs when the Sun is back to the antenna. Figure 6-45 shows the various contributors to the total flux. It can be seen that the highest flux is about 650/700 W/m2.

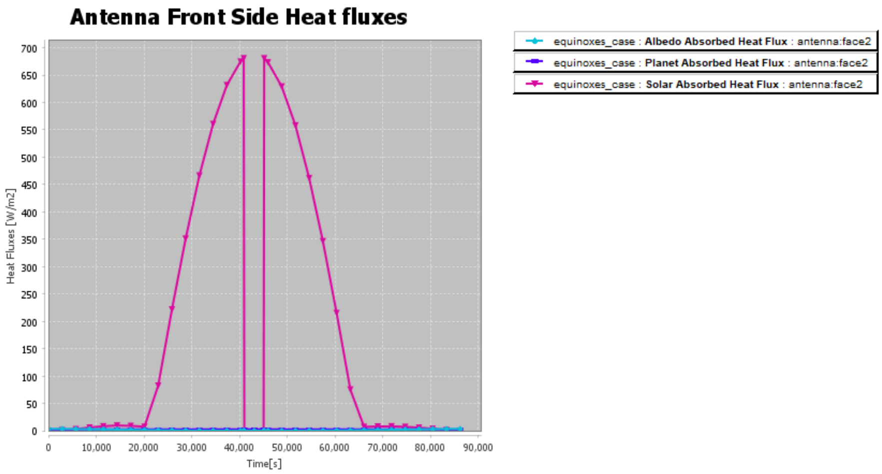

Figure 6-45 Heat fluxes received by antenna front side (no coating)

The temperatures are reported below in Figure 6-46. Temperature has a maximum when the Sun gets in front of the S/C followed by a minimum when the satellites enters into the eclipse. Like the solar panels, the quick drop of temperature can be explained by the low heat capacity of antenna. It must be also re-marked that during eclipse antenna does not dissipate heat power (it does not send power to Earth) and so the 430 MW of power is not considered during this period. The highest temperature is about 112°C while the lowest is about -7°C (during eclipse).

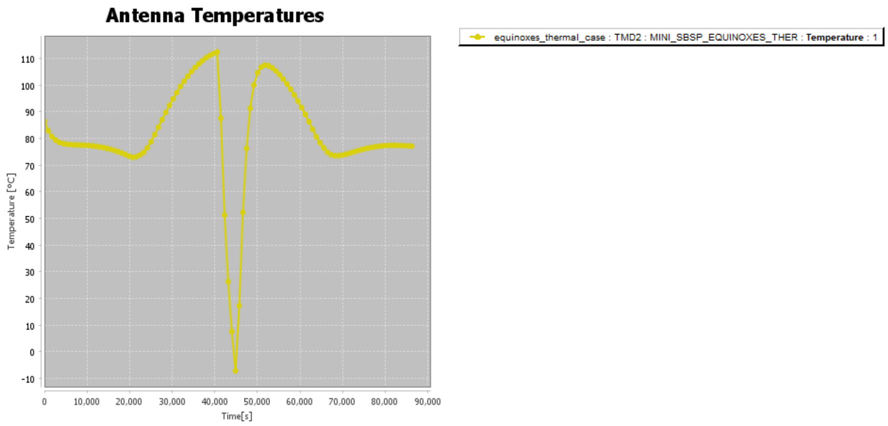

Figure 6-46 Temperatures of Antenna (no coating case)

The temperatures found are likely out of the operational temperature range of antenna, although further assessment shall be performed in future to define more precise requirements. What is more, it is expected in the future new material and technologies will be investigated to withstand these harsh temperatures. To lower the maximum temperature on antenna it is possible to consider coating on the front side of this.

6.3.7.4.2 Case 2: White Paint on Front side of Antenna

The second case assumes to cover the front side of antenna with white paint to lower the power received when the Sun is in front to S/C and increase the power rejected by the surface; the reference values come from TAS-I heritage. Thermo-optical values are:

- α=0.2
- ε=0.81

It is worth to highlight that the heat power received by rear side of antenna is the same received in the previous "no coating" case. Therefore, only the heat fluxes received by the active side of the antenna are reported in the following figure.

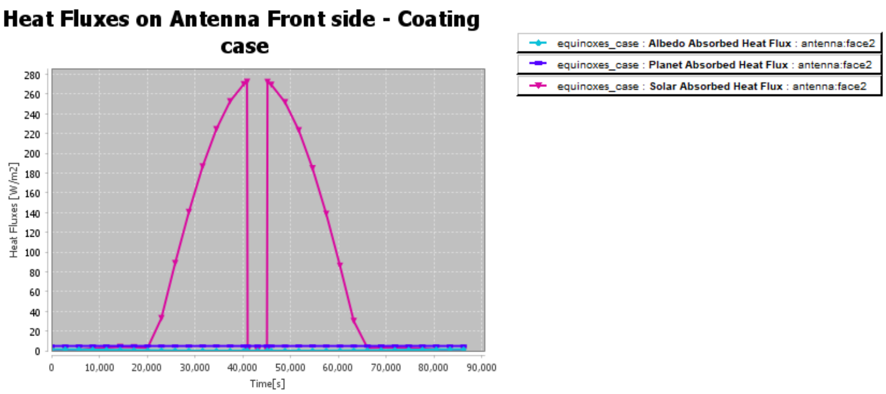

Figure 6-47 Heat fluxes received by antenna front side (coating case)

The effect of applying paint to the active side of the antenna appears to be beneficial, significantly attenuating the peaks of the heat fluxes. The maximum flux achieved in this case is 270 W/m2, against a value that reached 700 W/m2 when no coating was applied.

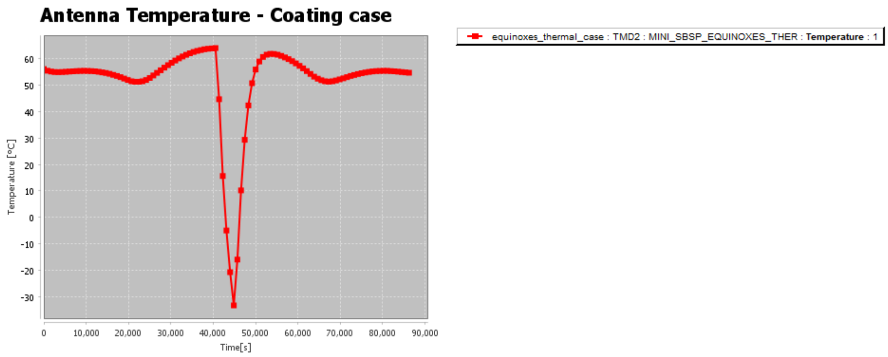

Figure 6-48 Temperatures of Antenna (coating case)

The temperature achieved by the antenna is reported in Figure 6-48. In this second case, as expected, the thermo-optical values modulates the temperature, which is significantly reduced with respect to the previous case. Both the maximum (64°C) and the minimum (-35°C) temperature remains within the reference requirements, with some margin helping to cover the uncertainty embedded in this preliminary model. This confirms the design indication.

6.3.7.5 Conclusions

The selection of the SPS architecture is driven by the strong constraints of the mass budget and the transmission to Earth function, resulting in a very large and modular concept equipped with huge solar panel fields and flat phased array antenna. The outcomes of the literature review and of our preliminary assessment indicate that the thermal control of this kind of space system shall be achieved with the use of passive solutions, due to the complexity and the enormous mass and reliability penalties that would be associated to the application of an active control (e.g. fluid loops, dedicated radiators) to such a huge and modular system. The thermal analyses therefore assumed a fully passive thermal control, defined by the choice of the modules material, and in particular the thermo-optical characteristics of the solar panel and the phased array antenna.

The thermal analyses of SPS in GEO orbit show, as expected, that the temperatures of the modules are mainly affected by the power dissipation, the solar flux and the thermal capacitance of the system, being the planetary contribution negligible. On both the hot and cold sides, the most critical scenario occurs during the equinoxes when the Sun is perpendicular to the S/C surfaces (and so the heat fluxes are maximum) and the S/C experiences the longest eclipse periods. Due to the low thermal capacitance per unit area of both the antenna and, especially, the solar panels, temperature drops a lot, and quickly, while entering the eclipse periods. This represents a significant challenge for the thermal design.

Overall, the results on solar panels show compliance against the maximum temperature in all mission conditions, but are borderline on the cold side with respect to the typical operating range found in bibliography for this type of arrays. Indeed, various assumptions and conservativism are embedded in the model about the composition, mass and thermal properties of the cells and the deployable supporting structure, and the temperature requirements need consolidation as well. In conclusion, the outcomes of the analysis suggest that the project is feasible with passive thermal control means but will probably require dedicated technologies (e.g. materials able to withstand extreme temperatures) and/or some design solutions to limit a bit the temperature excursion (for instance increasing the thermal capacitance of the support).

Temperatures on the antenna are compliant to the reference requirements (although marginally, if uncertainty is considered), provided that radiator-like optical properties are assured to radiate the enormous power dissipation. Also concerning the antenna the project is considered feasible, in this case with technologies and design solutions that are already available (namely, use of the First-Flex coating on the rear side and white paint on the front one have been preliminarily assumed in the analysis).

In conclusion, the thermal analyses demonstrate that the proposed SPS concept can function within the expected parameters. No show-stoppers have been identified. Indeed, the analyses confirmed that a passive control solution is feasible and adequate as long as a meticulous selection of materials and coatings is included into the design.

In this sense, it will be necessary to select or develop materials and passive control solution allowing satisfaction of requirements without major impacts on mass and system complexity; in particular fine trimming of thermo-optical properties and increasing of thermal capacitance.

Concerning the path forward, although considerations about the thermal control definition of thrusters, avionics and other service functions of the spacecraft bus are premature at the current stage, this aspect shall obviously be investigated in the future phases of the study.

6.4 Ground Segment

6.4.1 Ground Power Station

The Ground Power Station dimensions depend on:

- Transmission frequency (the higher the frequency the lower will be the GPS area, if the antenna area is fixed)
- GPS latitude (the higher the latitude the longer will be the footprint of the power beam)
- On-board antenna area (the higher the antenna area the lower will be the GPS area, if the frequency is fixed)

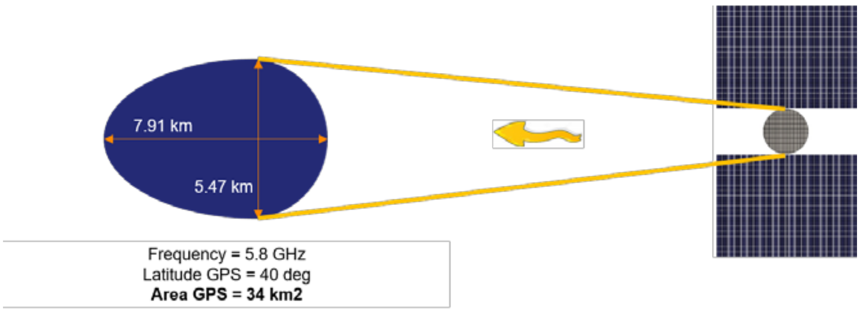

Figure 6-49 GPS footprint

Two options for the rectennas layout in the GPS:

1. Rectennas are laid flat on the ground and cover the entire surface of the elliptical footprint of the beam. More rectennas required (34 km²), simple accommodation (stretched net), no pointing constraint
2. Rectennas are put on inclined mesh panels. To avoid shadowing the panel lines are separated by some distance (1/sin(e)). Less rectennas required (23.8 km²), need panel infrastructure, requires fixed pointing

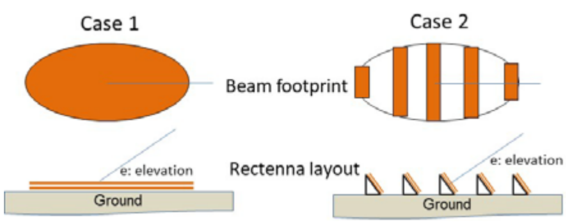

Figure 6-50 Rectennas layout

The selected option, based on inclined mesh panels, and the retrodirective beam pointing concept is shown below.

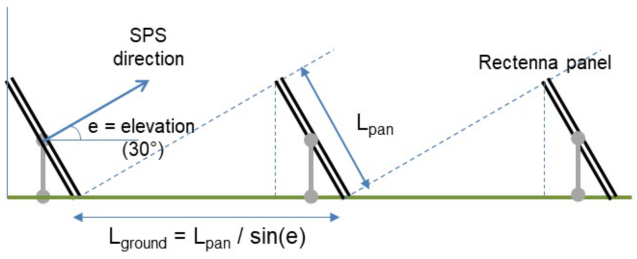

Figure 6-51 Inclined mesh panel

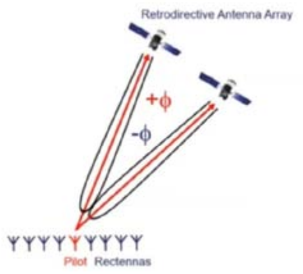

Figure 6-52 Retrodirective beam pointing concept (Credits: CWI)

The free area between the inclined mesh panels could be used for dual purpose, such as crop production.

6.4.2 Ground Stations & Control Centers

Ground stations are terrestrial facilities designed to receive and transmit signals to and from satellites in orbit. They form a crucial link in the communication chain between satellites and operators on the ground. The key aspects of ground stations are:

- Communication: receive downlink signals from SBSP S/C and transmit uplink signals to them;
- Tracking and Data Acquisition: track the position of SBSP S/C and collect data from them
- Control and Monitoring: control the operation (sending commands and software updates) and monitor SBSP S/C health & status;
- Orbit Determination and Navigation: help determine the precise position of SBSP S/C and contribute to navigation systems by providing accurate time signals;
- Data Processing: process the received data and distribute it to relevant Control Centers or user applications. They may also perform initial data analysis and quality checks.

Control Centers serve as central command hubs that manage and oversee the operation of satellites, space missions, or any complex systems. The key aspects of control centers are:

- Satellite Operations: control and operate SBSP S/C in space ensuring that the S/C is functioning as intended, perform necessary maneuvers, and execute mission objectives;
- Command and Control: send command to SBSP S/C for various purposes, such as reconfiguring payload settings or performing maintenance tasks;
- Mission Planning: develop mission plans and schedules that align with SBSP S/C objectives and scientific requirements. They analyze data collected from Ground Stations and collaborate with other teams to optimize mission success;
- Payload Management: in control centers operators manage SBSP S/C payload;
- Anomaly Investigation: control centers are responsible for investigating and troubleshooting any anomalies or unexpected behavior exhibited by SBSP S/C. They analyze telemetry data and work towards resolving issues;
- System Monitoring: monitor health & performance of SBSP S/C ensuring compliance with safety and operational constraints.

In summary Ground Stations provide the necessary infrastructure for SBSP S/C communication, while Control Centers manage and operate the S/C ensuring its smooth functioning and fulfillment of mission objectives.

6.4.3 Electrical Substation

6.4.3.1 Criteria for connection to the transmission grid: minimum design and equipment requirements

The system operator carries out specific studies to determine the access capacity of generation facilities. This assessment will be based on compliance with the technical criteria of safety, regularity, quality of supply and sustainability and efficiency established in the regulations in force.

The network access capacity for generation in a node or zone of the transmission network shall constitute the limit for granting the access permit to generation facilities connected to the transmission network in such node or zone.

The access capacity of a node or zone of the network for a type of generation (MGES or MPE) will be the minimum of the capacities resulting from the short-circuit power criteria (WSCR criteria), static behavior and dynamic behavior applicable to it.

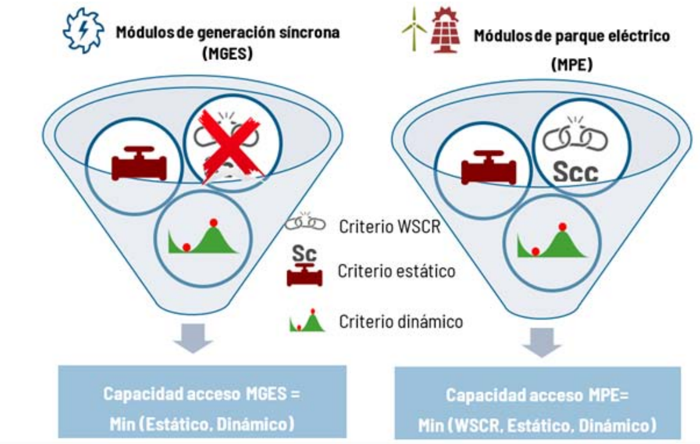

Figure 6-53 MGES/MPE

Any facility requesting connection to the transmission grid must comply with a series of requirements that guarantee that its operation will not interfere with the normal operation of the system and that it will behave as foreseen in both normal and exceptional situations. These requirements are defined in the current mandatory regulations.

Those included in the REE document "Facilities connected to the transmission grid: minimum design and equipment requirements" of June 2022, specify technical issues related to:

- Documentation to be provided in the connection processes: Project, report, budgets, etc.
- Energy exchange conditions: wave quality, perturbations, etc.
- Design and equipment requirements such as:
  - Short circuit power
  - Coordination of insulation and grounding network
  - Power equipment, (lines, transformers...)

- Definition of boundaries.
- Degree of criticity
- Protection systems and comunications.
- etc.
- Operating Conditions: Maintenance, maneuvers, etc..

The preferred configurations for application to the new ES are as follows:

- 400 kV one and a half breaker, evolutionary ring
- 220 kV breaker and a half, evolutionary ring, double busbar with coupling

The switch and a half will be required whenever 4 Inputs/Outputs at 400 kV or 5 I/O at 220 kV are required.

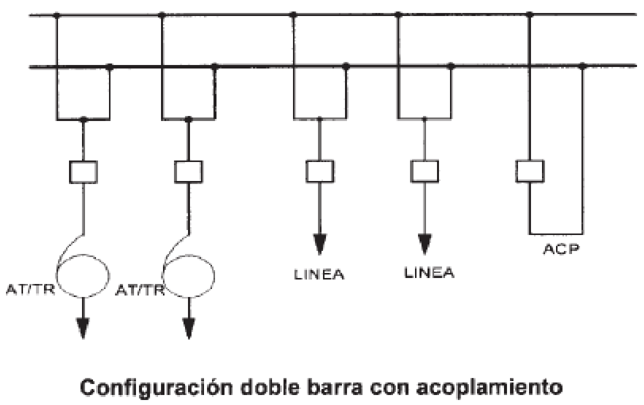

Figure 6-54 Double bar configuration with coupling

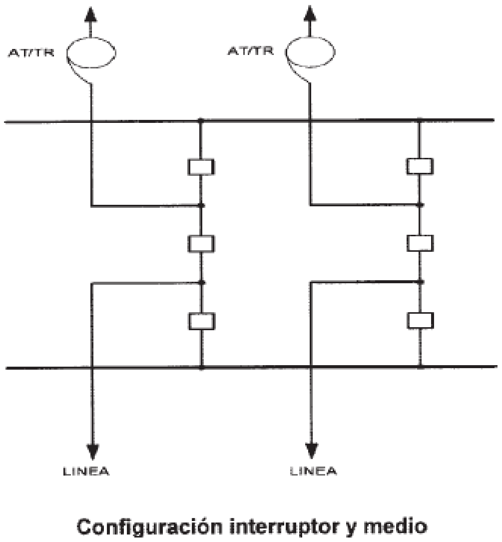

Figure 6-55 Configuration switch and a half

6.4.3.2 Limits of electromagnetic disturbances

The emission limits of the most significant characteristics of the voltage wave at the border points between the transmission grid with voltage levels greater than or equal to 220 kV and the generation or consumption facilities connected to the transmission grid are established:

- **Flicker:** The following flicker emission limits are established at each node of the transmission grid:
  - Perception of flicker short term <10 min (Pst) ≤ 0,8
  - Perception of flicker long term - 2 h (Plt) ≤ 0.6
- **Harmonics:** The following emission limits are established at the harmonic voltages of each node of the transmission system:

Not a multiple of 3		Multiple of 3			
Harmonic Order (n)	**Harmonic Voltage (%)**	**Harmonic Order (n)**	**Harmonic Stress (%)**	**Harmonic Order**	**Harmonic Voltage (%)**
5	1,8	3	1,8	2	1
7	1,8	9	0.9	4	0,7
11	1,3	15	0,3	6	0,3
13	1,3	21	0,2	8	0,3
17≤ n ≤ 49	$1{,}1 \cdot \frac{17}{n}$	21< n ≤ 45	0,2	10 ≤ n ≤ 50	$0{,}17 \cdot \frac{10}{n} + 0{,}14$
TOTAL HARMONIC DISTORTION RATE (THD) 3.00%					

- **Voltage unbalances:** emitters of this type shall not exceed the following limits of total voltage unbalance at each node of the transmission system:
  - short-term limit - μ < 0.7%
  - very short-term limit - μ < 1%

6.4.3.3 Costs and Costruction Timing

The costs and times described below refer only to the main HV substation: if other customers of the secondary distribution (MV or LV) shall be connected to the earth station, the costs and times of other HV/MV substations and further network branches shall be considered.

An indicative cost of the typical Transmission Station is 42 M€ and the total time for the design, development, component supplies and costruction is 36 months minimum.

The area required for the typical Station is approximately 30000 Sqm.

6.4.4 Electrical Storage System

This section defines the characteristics of the Electrical Energy Storage System (according to IEC 62933 series) based on energy intensive supercapacitors to be installed in a.c. systems with a declared fundamental frequency of 50 Hz.

6.4.4.1 EESS architecture

By according to IEC 62933 series, EESS must be designed in several subsystems with the following hierarchy:

a. primary subsystem;
   a. accumulation subsystem;
   b. power conversion subsystem;

b. auxiliary subsystem;

c. control subsystem;

a. communication subsystem;
b. management subsystem;
c. protection subsystem.

By according to IEC 62933 series two different architectures may be required:

d. EES system architecture with one POC type (Figure 6-56)

e. EES system architecture with two POC types (Figure 6-57)

EESS architecture with two POC types includes also the second one, that means that auxiliary subsystem can be configured to take the energy from the primary subsystem. This transition must be possible also during any EESS operating mode, without any impact to that operating mode. EES system architecture with two POC type is selected in this specification; in order to have the maximum level of reliability.

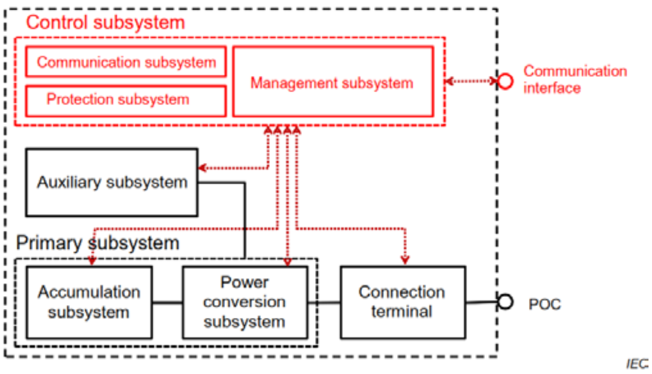

Figure 6-56 EES system architecture with one POC type

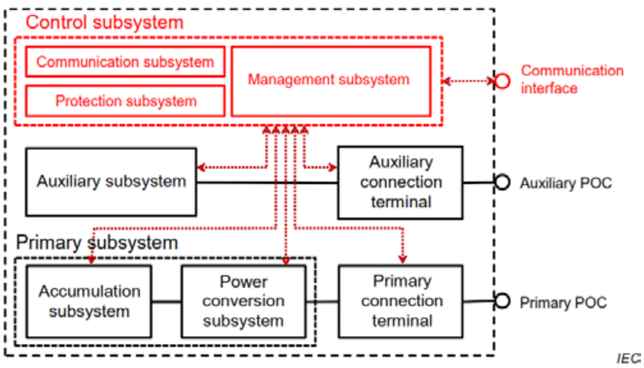

Figure 6-57 EES system architecture with two POC types

6.4.4.2 EESS modularity and reliability

By according to IEC 62933-1 an EESS module (or EESS unit) is a part of an EESS, which is itself, an EESS, so in according to the possible architectures; nevertheless the terminals, the auxiliary and the control subsystems may be absent in an EESS module, because they may be centralized at EESS level.

The EESS module is a specific EESS subsystem, in fact the EESS subsystem is a part of an EES system, which is itself, a system; a subsystem is normally at a lower indenture level than the system of which it is a part.

The EESS must be modular, following two possible modular approach:

a. full modular;
b. modularity for redundancy.

Any failure or lack of operation inside an EESS module must not impact the other modules.

In the full modular approach, all the EESS module must be an EESS able to work autonomously if needed. The EESS module must respect the architecture of the EESS; so they will share only the POCs.

In the modularity for redundancy, all the EESS module must share terminals, the auxiliary and the control subsystem; that are centralized at EESS level. Where present as a final stage of power conversion subsystem (immediately before the connection terminal) also transformers may be centralized.

Again, in order to stress the reliability the full modular approach is selected.

6.4.4.3 EESS on field

With the mentioned assumption, the EESS module may be included inside a 40ft standard container, by obtaining an on field installation based on:

- 1 single delivery substation (40ft container).
- Several 3 MVA / 3 MWh EESS modules (40ft containers).

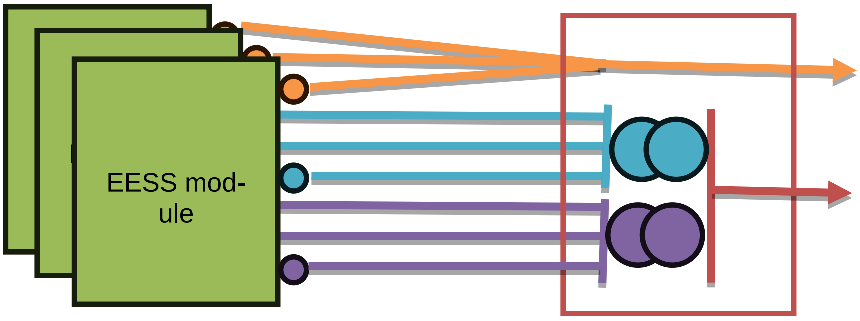

Figure 6-58 EES system installation

The delivery substation may be incorporated inside the electrical substation (refer to section 6.4.3). The delivery substation:

- Will receive cables from the primary connection terminals (400 V threephase in EU), for each of them will offer protection and switching arriving to a bus bar where a MV/LV transformer will adapt the voltage to the electrical substation requirements, then from the MV busbar a protected cable will be extended to the electrical substation.
- Will receive cables from the auxiliary connection terminals (400 V threephase in EU), for each of them will offer protection and switching arriving to a bus bar where a MV/LV transformer will adapt the voltage to the electrical substation requirements, then from the MV busbar aprotected cable will be extended to the electrical substation. The need to have a separated transformer is to improve reliability and to avoid to maintain the bigger transformer energized only to fed the auxiliary subsystems.
- Will receive cables from the communication interfaces connecting them to the external control link.

The final on site installation will be very similar to the traditional BESS installation with the exeption that the HVAC system are not required.

6.4.4.4 EESS module general requirements

Table 6-14 presents the EESS general requirements needed for the system identification; IEC 62933 series and the additional clarifications in this document are fundamental for its correct understanding.

Parameter	Requested values
Nominal frequency (f_N)	$f_N = 50$ Hz
Nominal voltage (V_N)	$V_N = 400$ V
Rated frequency and continuous operating frequency range (f_R)	$f_R = 50$ Hz ± 5 Hz
Rated voltage and continuous operating voltage range (V_R)	$V_R = 400$ V ± 60 V
Nominal energy capacity (E_{NC})	$E_{NC} \geq 3$ MWh
Nominal powers (S_N, P_N, Q_N)	$S_N \geq 3$ MVA circular power capability chart
Rated voltage of the auxiliary subsystem (V_{AN})	$V_{AN} = 400$ V ± 60 V
Rated apparent power of the auxiliary subsystem (S_{AN})	$S_{AN} \leq 20$ kVA
Expected service life expressed in C_{pcd1} (T_{SLC})	$T_{SLC} \geq 100000$
Expected service life expressed in years (T_{SLY})	$T_{SLY} \geq 10$ years
Nominal charging time ($T_{NC} = E_{NC}/P_{CN}$)	$T_{NC} = E_{NC}/P_{CN} = 1$ h
Nominal discharging time ($T_{ND} = E_{NC}/P_{DN}$)	$T_{ND} = E_{NC}/P_{DN} = 1$ h
Primary subsystem roundtrip efficiency (η_{PT})	$\eta_{PT} \geq 0.85$
Settling time (T_S)	$T_S \leq 300$ ms $T_S \leq 3$ s Depending to the operating mode
Specified tolerance limit ($\varepsilon=2\Delta y_S$)	$\varepsilon \leq 1\%$ of Y_∞ $\varepsilon \leq 0.1\%$ of f_∞ Depending to the operating mode
Self-discharge (E_{SD})	$E_{SD} \leq 15$ kWh per day per MWh of E_{NC}
Energy consumption of the auxiliary subsystems (E_X)	$E_X \leq 50$ kWh per day per MWh of E_{NC}
Energy stand-by consumption of the auxiliary subsystems (E_{XS})	$E_{XS} \leq 20$ kWh per day per MWh of E_{NC}
Reliability	MTTF ≥ 1350h MTTR ≤ 150h
Ordinary maintenance per year (M_O)	$M_O \leq 0.01$ FTE in one single intervention
Noise emission (DB_E)	$DB_E \leq 35$ dBA

Table 6-14 EESS general requirements

6.4.4.5 EESS module accumulation subsystem

The accumulation subsystem must be based on the energy intensive supercapacitor technologies; IEC 62391 series provides generic specifications, because of the earlier stage of energy intensive supercapacitor technologies, the adoption of LiIon based standards is possible to complement the overmentioned IEC 62391 series, in particular for planning, installation, operation and safety.

Components of the accumulation subsystem do not require heating or air conditioning to operate in the EESS reference environmental conditions. Ventilation may be accepted.

Encapsulated Hybrid Graphene Solid State and Tantalum Capacitor are used in this design.

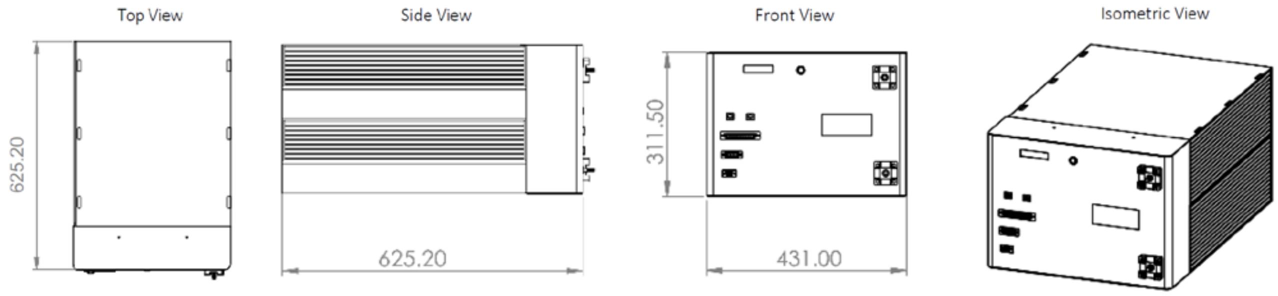

Figure 6-59 Encapsulated Hybrid Graphene Solid State and Tantalum Capacitor

- Cell Energy Density: 250Wh/kg
- Module Energy Density: 110Wh/kg
- Volumetric Density: 120Wh/Liter
- Weight: 90kg
- Upto 4MWh in a 40ft container
- Nominal voltage: 48VDC
- Voltage range: 43.2 V to 60.8V
- Capacity: 10kWh
- Compatible with all inverters
- Unlimited parallel connection
- Up to 1000VDC series connection
- Galvanic Isolation: 5000V
- Embedded Module Combiner

6.4.4.6 Final consideration about dimensions and cost

For >10 MVA / 10 MWh installations the following parameters are valid:

- 700 k€/MWh full cost EESS;
- 60 m^2/MWh land consumption.

6.5 Launch segment

With the operational orbit selected, the amount of launches required to bring the SPS in orbit can be further analysed. First, an estimation of the amount of Orbital Tugs required to bring the SPS in orbit is presented. Secondly, an evaluation based on the amount of transportable mass due to volume constraints is performed. Then, analysis based on the available launchers of ArianeGroup and RFA are developed.

6.5.1 Required Tugs based on time constraints

Considering an SPS mass of 6600 [tons] and assuming a Tug mass of 60 [tons] and a transportable payload of 100 [tons] both by the launcher and the Tug, it is possible to evaluate the time required for the Tug LEO-GEO roundtrip and the amount of Tugs required to bring all the SPS modules in GEO in 2 years.

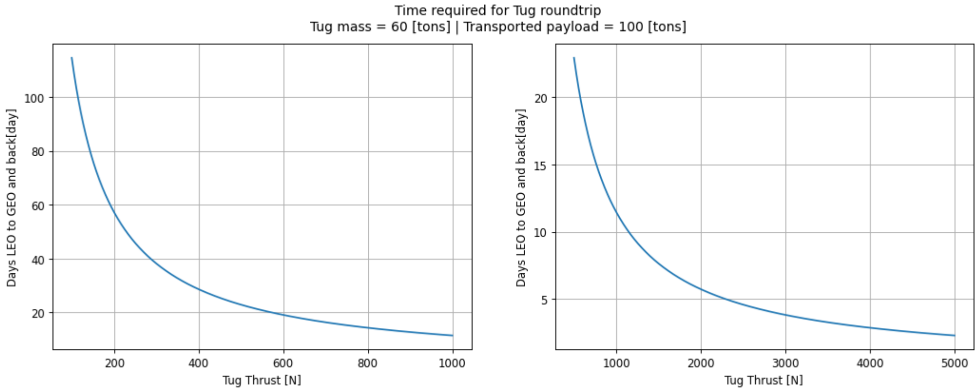

Figure 6-60 Time required for Tug roundtrip based on Tug thrust

Assuming a Tug thrust of 200 N, 60 days are required per roundtrip. This means that 6 Tugs need to work continuously to bring all the modules in GEO in 2 years.

6.5.2 Volume Constraints Analysis

Due to the limiting capacity of launchers' fairings in terms of volume, it is mandatory to assess the potential increment in term of launches due to this factor. For this evaluation, the Orbital Tug have a crucial role in determining the system's overall performances. All evaluation are done considering a 0 deg inclination, 500 km altitude parking LEO orbit and a 0 deg inclination operational GEO orbit, using finite burns with a Isp of 1000 s.

If no strategy is taken, considering an Orbital Tug with a mass of 60 tons that bring the amount of modules launched in a single launch in the operational orbit gives the following output:

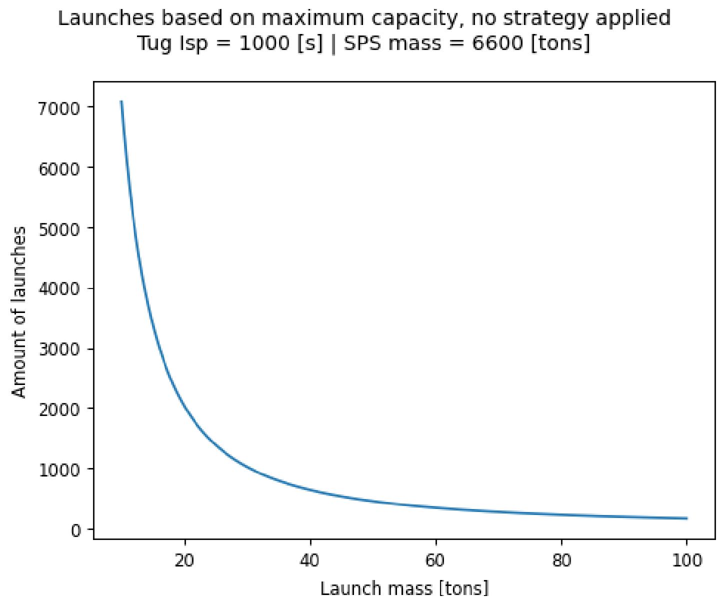

Figure 6-61 Launches based on maximum capacity without implementing strategies

The Figure 6-61 considers also the propellant launches with the volume constraints. A clearer plot can be done considering a full fairing when evaluating the propellant launches required:

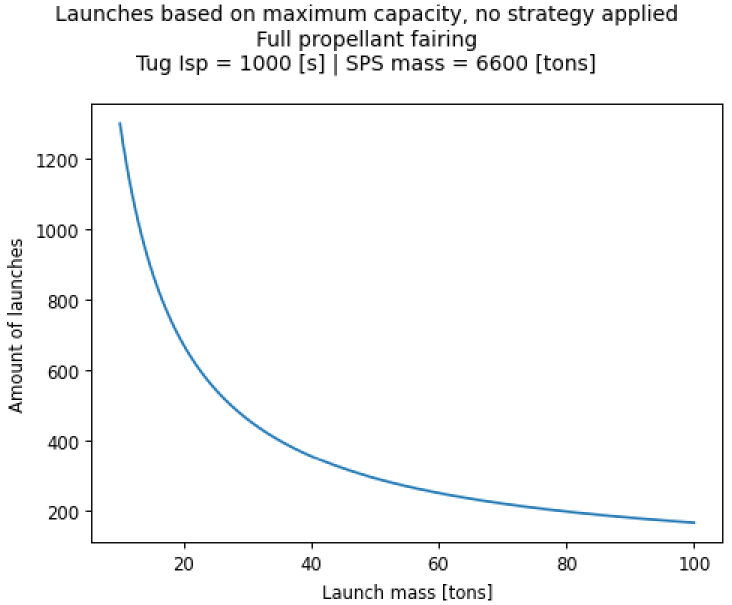

Figure 6-62 Launches based on maximum capacity with full propellant fairing

In order to prevent this escalation in terms of launches two possible strategies can be followed:

1. The Orbital Tug will have a mass of 60 tons and will carry for every trip 100 tons of structure. This means that the amount of modules launches will not coincide with the amount of Tug trips to GEO and back.
2. The Orbital Tug will have a mass equal to 60% of the launcher transportable mass. This means that the Tug is considered of proportional dimensions w.r.t. the fairing capacity.

The amount of launches required to bring the modules in orbit will change, while the amount required for the propellant will remain constant. The resultant amount of launches is shown in the Figure 6-63:

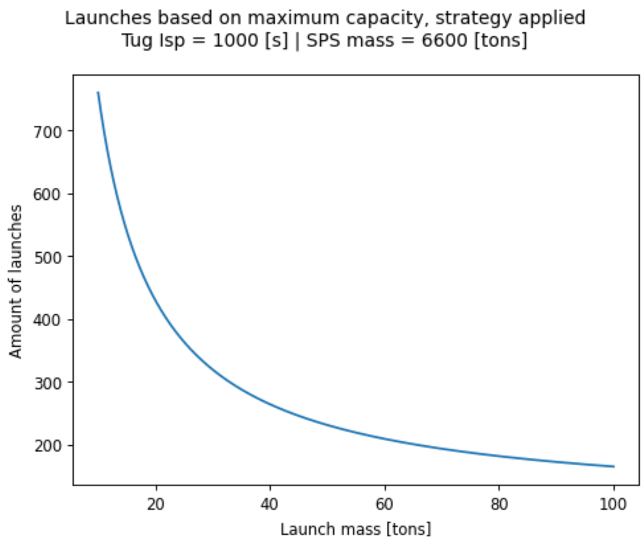

Figure 6-63 Launches based on maximum capacity with strategies implemented

Both strategies are feasible and will depend on the development of the Orbital Tug.

6.5.3 In-Orbit Assembly Highlights

The in-orbit manufacturing is a crucial technology allowing to fully exploit the launcher's fairing. With robotic systems capable of join components in the operational orbit it would be possible to maximize the amount of transported mass without modifying the modules design. By stacking the module's components in a tight configuration, the fairing can be fully exploited.

It would be possible to link each modules with no need of docking mechanisms. This means a a substantial decrease in LCOE. In fact, a single docking unit has been considered to cost around 3 M€. Considering the learning curve it adds up to more than 3 B€ which is the majority of the structure's cost.

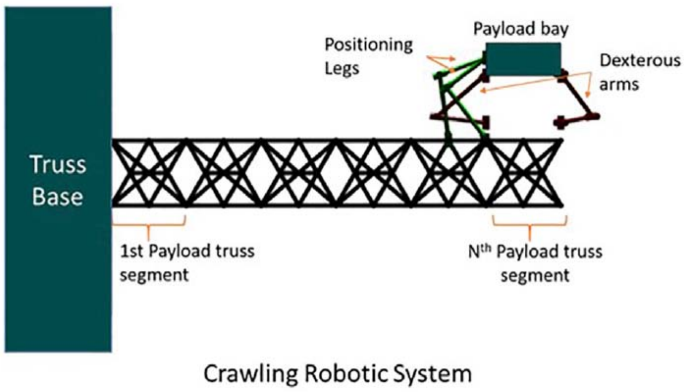

Figure 6-64 Robotic system example (Credits: U.S. Naval Research Laboratory)

In order to evaluate the amount of robotic systems required to perform the in-orbit assembly the following assumptions are taken:

- 4 robots to assembly 1 module in 4 hours
- 8 hours/day for robotic operations
- 100 modules arrive at the same time with the orbital tug and have to assembled in 11 days (before the next tug with other modules arrives)

With these assumptions, the required amount of robotic systems to build the SPS in 2 years is 24.

Space pallet meant to host assembly parts in space logistics, robotically actuated package fillers and fasteners and interfaces compatible with robots need to be studied.

6.5.4 Decommissioning launches evaluation

Based on the decommissioning strategy proposed in Section 4.4, it is possible to evaluate the required amount of launches of propellant required to bring all the disassembled SPS from GEO to Moon. Assuming a Tug mass of 60 [tons] and an SPS mass of 6600 [tons], a sensitivity analysis based on the Tug Isp is proposed below:

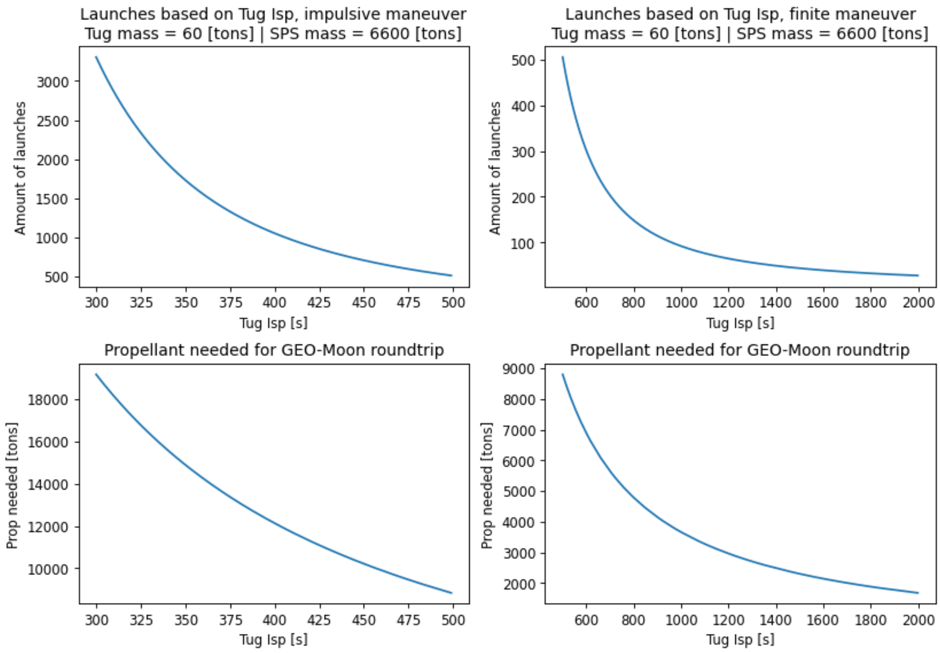

Figure 6-65 Propellant launches and mass required for decommissioning based on Tug Isp

The amount of launches is for both the propellant required for the GEO-Moon roundtrip and the one required to bring the fuel from LEO to GEO.

Similarly, a sensitivity analysis based on Tug mass is performed, considering both an Isp of 360 [s] and 1000 [s].

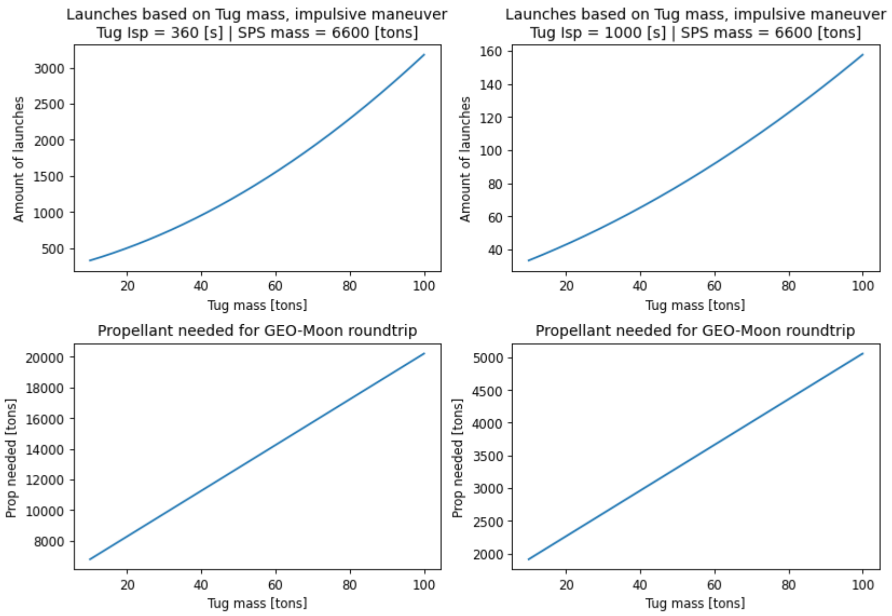

Figure 6-66 Propellant launches and mass required for decommissioning based on Tug mass

7 Functional Analysis & Physical Architecture

7.1 Functional Analysis

The functional analysis based on the logical layer is developed to define functions for the physical architecture. The following three macro functions containing all the sub-functions of the system are considered:

- Generate and trasform solar energy into RF;
- Convert RF in Electrical power and distribute to end-users;
- Perform & Support Satellite functions (specific functions for the SPS).

The functional tree related to the first function "**Generate and trasform solar energy into RF**", shown in the picture below, describes the process of transformation of the solar energy in electrical power on board, the transformation in radiofrequency waves and the transmission on ground.

The green functions are the ones allocated to our system, the blue ones are performed by external actors outside our area of responsibility (ground control segment or end users). These functions are used to specify the external interfaces with the system.

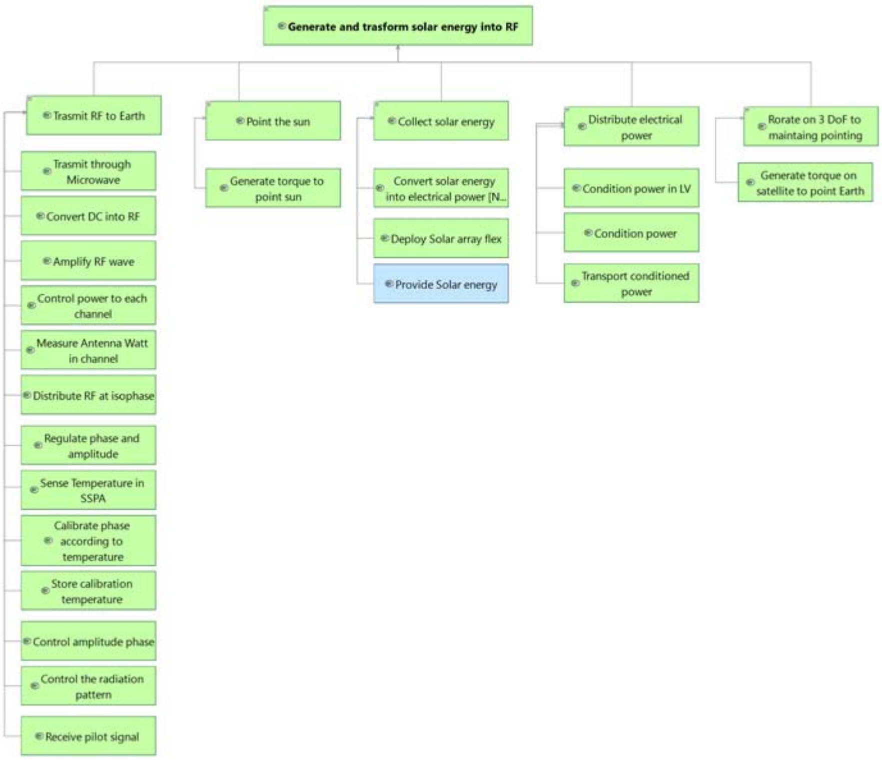

Figure 7-1 Functional tree (Generate and trasform solar energy into RF)

The functional architecture has been developed during the physical architecture elaboration and is detailed in section 7.2.

7.2 Physical Architecture

The functional architecture has been developed following the evolution of the sub-system design. Once the sub-system design has been frozen by the specialists, the integration in the Capella model has been performed.

The physical architecture is the result of a functional analysis detailed at component level and the definition of interfaces among components. Thus, functions and functional exchanges (data exchanged among functions) are allocated to the physical components and physical interfaces. The result is a preliminary design of a SBSP systems with his building blocks, components and the associated functions.

The space segment is composed of three building blocks:

1. Full wing assembly: it includes the flexible solar arrays with the deployment mechanism, the hall effect thruster assembly and the PCU to condition the electrical power to the desired voltage;
2. The satellite Platform: it includes the typical equipment of a standard satellite such as on-board computer, Low gain antenna and battery. In addition, the central truss which includes the main power bus is described as well as the motorized rotary joints allowing the motion of the antenna to point the GPS on Earth;
3. The phased array antenna assembly: it includes dedicated PCUs to condition power, the RF generation and transmission assembly and the Antenna central Unit controlling the phase shifters.

The yellow block represents the hardware components (e.g. the OBC or the Low Gain Antenna) that are under satellite platform responsibility and that will be distributed (e.g. hosted on the roll-out module) according to the configuration evolution.

The blue blocks represent the behaviour of the component and allow the allocation of the functions in the components.

The functions are described with green blocks and are allocated to each yellow component of the architecture. As already mentioned before, the functions are organized in functional trees and represent the leaves of the branches, satisfying ARCADIA rules.

The most important added value of the Physical Architecture, reported Figure 7-3, is the definition of the interfaces:

- the green exchanges represent the functional exchanges, meaning the data exchange between the executions of two functions;
- the blue exchanges represent the kind of interfaces between two component (electrical, data, hydraulic, etc.);
- The coloured ones, detailed in Figure 7-2, correspond to a preliminary definition of physical interfaces, in this case high voltage (20 KV), low voltage (28V, 50V, 120V), medium voltage (400-500V) and data interfaces.

The following legend has been developed to help the visual understanding of the model:

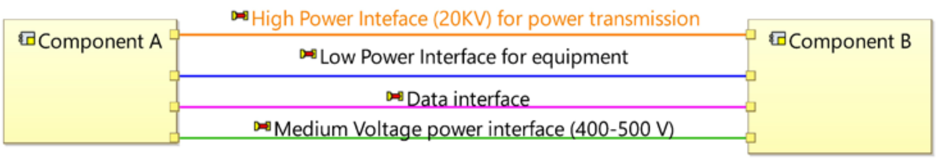

Figure 7-2 Interface legend

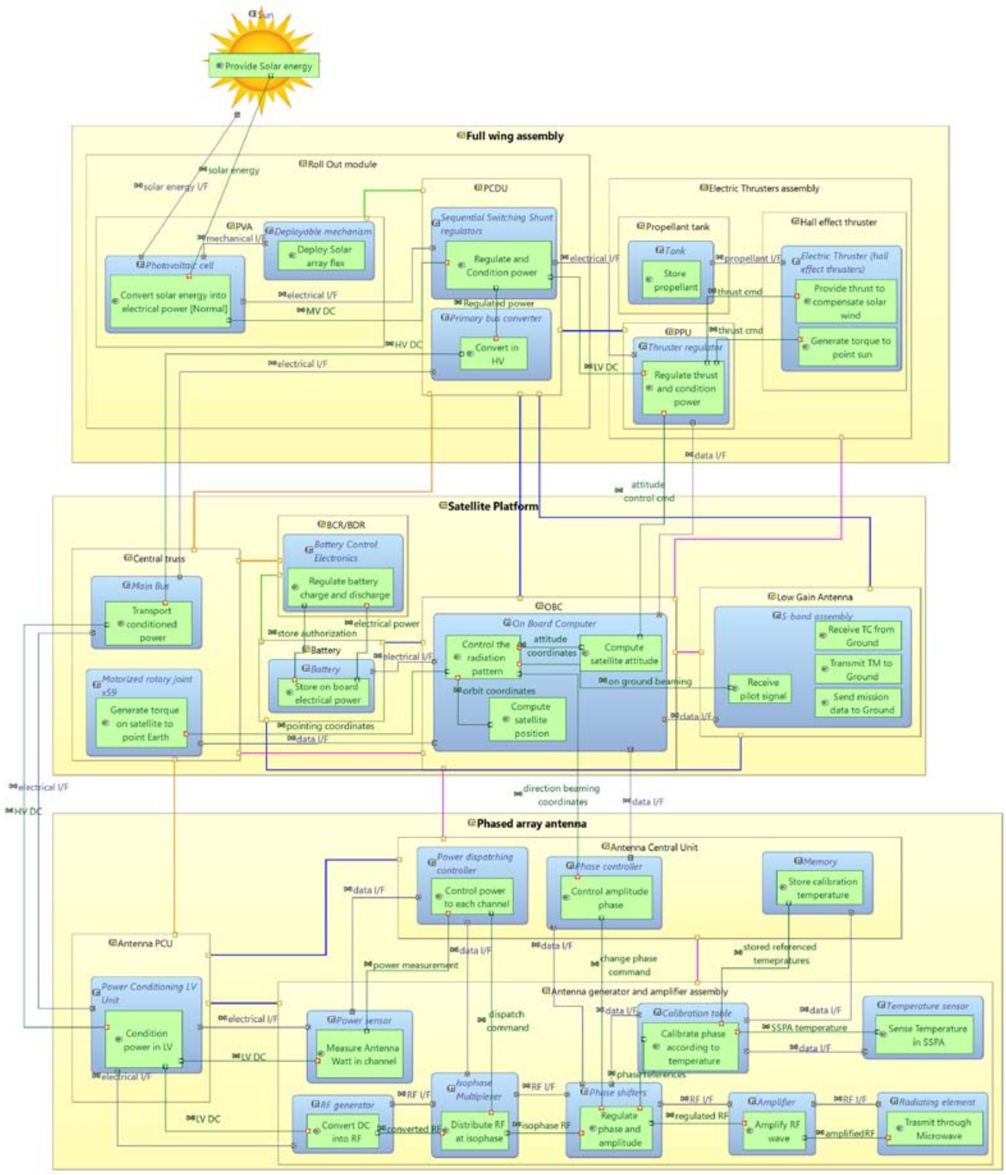

Figure 7-3 SBSP physical architecture

The on-ground architecture, shown in Figure 7-4, foresees the RF coming to ground through the beam emitted by the antenna, collected by the rectennas and transformed into electrical power before being distributed to the final users. The power is then regulated by an Electrical Substation that can be either dedicated to a specific end users (data center, desalination center,…) or to the national electric grid. If the specific end user is isolated without the connection on the public grid, it is an **off-grid configuration** otherwise (if there is a backup connection with the grid) is an **on grid configuration**.

Two functional chains (red and blue) describe the distribution to large scale end users into a national grid or the distribution to specific and high demanding end users.

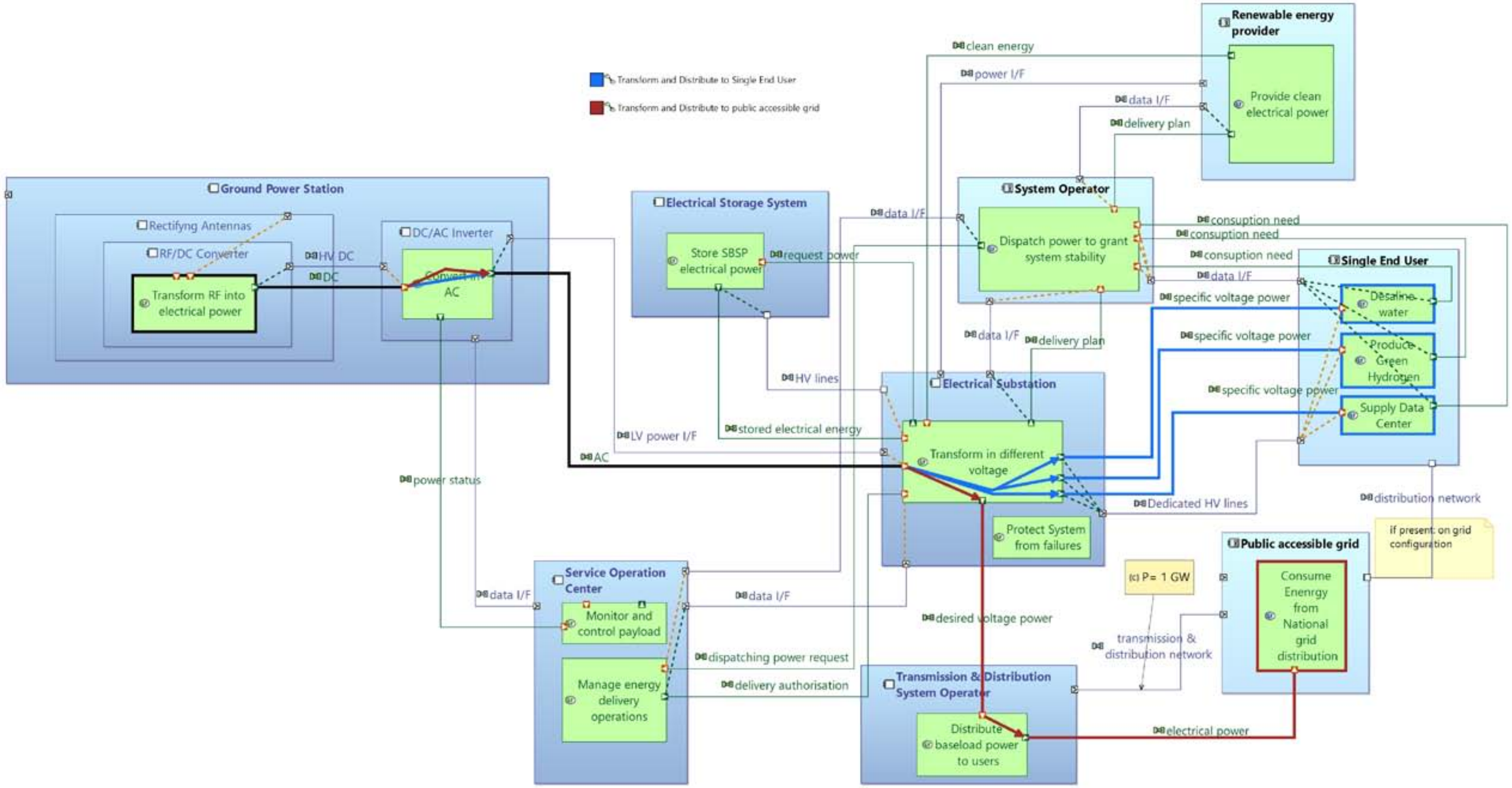

Figure 7-4 On-ground architecture

8 System Budgets

The mass budget of the proposed architecture is summarized in Table 8-1.

Item	Mass [tons]	Remarks
PVA	1870	This mass has been computed considering a PV area of 6 km2. We are considering Perovskite cells as the baseline solution with a weight of 0.08 kg/m2. Additionally, we are hypothesizing that the cell weight is only 25% of the full PV Assembly weight, which amounts to 0.3 kg/m2. The PVA density under consideration has been assesed as follows: • The photovoltaic layer of a perovskite cell is only 1-2 µm, which is equivalent on average to about 15 g/m². • Then, if electrical connections, an adapted packing factor, etc. are taken into account, an estimate of 80 g/m² as made by TAS-I seems realistic. • Similarly, at PVA level, assuming 0.3 kg/m² seems acceptable if a thin substrate and adequate encapsulation are taken into account; and in view of future technological developments. Refer to section 6.3.3
Phased Array Antenna	250	Considering Caltech ultra-lightweight phased array antenna technology [RD2]. The idea is to develop a lightweight RF IC (integrated circuit) glued on a foil of about 0.5 kg/m^2 of density (considering also SSPA and all the integrated circuit). Refer to section 6.3.3
Structure	3370	This mass has been computed considering a truss-like structure. Refer to section 6.3.3. This value is likely to fall considering the evolution of materials used.
AOCS	100	Thrusters + PPUs + Propellant for 1 year. Refer to section 6.3.4
EPS	1018	DC/DC converters + Harness. Refer to section 6.3.5
Mechanisms	30	Motorized rotary joints. Refer to section 6.3.2
TOTAL	**6640**	

Table 8-1 Mass budget

The power link budget is reported in Table 8-2.

Efficiency	Value	System efficiency	Power [MW]
	Solar Power Generator (0.24)		8593
Photovoltaic cell efficiency	0.29	0.29	2492
Solar panel surface efficiency	0.86	0.25	2143
Illumination efficiency	0.99	0.247	2122
Power line efficiency	0.99	0.245	2100
Power conditioning efficiency	0.98	0.24	2058
	Wireless Power Transfer (0.64)		
Power distribution network	0.98	0.235	2017
Power conditioning efficiency	0.98	0.23	1976
RF power generator	0.83	0.19	1641
Antenna efficiency	0.98	0.187	1608

Atmospheric attenuation	0.98	0.18	1575
Beam collection efficiency	0.833	0.153	1312
Ground Power Station (0.77)			
Rectenna panel surface efficiency	0.98	0.15	1285
Rectenna efficiency	0.833	0.125	1071
Power line efficiency	0.99	0.124	1060
Power conditioning efficiency	0.95	0.117	1007

Table 8-2 Power link budget

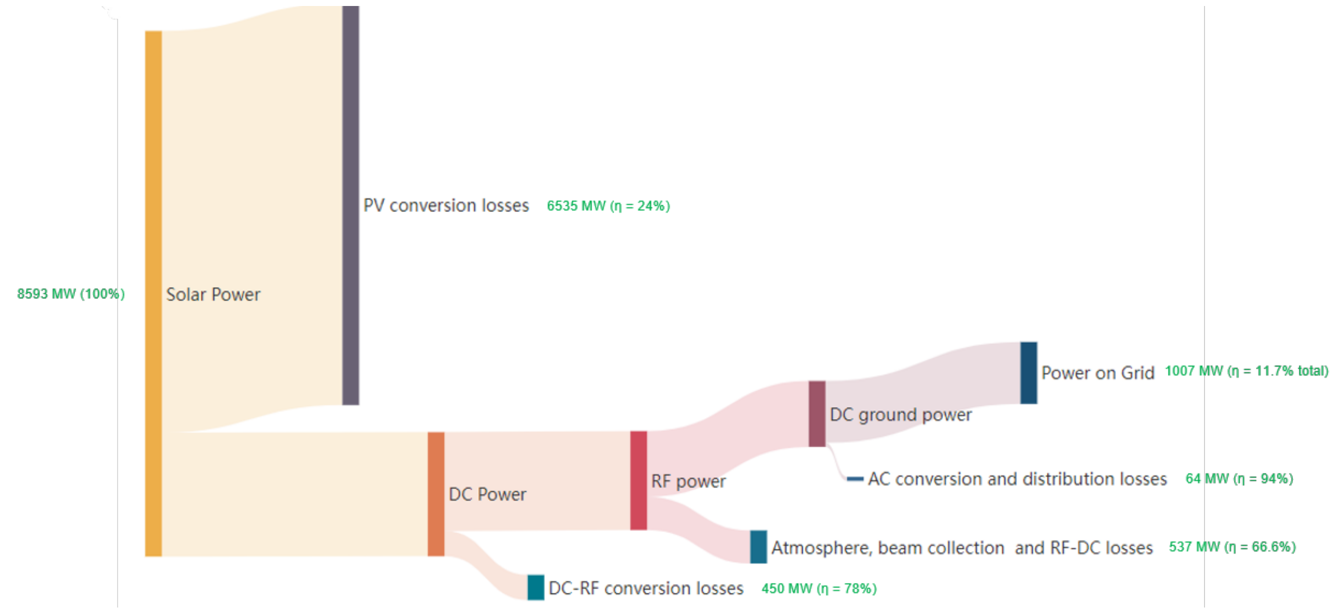

Figure 8-1 SBSP Sankey diagram

9 SPS Critical Areas & Technology Needs

The following table summarizes the SPS critical areas & technology needs.

S/S	Critical areas & technology needs	Remarks
PVA	Very-low cost, lightweight solar cells with ~30% efficiency and 30 yr lifetime are required	
Robotics & Mechanisms	Large Mechanisms (rotation of the Phased antenna structure)	Refer to section 6.3.2
	Assembly & Maintenance	The assembly and maintenance of big space infrastructures, performed by autonomous rendez-vous & Robotics systems is being tackled by ESA via the new Initiative on In-Orbit, Servicing, Construction and Recycling technologies (OSCAR). A workshop has been organized on 20/10/2023 and technology development activities will be pursued to raise the TRL of the necessary building blocks

Structure	Solar Arrays	Refer to section 6.3.3 **Boom:** development for 80 m boom either coilable or telescopic designs solutions **Flexible part with solar cells**: thin film e.g. Kapton internal joints and surface joining to flexible solar cells processes development. **Deployment Mechanisms:** development of unrolling mechanism e.g. controlled unrolling of coilable boom or extension mechanism for telescoping boom
	Roll-out Modules	Refer to section 6.3.3 **Modules**: development of the modules to provide the above reported section inertia properties for target stiffness achievement as well as intra-modules joints
	Central Truss	Refer to section 6.3.3 **Modules:** development of the modules to provide the above reported section inertia properties for target stiffness achievement as well as intra-modules joints
AOCS	Actuators	Refer to section 6.3.4 Advancements in electric propulsion are required to support control.
	Structure/Control Interaction	Refer to section 6.3.4 Interaction with structure needs to be further investigated to ensure robustness of control concept.
EPS		Refer to section 6.3.5 The huge amount of power involved in SBSP applications makes necessary managing very high voltage ranges. Thus, highly performant power conversion technologies will be needed as well as high-power cables, which represent a big challenge in space. Another issue could be related to the power management of a complex high power space system like this.
Phased Array Antenna	Beam forming & pointing	Refer to sections 6.3.6.5 Methods for forming & pointing power beam within a very large phase array (millions of controls) to be developed and validated
	High Power Amplifier with very high Power Added Efficiency (PAE)	Refer to sections 6.3.6.2 and 6.3.6.6

		Large technological effort is required to increase SSPA PAE to the expected efficiency.
	In-orbit assembly of very large planar phase array (from 10's of thousands of sub-panels)	Refer to sections 6.3.6
	Industrial mass production (millions of units) of space grade electronics for bricks and sub-panels (SSPA, EPC, phase shifter,…)	Refer to sections 6.3.6.10 Table 6-11.
TCS	New material to withstand extreme temperature	Refer to section 6.3.7
	New solutions to manage thermo-optical properties	
	New solutions to increase thermal capacitance	
Launch and deployment	In-Orbit Servicer	Refer to section 3.2.7 The Orbital Tug is a critical technology as it allows to bring the modules in the operative orbit and assemble the SPS
	Launcher Fairing	Refer to section 6.5.2
	In-Orbit Manufacturer	Refer to section 6.5.3 If a servicer satellite is capable to link modules there would be a great advantage in term of cost and overall mass, as well as maximize fairing capability

Table 9-1 Critical areas & technology needs

10 Digital Model Overview

The comprehensive digital model, developed in collaboration with MathWorks®, is denominated "SBSP Analysis Framework". This digital model integrates multiple optimization and parametric models and includes a user interface, allowing for the simulation of various scenarios.

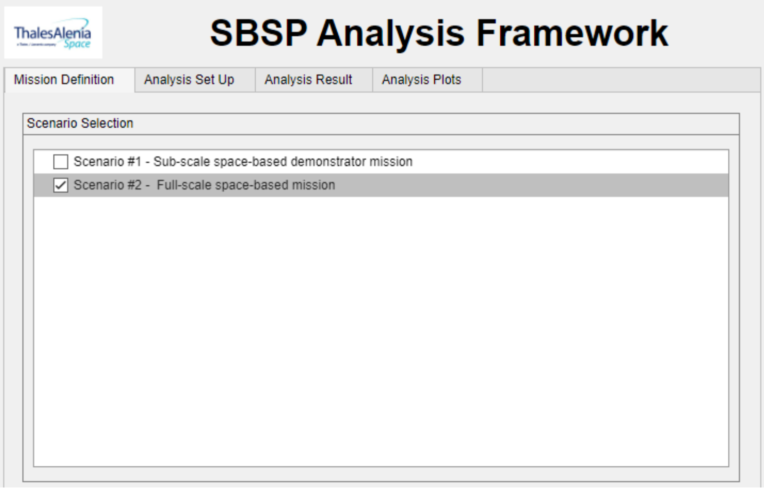

Figure 10-1 High-level scenarios of the SBSP Analysis Framework

10.1 Full-scale SBSP mission model

In the context of the full-scale SBSP mission, the framework allows for two types of analysis, each with distinct objectives:

- **Low-Fidelity Analysis**: an optimization model is used to assess the optimal combination of the three primary SBSP areas – the Photovoltaic (PV) area, antenna area, and GPS area. This evaluation is based on a range of variable inputs and user-defined optimization weight factors. All the analyses presented in chapter 5 have been conducted using this model.
- **High-Fidelity Analysis**: after selecting one of the optimized options derived from the low-fidelity analysis, the subsequent outputs are imported into a System Composer® architecture for the complete system. This architecture incorporates various models that enable different evaluations of the specific set of inputs derived from the low-fidelity analysis. These evaluations include high-level power simulations in various scenarios as well as preliminary assessments of mass and cost. The majority of the analyses presented in chapters 9 and 14 have been carried out using this particular feature of the tool.

10.1.1 Low-Fidelity Analysis

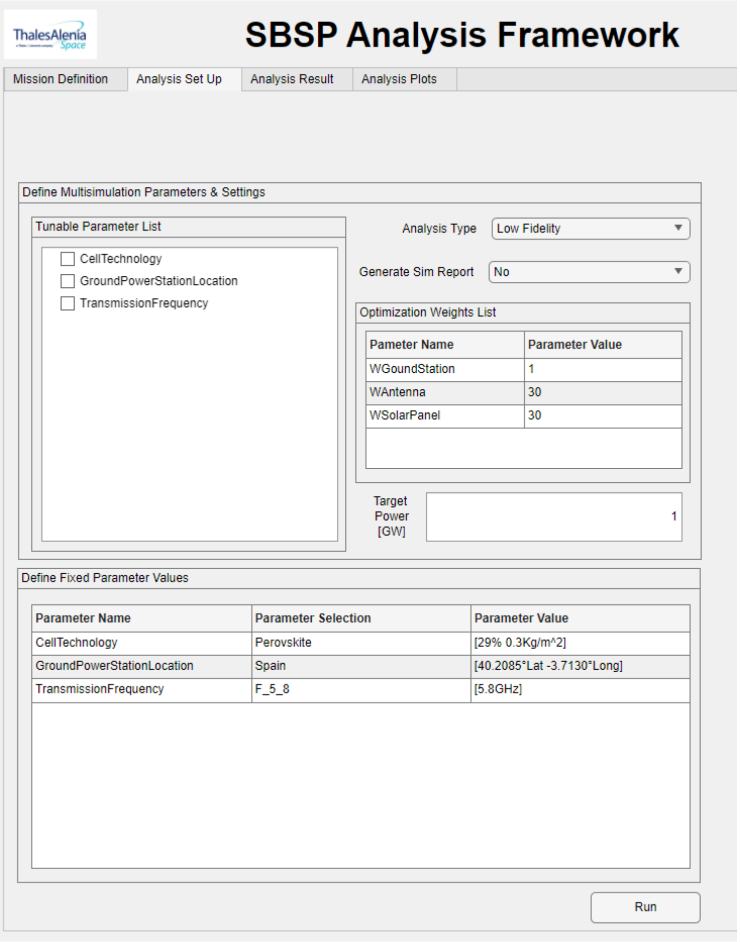

Figure 10-2 Low Fidelity analysis interface

The optimization model is used to assess the optimal combination of the three primary SBSP areas – the Photovoltaic (PV) area, antenna area, and GPS area. This assessment is conducted using a spectrum of variable inputs, which can be either set to specific values or left adjustable, allowing the tool to generate an optimized solution for each of these options.

Once, among all the optimized solutions, one of the possible configurations is selected, this can be exported to a SBSP high-level architecture transported from Capella MBSE tool in System Composer MathWorks® tool.

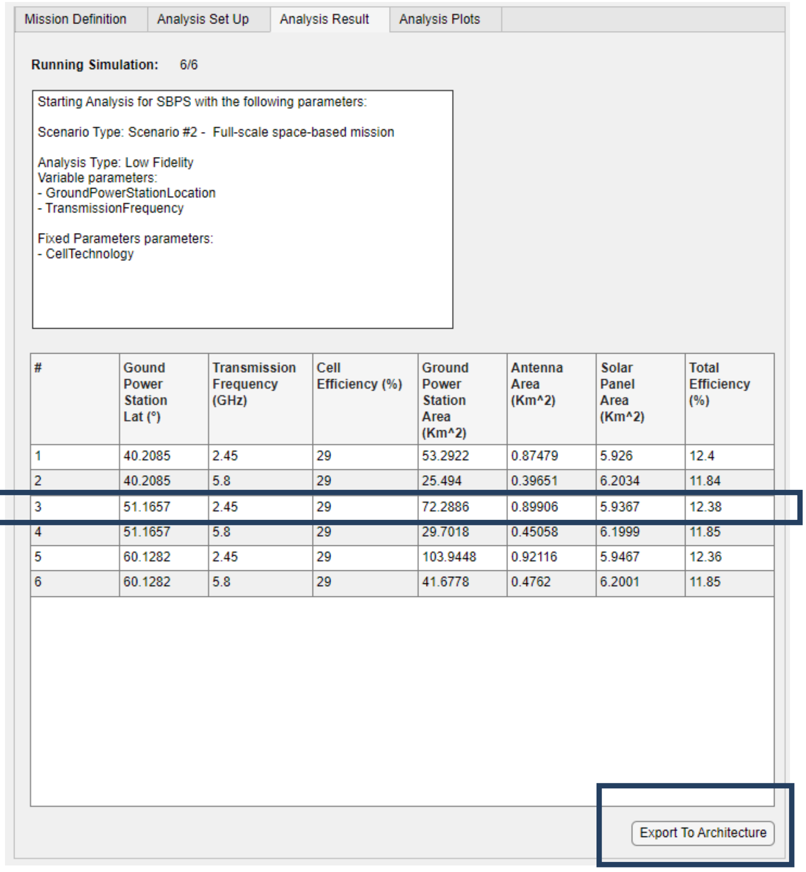

#	Gound Power Station Lat (°)	Transmission Frequency (GHz)	Cell Efficiency (%)	Ground Power Station Area (Km^2)	Antenna Area (Km^2)	Solar Panel Area (Km^2)	Total Efficiency (%)
1	40.2085	2.45	29	53.2922	0.87479	5.926	12.4
2	40.2085	5.8	29	25.494	0.39651	6.2034	11.84
3	51.1657	2.45	29	72.2886	0.89906	5.9367	12.38
4	51.1657	5.8	29	29.7018	0.45058	6.1999	11.85
5	60.1282	2.45	29	103.9448	0.92116	5.9467	12.36
6	60.1282	5.8	29	41.6778	0.4762	6.2001	11.85

Figure 10-3 Example of end simulation results with possibility to export to architecture

10.1.2 High-Fidelity Analysis

Once the desired solution is exported, these outputs are incorporated as inputs into the high-fidelity analysis. This process involves importing and saving all the relevant variables within the high-level architecture, which is used for detailed simulations and additional comprehensive system assessments.

With all the critical values now integrated into the architecture, we can proceed with the high-fidelity analysis. This set of functions allows us to:

- Assess the overall power transmission performance in various sections of the architecture throughout a simulation day;
- Evaluate the mass and total number of launches required for the chosen architecture;
- Calculate the mission cost and Levelized Cost of Energy (LCOE) for the selected architecture;
- Determine the Energy Return on Energy Invested (ERoEI) and Energy Payback Time (EPBT) for the selected architecture.

The assessments are based on the hypotheses outlined in chapter 14, and these evaluations can be conducted for any potential output architecture resulting from the Low-Fidelity analysis.

Similar to the Low-Fidelity case, certain parameters that serve as inputs (for either the power simulations and/or the mass and costs evaluation) can be either set as constants or adjusted among all the available options:

Parameter	Options	Main impact on the SBSP System
DC-RF technology	SSPA	DC-RF technology and the associated output power and mass per unit influence the mass (and all the related parameters) of the overall SPS
	Klystrons	
	Magnetron	
Simulation Day	Nominal day	The term "nominal day" refers to a day with uninterrupted 24/7 illumination of the solar panels, whereas the "worst day" represents the most challenging scenario with 71 minutes of eclipse during a day. It is important to note that the selection of the simulation day significantly affects the power profile throughout the day for different SBSP systems.
	Worst day	
Ecliptic inclination	Nominal	The term "Nominal" is used to describe a day with an average solar flux inclination toward the solar panels, while "Worst case" refers to the scenario with the maximum inclination of incident power, which is 23 degrees (ecliptic inclination).
	Worst case	
SPS alignment	Well aligned	A logical architecture has been established to simulate retro-directive beaming and implement potential safety measures associated with misalignment of the SPS. This architecture allows to model a scenario in which the antenna power beam is aimed at the designated target (Well aligned) and one with a certain error, that exceeds acceptable safety threshold (Bad aligned).
	Bad aligned	

Table 10-1 Parameters and options for the High Fidelity analysis

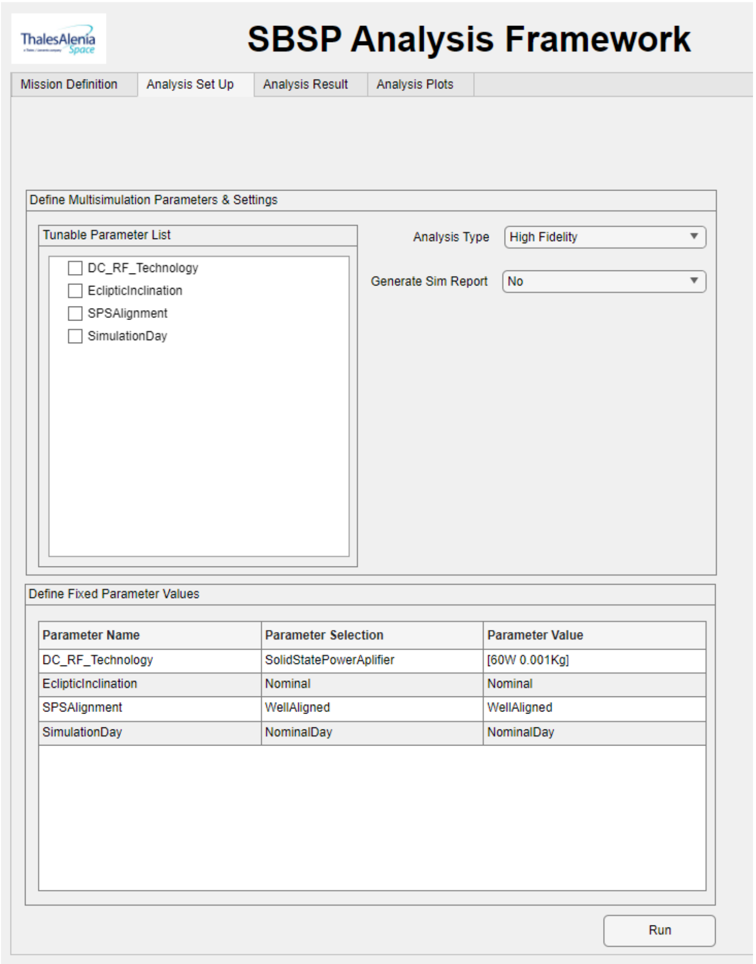

Figure 10-4 High Fidelity analysis interface

Once a specific combination of parameters is selected (or multiple combinations if certain parameters are left variable), the analysis produces various results, including those from the power transmission simulation and estimations of mass and cost (see Figure 10-5 and Figure 10-6). These results are invaluable for assessing and comparing different solutions, as seen also in the Low-Fidelity case.

#	DC_RF Technology	SPS Signal Alignment [-]	Simulation Day [-]	Ecliptic Inclination [-]	Average Transmission Power (MW)	Total Mass (T) & Total Launch(-)	Misson Cost (B$) & LCOE ($/MWh)	EROEI (-) & Energy Paybacktime (days)
1	SolidStatePowerAplifier	WellAligned	NominalDay	Nominal	• @PVA=2064 • @PMainBus=1979 • @On-board Antenna=1577 • @GPS=1051 • @Grid=993	• tot_mass=6591 • tot_launch=106	• miss_cost=14 • LCOE=191	• EROEI=42 • EPBT=219
2	SolidStatePowerAplifier	WellAligned	WorstDay	Nominal	• @PVA=1883 • @PMainBus=1805 • @On-board Antenna=1439 • @GPS=959 • @Grid=993	• tot_mass=6591 • tot_launch=106	• miss_cost=14 • LCOE=191	• EROEI=42 • EPBT=219

Figure 10-5 Example of High Fidelity analysis results 1/2

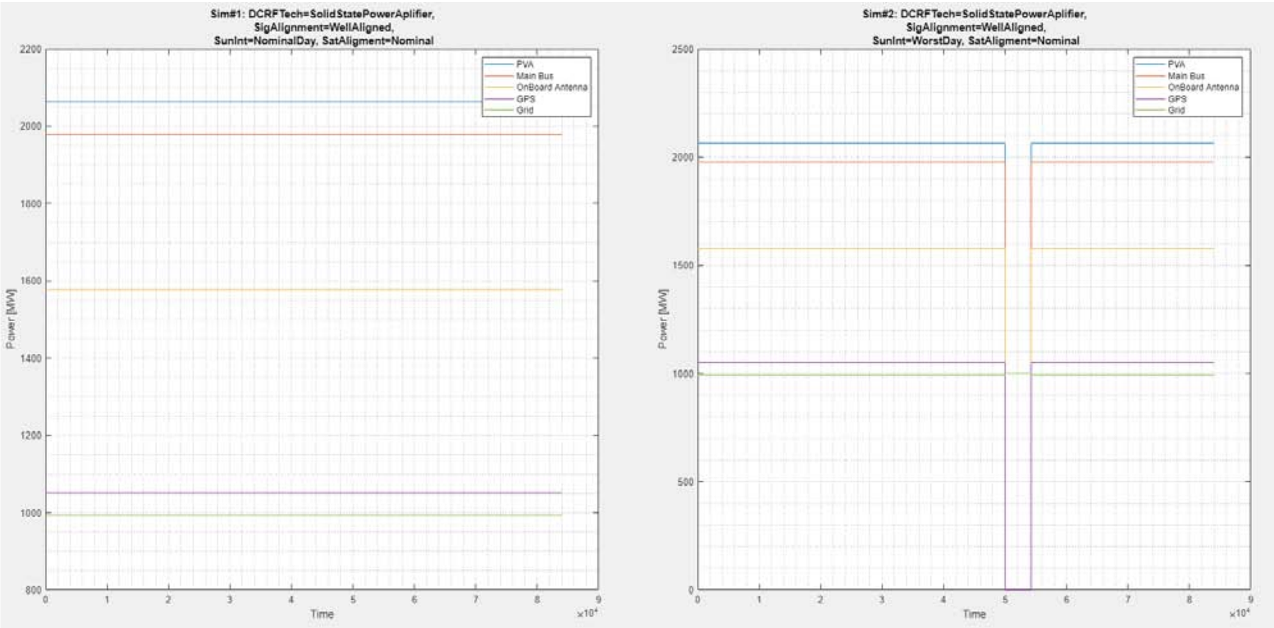

Figure 10-6 Example of High Fidelity analysis results 2/2

10.2 Sub-scale demonstrator mission model

A dedicated parametric model has been developed and seamlessly integrated into the SBSP Analysis Framework for the sub-scale demonstrator (see Figure 10-7). In this context, the following inputs can be modified:

- Orbit Type: having the flexibility to choose between Low Earth Orbit (LEO), Medium Earth Orbit (MEO), and Geostationary Orbit (GEO) as potential operational orbits for the demonstrator;
- Ground Station Area: the tool performs parametric simulations for each Ground Power Station (GPS) area input provided in the section;
- Target Power Requirement: for each GPS area, the tool generates a dedicated curve for every specified target power on the ground, demonstrating the options included in that section.

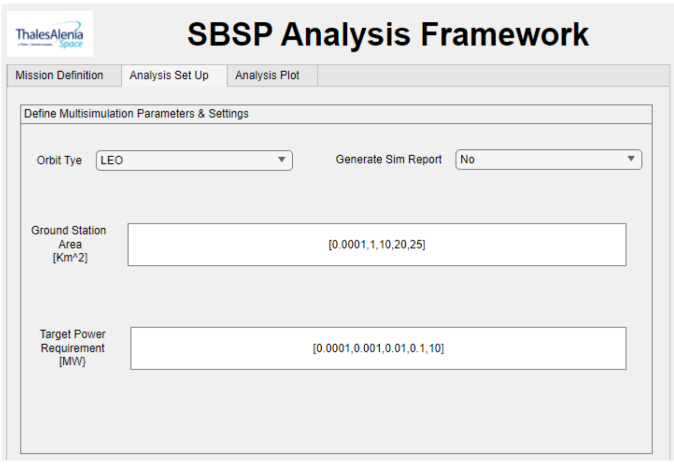

Figure 10-7 Sub-scale demonstrator mission scenario interface

The scenario has as results the plotting of a figure for every GPS inserted to be analysed (see Figure 10-8). In each plot is possible to observe a curve (that depends on the target power delivered) which correlates solar panel area and antenna area. These plots are fundamental to understand the expected scale of a demonstrator in function of the target power and other considerations.

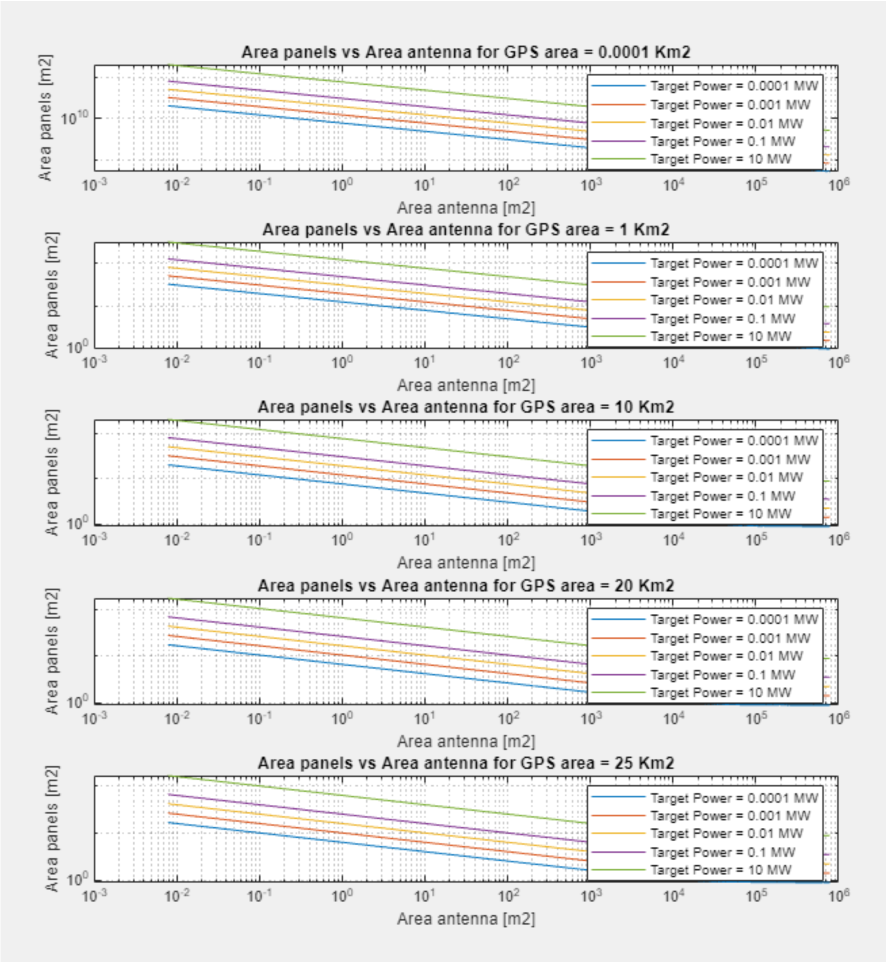

Figure 10-8 Example of Sub-scale demonstrator mission scenario interface results

11 System & Performance Simulations

The SBSP Analysis Framework, as elucidated in the preceding chapter, serves also the purpose of simulating the power link budget and wireless power transmission in different scenarios. This simulation takes into account the SBSP power link budget, which has been revised and updated following a more comprehensive analysis (see Table 8-2).

As previously elucidated in the SBSP Framework Analysis presentation on High-Fidelity simulations, the incorporation of the SBSP platform architecture within System Composer, replete with Simulink circuits, enables the power simulation of diverse high-level scenarios:

- Nominal day simulation;
- Worst day (71 minutes of eclipse) simulation;
- Worst case ecliptic inclination (23 deg) simulation;
- SPS alignment logic simulation.

11.1 Nominal Day Simulation

When discussing a typical operational day, it is plausible to assume a continuous 24-hour period of full nominal illumination for the Solar Power Satellite. Under these conditions, the on-board batteries and the ground-based super capacitors remain inactive because the solar power reaching the solar panels remains relatively constant, and there are no instances of eclipses. It is important to emphasize that, in addition to the energy supply, one must also consider the power requirements for various on-board systems, with a specific focus on the Attitude and Orbit Control System (AOCS) hall thrusters, and for the batteries recharge if needed.

In the following figures, it is possible to observe the power profile throughout the day at various critical points within the SBSP system:

- PVA power output;
- Main bus power;
- Antenna power output;
- GPS power output;
- Grid power.

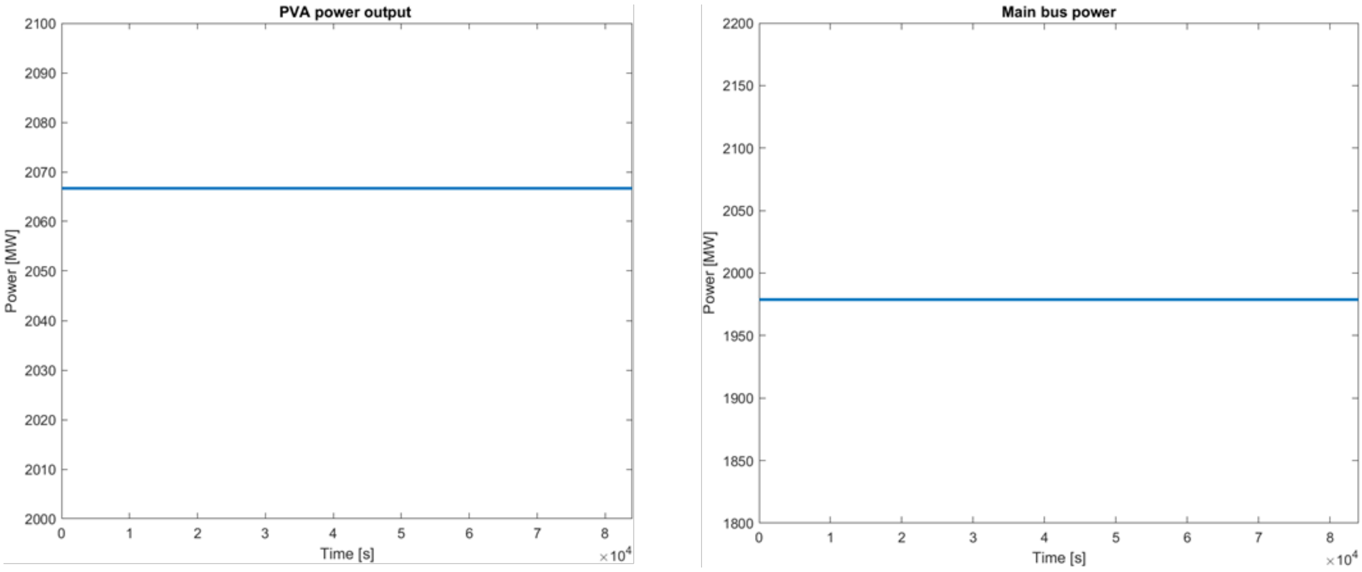

Figure 11-1 PVA power output (left) and Main bus power (right) during a nominal day

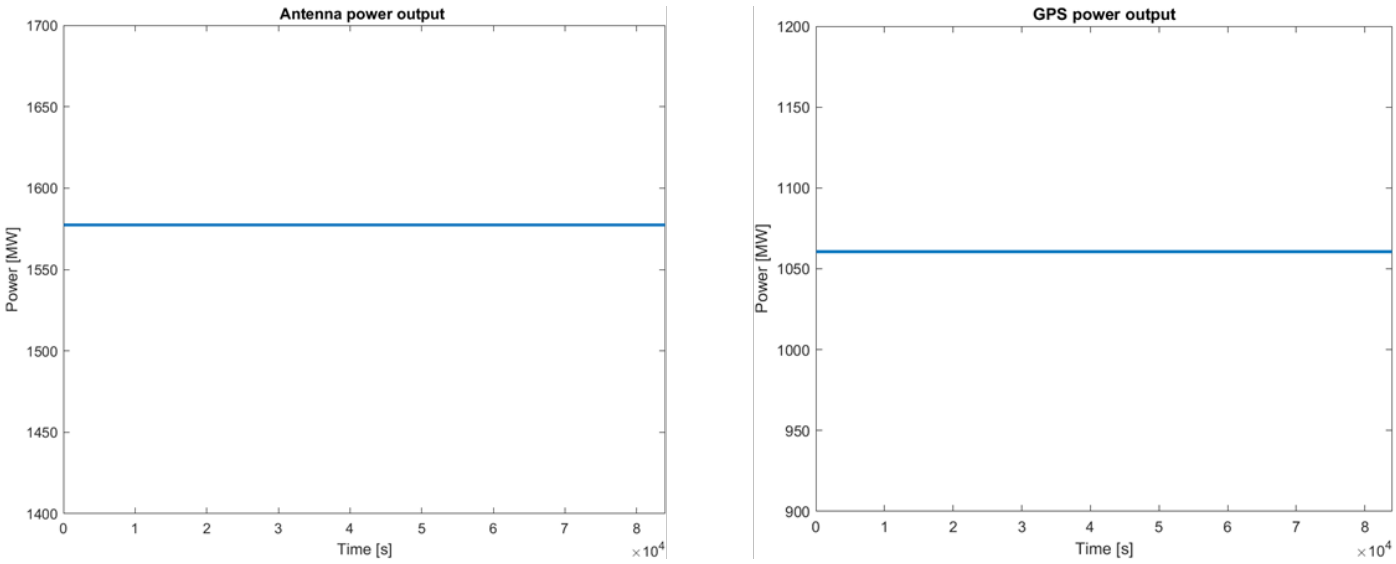

Figure 11-2 Antenna power output (left) and GPS power output (right) during a nominal day

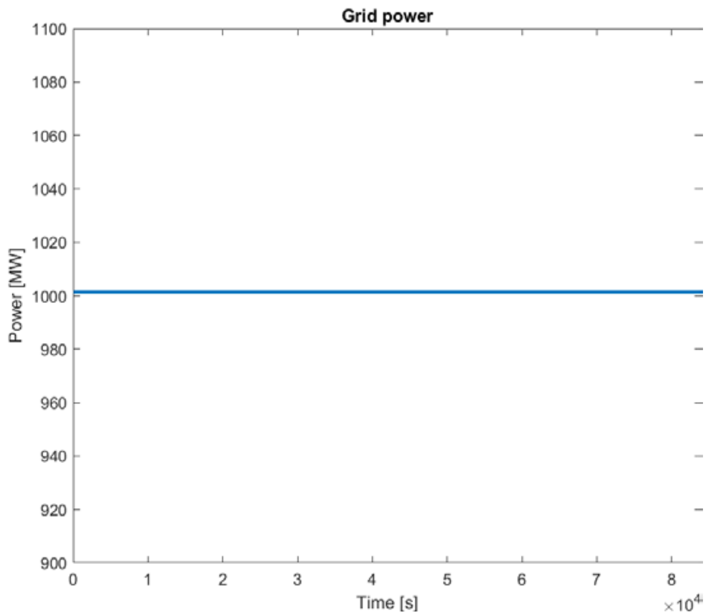

Figure 11-3 Grid power during a nominal day

As evident from Figure 11-3, the baseline of 1 GW of grid power is assured continuously throughout the day.

11.2 Worst Day Simulation (71 minutes of eclipse)

When examining the worst-case scenario, which occurs during equinoxes and involves the maximum duration of eclipses within a day (71 minutes), the tool's utility lies in high-level simulating the logic of compensations from on-board batteries and ground-based supercapacitors to address the absence of power generation during those brief periods.

In the following figures, it is possible to observe the power profile throughout the day at various critical points within the SBSP system:

- PVA power output;
- Main bus power;
- Other on-board loads power (with batteries compensation, it is observable how power does not arrive to zero in the eclipse period);
- GRID power (with super capacitors compensation, it is observable how the grid power does not arrive to zero in the eclipse period).

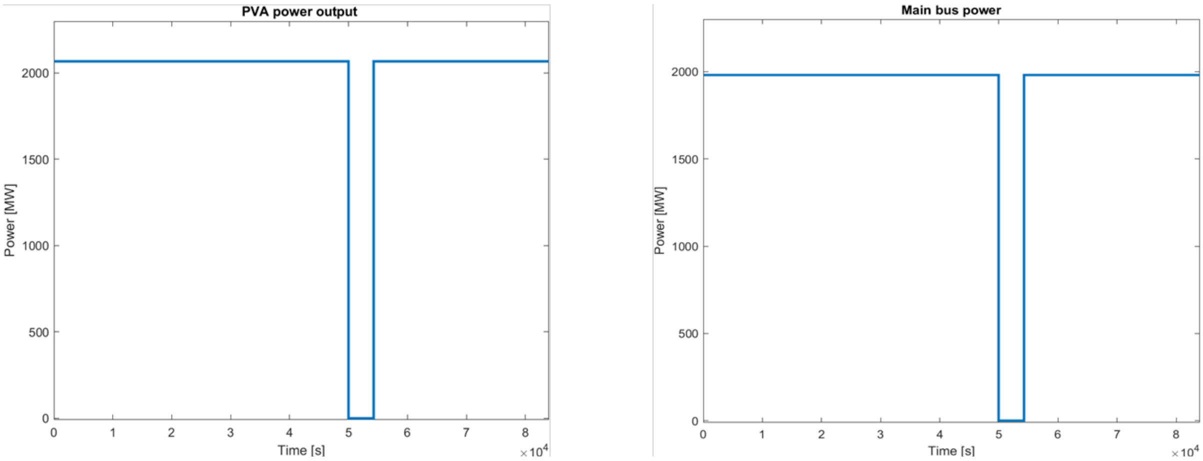

Figure 11-4 PVA power output (left) and Main bus power (right) during the worst day case

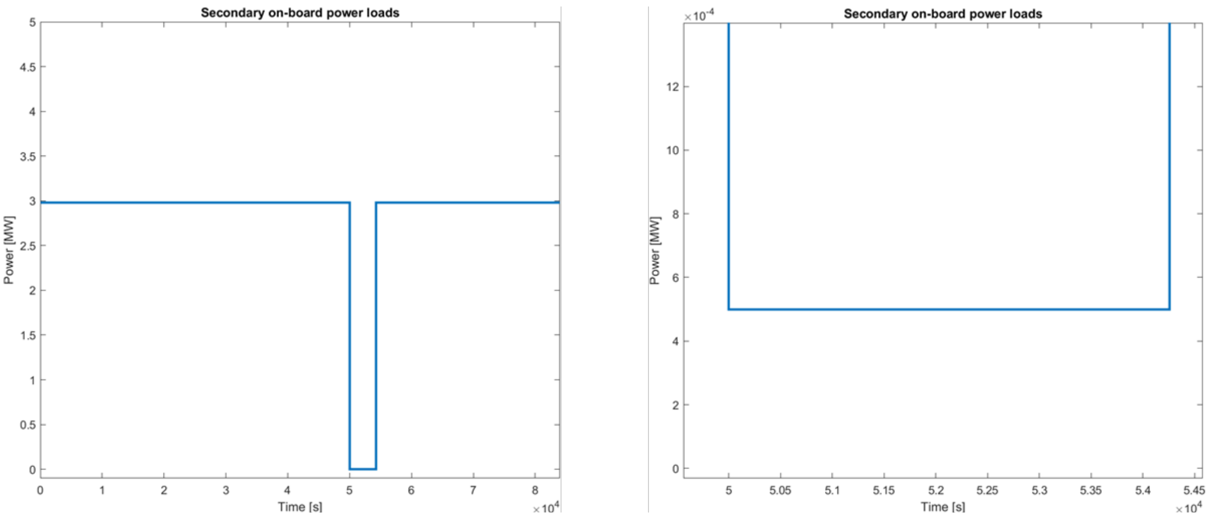

Figure 11-5 Secondary power loads on-board during the worst day case (right: detail of eclipse period)

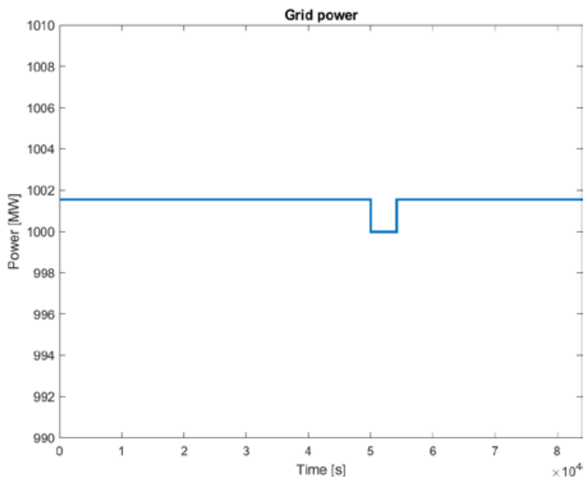

Figure 11-6 Grid power during a worst day case

Despite the 71-minute eclipse, as evident from Figure 11-6, the baseline of 1 GW of grid power is assured continuously throughout the worst day too. This is made possible by the ground-based super capacitors, which are activated when the SPS is not generating power.

11.3 Worst Case For Ecliptic Inclination

In Geostationary Orbit (GEO), the Solar Power Generator, represented by the solar panels, is positioned to continuously rotate around the North/South axis, ensuring it always directly faces the sun. The Solar Power Satellite, located on the celestial or equatorial equator, aligns the perpendicular to the plane of the solar panels with the equatorial plane. As a result, the angle at which the sun's rays arrive at the solar panels corresponds to the sun's declination.

The ecliptic plane, on the other hand, represents Earth's orbital plane around the Sun and is inclined to the equatorial plane at an angle of 23.4 degrees. This inclination causes the angle of incidence of the sun's rays on the solar panels to change with the sun's declination. For the purposes of this simulation, we have focused on assessing the impact on performance under the most challenging conditions, considering a 23.4-degree inclination.

In particular, in the subsequent figures, it is possible to observe the following power output profiles through a nominal day (but considering a 23.4-degree inclination of sun incident power):

- PVA output power;
- Grid power.

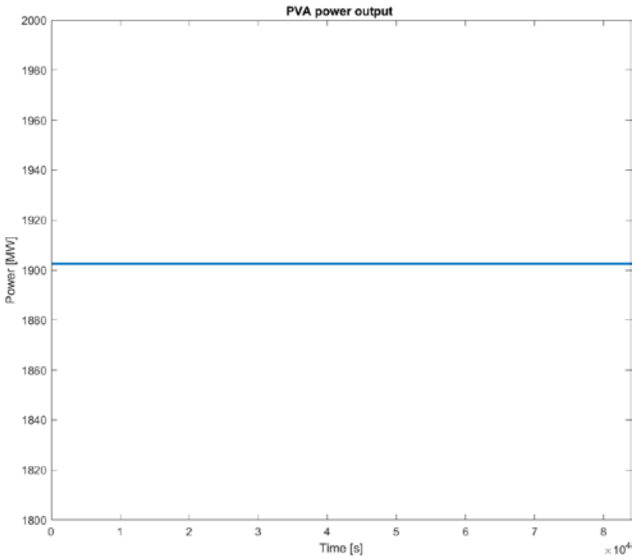

Figure 11-7 PVA power output in worst-case day for ecliptic inclination

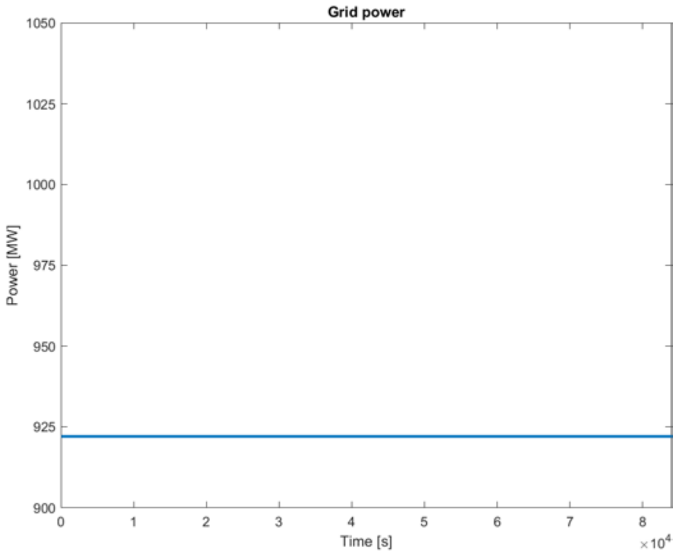

Figure 11-8 Grid power in worst-case day for ecliptic inclination

Looking at the last graph, one can see that the power loss is still acceptable and falls within the baseload power use-case definition of 1 GW + TBD%. In fact, this TBD can be quantified precisely by considering this worst-case as around 7%.

11.4 SPS Alignment Logic Simulation

Finally, a logical architecture is established to simulate retro-directive beaming and implement potential safety measures associated with misalignment of the SPS. This architecture allows to model a scenario in which the antenna power beam is aimed at the designated target (a GPS) but with a certain error, that exceeds acceptable safety thresholds.

In such cases, the antenna's central unit and the phase shifters collaborate to interrupt the power beaming if the angle error surpasses specified safety standards. As evident from the graphs below, it is possible to observe that the power generated by the Photovoltaic Assembly (PVA) is no longer transmitted to Earth due to the antenna's disconnection (in this simulation this period is 10 seconds).

Nevertheless, at ground level, the baseline power requirements for the grid, easily during brief intervals, can be compensated by the utilization of super capacitors. This provision of additional power facilitates the SPS in its process of realigning with the GPS centre through retro-directive beaming and AOCS.

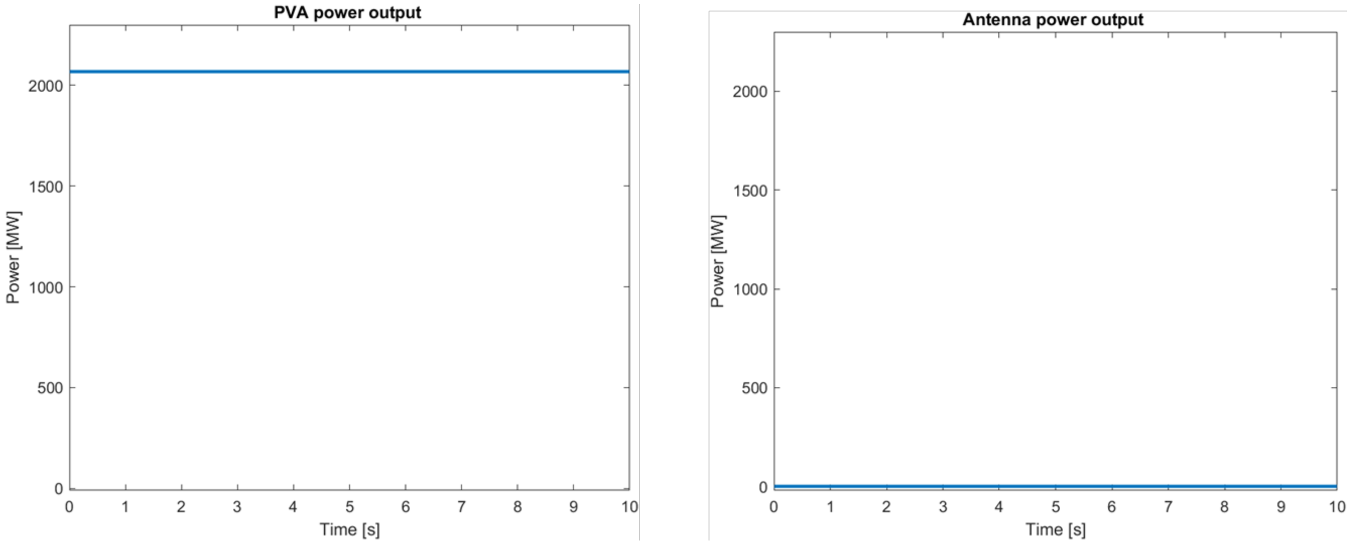

Figure 11-9 PVA power output (left) and antenna power output (right) during 10 seconds of SPS high misalignment

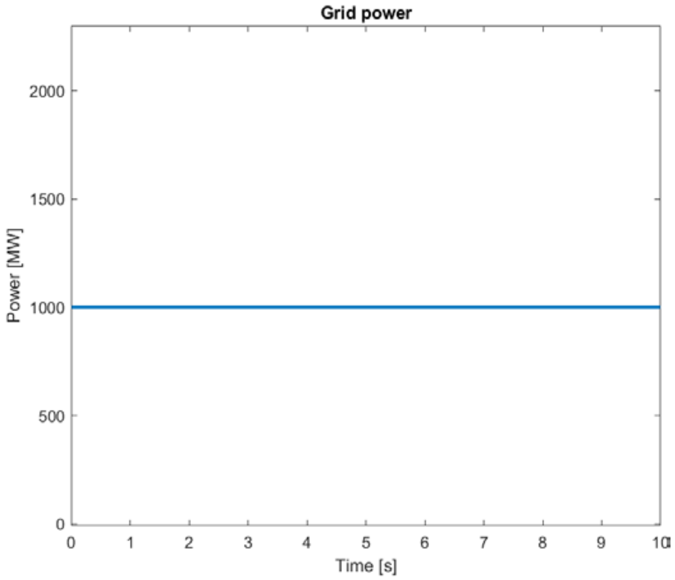

Figure 11-10 Grid power during 10 seconds of SPS high misalignment (compensated with super-capacitors)

12 Environmental Impact Analyses

Conducting a preliminary LCA for a space-based solar power mission is essential for understanding and mitigating potential environmental impacts. While it has limitations due to data uncertainty and the incomplete picture of the project, it serves as a valuable tool for early decision-making and promoting sustainability. As the project progresses, more detailed and accurate LCAs should be conducted to refine sustainability strategies applying [AD2].

To obtain an initial approximation of the GHG parameter (greenhouse gas emission), it is necessary to conduct a preliminary evaluation of the CO_2 for SBSP deployment considering mainly material productions and launches. To achieve this, the energy expenses associated with the SBSP mission are categorized into distinct macro-areas for estimation and the main formulas are implemented into the parametric model used also for energy investment calculations.

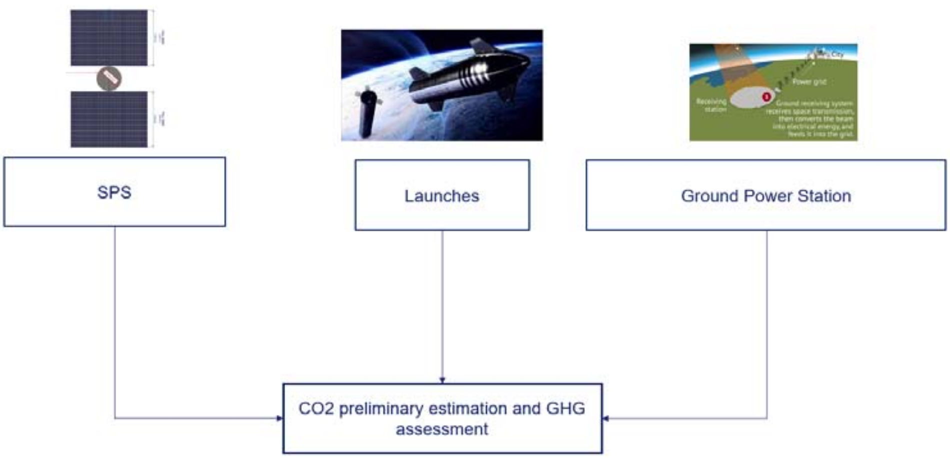

Figure 12-1 SBSP CO_2 production breakdown

12.1 Preliminary Assessment Of CO_2 Production For SBSP Mission

For what concerns the SPS, as for the energy investment calculations, it is plausible to assume that the platform predominantly consists of composites, aluminum or other more readily processed materials (60%), steel or materials akin to it (17%), silicon or similar materials (3%) and in the end perovskite for PV cells (20%). In particular, perovskite cells are surely greener solution when compared to other technologies such as Si-based solar panels.

With this foundation, considering the appropriate CO_2kg_{eq}/kg for every material, it is possible to calculate the preliminary estimated CO_2 production for the SPS parts production.

CO_2 for SPS materials production	**270 kt_{eCO2}**

Table 12-1 SPS materials production

The Ground Power Station, weighting approximately 2 kg per square meter, includes a steel mesh, minimal electronic components (e.g., diodes), and power cabling. For a 1 GW ground power station covering an area of approximately 34 km², this results in an estimated receiver mass of approximately 70000 tons. To simplify the calculation and avoid delving into intricate details, it is possible to assume that the GPS is primarily composed of steel or materials resembling it (80%), aluminum or other more easily processed materials (19%), and silicon or similar materials (1%). With this hypothesis, the CO_2 for the GPS materials production can be straightforwardly computed.

CO_2 for GPS materials production	**150 kt_{eCO2}**

Table 12-2 GPS materials production

Considering the input values provided by RFA and AG it is possible to estimate the total amount of CO_2 for launches, which is the predominant factor.

CO_2 for Launches	**12 109 kt_{eCO2}**

Table 12-3 Launches

12.2 Greenhouse Gas Emission Estimation For CO_2

Taking into account these preliminary evaluations, it is possible to calculate a first estimate of the GHG parameter for CO_2. This is evaluated as the total amount of CO2 divided for the energy provided during the entire SPS lifetime.

CO$_2$ for SBSP deployment	12 527 kt$_{eCO2}$
GHG (CO$_2$)	56 g$_e$/kWh

Table 12-4 GHG emission estimation

The preliminary result obtained is compatible with other energy sources already available on the market.

13 Energy & System Cost Analyses

All the cost evaluations reported in this chapter are based on assumptions taken from the relevant literature, including the cost-benefit analysis documents provided by ESA as input of the study (e.g. SOW RD1 and RD2). This cost assessment is not to be considered as a commitment on the part of Thales Alenia Space.

13.1 Methodology For SBSP Preliminary Cost Assessment

Many cost estimation methodologies employ mass-based (referred to as 'weight-based') cost estimation relationships (CERs), like the 'cost per kilogram' for a specific system or module. These CERs are influenced by various factors, including design complexity, similarities to other technologies and systems, etc.

Referring to the baseline CER mentioned above, the industrial history of the 20th century shows that, for a regularly produced item, there is a statistical correlation between the quantity of units manufactured and the anticipated change in the initial CER (for a single unit) as production quantities increase. This phenomenon, initially observed by Wright while employed at the Boeing Aircraft Company in the 1930s, is commonly referred to as the 'learning curve' (LC) or 'manufacturing curve'.

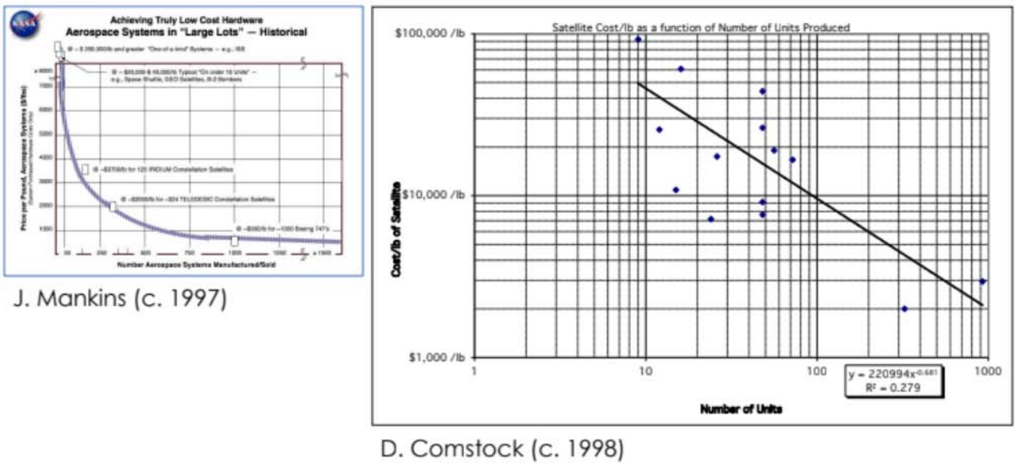

Figure 13-1 Examples of learning curve approach in space applications

The learning curve is a mathematical relationship that takes into account productivity improvement for larger number of produced units considering cost reductions due to the economics of scale, setup time and human learning as the number of units increase. The total production cost for N units (as showed in Figure 13-1) is modelled as follows [RD2]:

$$\text{Production Cost} = \text{TFU x L}$$

$$L = N^{B}$$

$$B = 1 - \frac{\ln(\frac{100\%}{S})}{ln2}$$

Where:

- TFU: Theoretical first unit cost;
- L: Learning curve factor;
- S: Learning curve slope, represents the percentage reduction in cumulative average cost when the number of production is doubled (it depends on the number of equal items is considered).

This approach, already used in several cost assessment for SBSP missions [RD1] [RD2], is the most suitable when considering very big and complex systems.

The SBSP mission costs are divided in four areas as shown below.

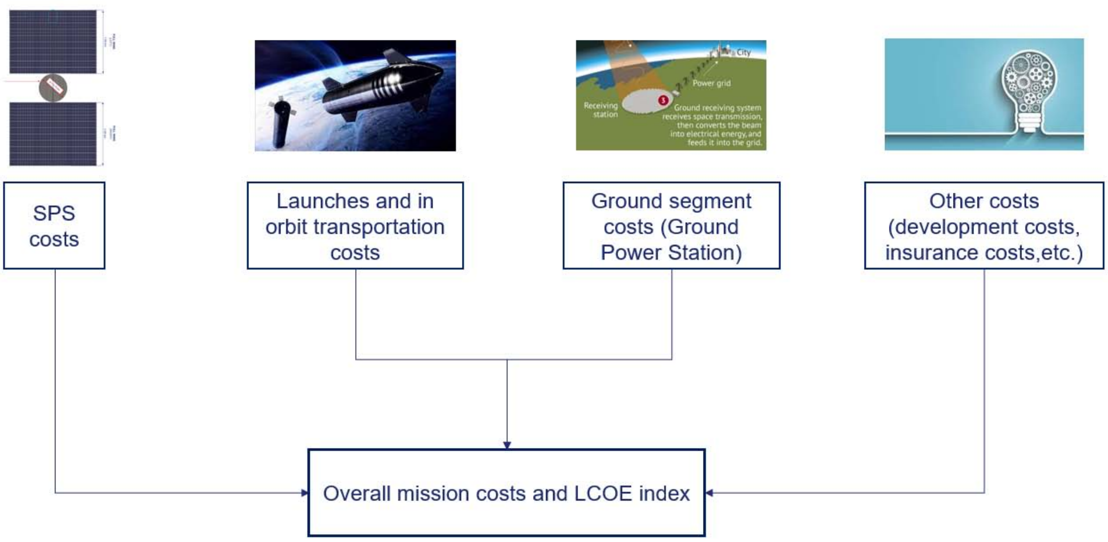

Figure 13-2 High level cost division

13.2 Costs Breakdown

The four main cost areas are analyzed considering for each area the different subdivisions and specializations. All the relationships are implemented in a parametric cost model (integrated within the SBSP Analysis Framework) allowing different sensitivity analysis for the main parameters affecting the overall mission costs.

Regarding the SPS costs, an high-level bottom-up approach is utilized to estimate the cost of each component type comprising the entire SPS.

Various cost estimation relationships (CERs) as cited in [RD1] and [RD2] are used to evaluate the expenses associated to each unit type. Subsequently, the learning curve approach is applied to derive an overall cost for each group of similar units within the system (which are listed in Table 13-1).

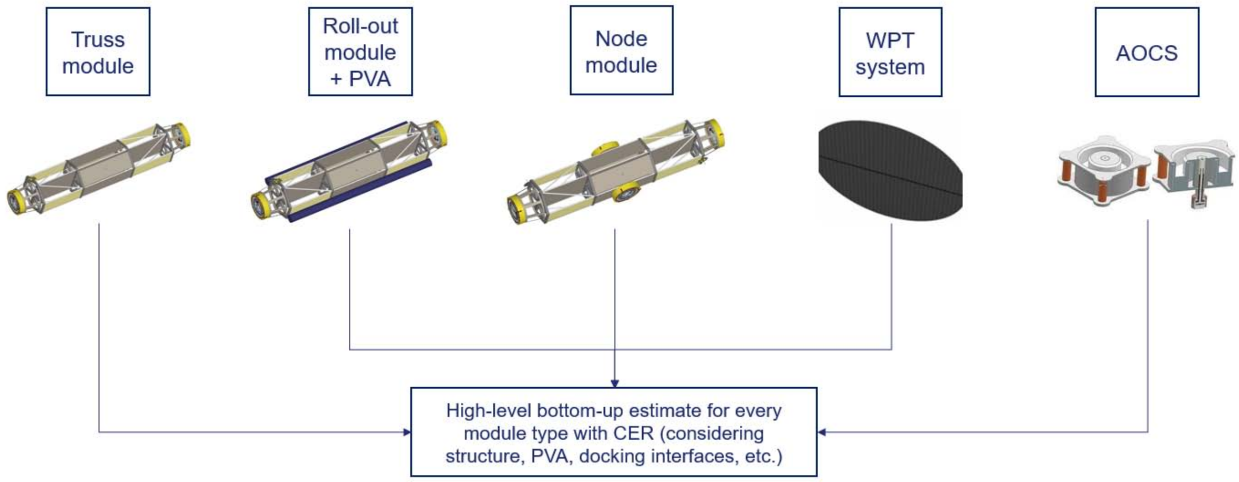

Figure 13-3 Main unit groups composing the SPS system

Unit Group	Cost
Truss modules	0.01 B$
Roll-out modules (with PVA)	0.18 B$
Node modules	0.002 B$
WPT system	0.50 B$
AOCS	1.43 B$
SPS cost	**2.06 B$**

Table 13-1 Summary results for SPS costs

Launch costs are, on the other hand, one of the crucial cost areas, contingent upon the assumptions under consideration. Extensive sensitivity analyses have been conducted in the relevant section to account for various parameters that could substantially influence launch expenses. A few notable factors include:

- Launch cost per kg [$/kg];
- Usable volume of the launcher fairing (considering 100 tons of maximum mass capability);
- Orbital tug mass;
- Type of manoeuvre considered for LEO-GEO transfers (impulsive or continuous);
- Specific impulse of propellant considered for the LEO-GEO transfer.

Launch costs	**3.31 B$**

Table 13-2 Launch costs

This value is computed considering the following assumptions on the driving parameters listed before:

- Launch cost per kg = 200 $/kg;
- Usable volume of the launcher fairing (considering 100 tons of maximum mass capability) = 100 %;
- Orbital tug mass = 60% of the launcher transportable mass;
- Type of manoeuvre considered for LEO-GEO transfers = continuous;
- Specific impulse of propellant considered for the LEO-GEO transfer = 1000 s (it could be possible considering higher values, however the assumption would be very strong in particular when considering time constraints in the problem for in-orbit transportation and assembly).

For in-orbit transportation from LEO to GEO a cost per kg of 100$/kg for the orbital tug utilization is estimated.

In-orbit transportation costs	**1.65 B$**

Table 13-3 In-orbit transportation costs

For Ground costs a series of values are considered in order to compute the final cost [RD1]. The most relevant are:

- Land occupation costs;
- Rectenna mesh costs;
- GPS power control costs.

Ground costs	**682 M$**

Table 13-4 Ground costs

Finally, a list of other costs are included in the SBSP cost model such as:

- Insurance costs (considering both launch insurance and satellite insurance [RD1]);
- OM costs (the yearly operational expenses of the system comprise two components: ground operation and satellite operation. These expenses are determined by applying the O&M Factor to the respective construction costs. [RD1]);
- AOCS refuelling launches;
- Assembly costs (considering a $/kg relationship for every robotic system needed on-board for assembly).

Other costs	**3.66 B$**

Table 13-5 Other costs

13.3 Cost Assessment & LCOE Results

Considering the cost breakdown presented above and a plausible estimation for launch costs (which will be further elaborated in appropriated sensitivity analyses), the total cost for a FOAK (First Of a Kind) SBSP system is evaluated.

Also the CAPEX (capital expenditure) and the OPEX (operational expenditure) are estimated considering an appropriate cost grouping showed below with the correspondent values (see Table 13-6).

<table>
<tr><th>Parameter</th><th colspan="4">Composition and value</th></tr>
<tr><td rowspan="11">CAPEX</td><td rowspan="5">SPS costs</td><td>Truss module costs</td><td>0.01 B$</td><td rowspan="11">7.71 B$</td></tr>
<tr><td>Roll-out modules (with PVA) costs</td><td>0.18 B$</td></tr>
<tr><td>Node modules costs</td><td>0.002 B$</td></tr>
<tr><td>WPT system costs</td><td>0.50 B$</td></tr>
<tr><td>AOCS costs</td><td>1.43 B$</td></tr>
<tr><td rowspan="3">Launch and in-orbit transportation/assembly costs</td><td>Launch costs</td><td>3.31 B$</td></tr>
<tr><td>In-orbit transportation costs</td><td>1.65 B$</td></tr>
<tr><td>Robotic hardware costs for assembly</td><td>0.004 B$</td></tr>
<tr><td rowspan="3">GPS costs</td><td>Land occupation costs</td><td>0.06 B$</td></tr>
<tr><td>Rectenna mesh costs</td><td>0.17 B$</td></tr>
<tr><td>GPS power control costs</td><td>0.36 B$</td></tr>
<tr><td rowspan="3">OPEX</td><td colspan="2">Insurance costs</td><td>1.7 B$</td><td rowspan="3">3.66 B$</td></tr>
<tr><td colspan="2">OM costs</td><td>1.6 B$</td></tr>
<tr><td colspan="2">AOCS thrusters refueling costs</td><td>0.36 B$</td></tr>
<tr><td>TOTAL SBSP MISSION COST</td><td colspan="4">11.4 B$</td></tr>
</table>

Table 13-6 : Cost assessment results

Considering these values, the LCOE is calculated, and its fluctuations are scrutinized in response to changes in the primary cost-driving parameters.

The levelized cost of electricity (LCOE) serves as a metric to assess the average net present cost of electricity generation for a given generator throughout its operational life. It proves very useful for investment planning and facilitates a consistent basis for comparing various electricity generation methods.

$$\mathrm{LCOE} = \frac{\text{sum of costs over lifetime}}{\text{sum of electrical energy produced over lifetime}}$$

While the sum of costs over lifetime has already been discussed, the total amount of energy produced over lifetime has not been discussed yet.

Considering a BOL (beginning of life) power delivered of 1 GW 24/7/365 (apart from the very short eclipse periods) and 30 years of SPS lifetime (UR-REQ-0070), the annual performance degradation rate is estimated to 1% in order to have a plausible estimate of the evolution of power produced over this timespan. This value is considered due to:

- 0.1-0.5 %/year expected radiation degradation ratio for perovskite cells. This value is based on recent laboratory tests assessing perovskite radiation resistance. Notably, research conducted by Sydney University highlights the remarkable potential and viability of "self-recovery" in perovskite cells through the strategic use of specific dopants. The selection of the right dopant could have the dual benefit of limiting radiation damage and enabling cells to undergo a "self-healing" process through TV treatment, ultimately restoring their Power Conversion Efficiencies (PCEs). Further exploration of this potential could mark a pivotal moment in PV space applications, such as SBSP, by curbing the rate of system performance degradation;
- Possible system failures, debris impacts or space weather events, which could affect system performances. However, it is to be expected that a fully developed system will have a comprehensive in-orbit maintenance and resupply programme. This should be fundamental to reduce the impact on system capacity factor in a long lifespan such as the one considered for an SPS.

According to the above considerations and given the assumptions taken for system costs (further LCOE sensitivity analyses will be showed in the paragraph 13.6) the following LCOE is obtained for a FOAK SBSP system:

Parameter	Value	
Expected energy generated over the system lifetime	Lifetime = 30 years 1 %/year degradation rate 1 GW 24h 365 days BOL	**223.4 TWh**
LCOE	**158 $/MWh (≈ 15.8 ₵/kWh)**	
LCOE for the 10th of a kind SBSP system	**143 $/MWh (≈ 14.3 ₵/kWh)**	

Table 13-7 Total energy delivered and LCOE results

The LCOE for the 10^{th} of a kind SBSP system is also computed and reported in Table 13-8

Parameter	Value

LCOE for the 10th of a kind SBSP system	**143 $/MWh (≈ 14.3 ₵/kWh)**

Table 13-8 : LCOE result for 10th of a kind system

The resulting LCOE are calculated using a 15% discount rate, a reasonable choice given the complexity and uncertainties associated with the SBSP project. Nonetheless, a dedicated sensitivity analysis is performed to assess the impact of this value, considering that various studies have explored a range of discount rates from 10% [RD2] to 20% [RD1].

A discount rate is a financial metric used to evaluate the present value of future cash flows or benefits. It represents the rate of return required to make an investment or project's net present value equal to zero. In other words, it reflects the opportunity cost of allocating resources to a specific project or investment rather than pursuing alternative opportunities with a similar level of risk. The discount rate is a critical component in financial decision-making, cost-benefit analysis, and investment appraisal, helping to account for the time value of money and assess the attractiveness of an investment or project over time. It is typically expressed as a percentage or a decimal.

The results obtained for the LCOE are competitive with respect to other energy sources now available.

13.4 FOAK vs NOAK System Costs

To attain the baseload objectives for achieving net zero emissions in Europe by 2050, multiple SBSP system need to be deployed. It is reasonable to anticipate that, as the number of SPS deployed increases, the cost per satellite is likely to decrease so as the cost per SBSP mission.

The learning curve approach is applied to assess a preliminary estimation of what could be the cost for an n-of-a-kind (NOAK) system with respect to a first-of-a-kind (FOAK), which have been calculated in the section 13.3. The slope of the curve applied for these calculations is 0.90 [RD2], which is a credible assumption based on the experience gained from more than 10 SPS deployments. Consequently, for cases involving fewer than 10 systems, a slightly more conservative curve slope of 0.95 is adopted (see Table 13-9). For what concerns the cost per SBSP mission for the NOAK, the learning curve is applied only to the hardware costs (and not for example launch or orbit transportation costs).

Number of SPS	Cost per SPS [B$]	Cost per SBSP mission [B$]
1	2.06	11.4
5	1.81	11.0
10	1.43	10.5
30	1.25	10.3
50	1.15	10.1
86	1.05	10

Table 13-9 Results of learning curve approach for multiple SPS deployment

13.5 Energy Investment & ERoEI assessment

After having calculated the energy delivered during SPS lifetime, a critical performance indicator for sustainable energy systems revolves around the speed at which the energy needed to manufacture and install the system can be recovered once the system becomes operational; this metric is commonly referred to as the "energy payback time" (EPBT).

Furthermore, the comprehensive energy commitment required to establish a SBSP mission in comparison to the energy yield over the SPS's operational lifespan serves as a pivotal measure for evaluating the feasibility of the concept in relation to alternative energy sources. This parameter is commonly known as ERoEI (Energy Return on Energy Invested). This value is a derivation of the RoI economic parameter for energy investment applications.

To obtain an initial approximation of these two metrics, conducting an essential preliminary evaluation of the energy investment for SBSP is imperative. To achieve this, the energy expenses associated with the SBSP mission have been categorized into distinct macro-areas for estimation and the main formulas have been implemented into the parametric cost model (see Figure 13-4).

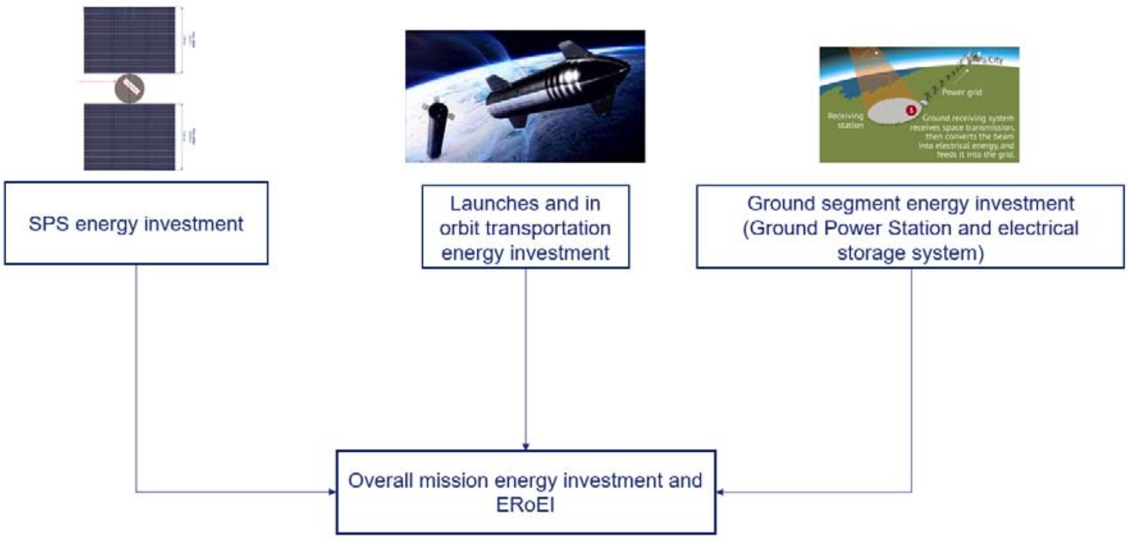

Figure 13-4 SBSP energy investment breakdown

For what concerns the SPS, without delving into intricate specifics, for the purpose of this computation, it is plausible to assume that the platform predominantly consists of composites, aluminum or other more readily processed materials (60%), steel or materials akin to it (17%), silicon or similar materials (3%) and in the end perovskite for PV cells (20%).

With this foundation, considering the appropriate kWh/kg for every material, it is possible to calculate the estimated energy cost for SPS.

SPS energy investment	**789 GWh**

Table 13-10 SPS energy investment

The Ground Power Station, weighting approximately 2 kg per square meter, includes a steel mesh, minimal electronic components (e.g., diodes), and power cabling. For a 1 GW ground power station covering an area of approximately 34 km², this results in an estimated receiver mass of approximately 70000 tons. To simplify the calculation and avoid delving into intricate details, it is possible to assume that the GPS is primarily composed of steel or materials resembling it (80%), aluminum or other more easily processed materials (19%), and silicon or similar materials (1%). With this hypothesis, the estimated energy cost for the GPS can be straightforwardly computed.

GPS energy investment	**3209 GWh**

Table 13-11 GPS energy investment

In the available literature, it is well documented that the production of each kilowatt-hour (kWh), equivalent to approximately 10 kg of Lithium-Ion battery, requires around 55-65 kWh of energy. For a system with the capacity to store approximately 1,120,000 kWh (equal to 1 GW for 71 minutes, the maximum duration of shadowing of GEO at the Equinox) the energy investment can be calculated with the previous numbers.

Electrical storage system energy investment	**58 GWh**

Table 13-12 ESS energy investment

As mentioned earlier, the cost model includes a dedicated section aimed at assessing the number of launches required for the entire payload and the propellant necessary for transferring and assembling the SPS in GEO. This evaluation takes into account various inputs such as the type of maneuver for LEO-GEO transfer, specific impulse, and the mass of the propulsion system.

Utilizing the preliminary estimation, and considering Methane and LOX as the launch propellants (with quantities of 1000 tons and 3600 tons per launch for a heavy reusable two-stage launcher with a maximum cargo capacity of 100 tons), along with the established energy content values for these propellants in kWh, the launch energy investment required has been estimated. This calculation is based on the total number of launches and follows the same assumptions applied in calculating the LCOE.

Launches energy investment	**3179 GWh**

Table 13-13 Launches energy investment

Finally, the last energy investment area is the in-orbit transportation. It is plausible to consider the kinetic energy of every single transfer from LEO to GEO (about 4.5 km/s for Edelbaum approximation in case of continuous maneuver) of the orbital tug with the correspondent payload and an inefficiency of about 50% of the overall energy produced. Considering this approach, it is possible to have a preliminary estimate of the in-orbit transportation energy investment needed (considering the same assumptions as for the LCOE calculations).

In-orbit transportation energy investment	**62 GWh**

Table 13-14 In-orbit transportation energy investment

After having analyzed the entire energy cost breakdown, the main results are showed below:

Parameter	Formula	Value
SBSP Energy investment (e.i)	SPS e.i + GPS e.i + Electrical storage system e.i + Launches e.i + In-orbit transportation e.i	**7.30 TWh**
EPBT	SBSP Energy investment / Energy delivered per day	**300 days**
ERoEI	SBSP Energy returned / SBSP Energy investment	**31: 1**

Table 13-15 Final energy analyses results

With respect to other renewable technologies such as PV farms, the EPBT is minimal, making clear the possible advantages of SBSP and its economic potential:

Energy Investment Item	Winter Case (Overcast 7 day)	Summer Case (Overcast 1 day)
Ground PV System		
PV Array	– 756,800,000,000 kWh	– TBD kWh
Energy Storage System	– 336,000,000 kWh	– TBD kWh
Energy Produced per Day	+ 48,000,000 kWh / day	+ 48,000,000 kWh / day
Energy Payback Time	~40 Years	~6 Years

Table 13-16 EPBT example for solar farms on Earth

13.6 Cost & Energy Investment Sensitivity Analyses

The LCOE value presented for our SBSP concept is very sensitive to certain parameters, which make the final mission costs quite complex to assess.

For this reasons, it becomes fundamental to have some cost sensitivity analysis taking into account the main cost driving parameters and the ones with the largest uncertainty. These parameters are listed below (with the respective plausible ranges) and a sensitivity analysis have been performed for each one:

- SPS mass [20% +100%] (with respect to baseline mass)

- Usable volume of the launcher fairing : [10% - 100%];
- Tug mass percentage with respect to transportable mass : [10% - 200%];
- Tug propulsion system specific impulse [400 s – 3000 s];
- Specific cost per launch [100 $/kg – 1500 $/kg];
- System Lifetime [15 years – 40 years];
- Performance degradation rate during SPS lifetime [0.1% - 2%];
- Learning curve slope for roll-out module group cost estimation [0.75 - 0.95];
- Discount rate [10% - 20%].

In the following sensitivity analyses the LCOE and/or ERoEI variations w.r.t. the parameters listed above will be shown in a graph. When selecting a parameter to be analyzed the others will be fixed according to the assumptions reported in section 13.2 and 13.3.

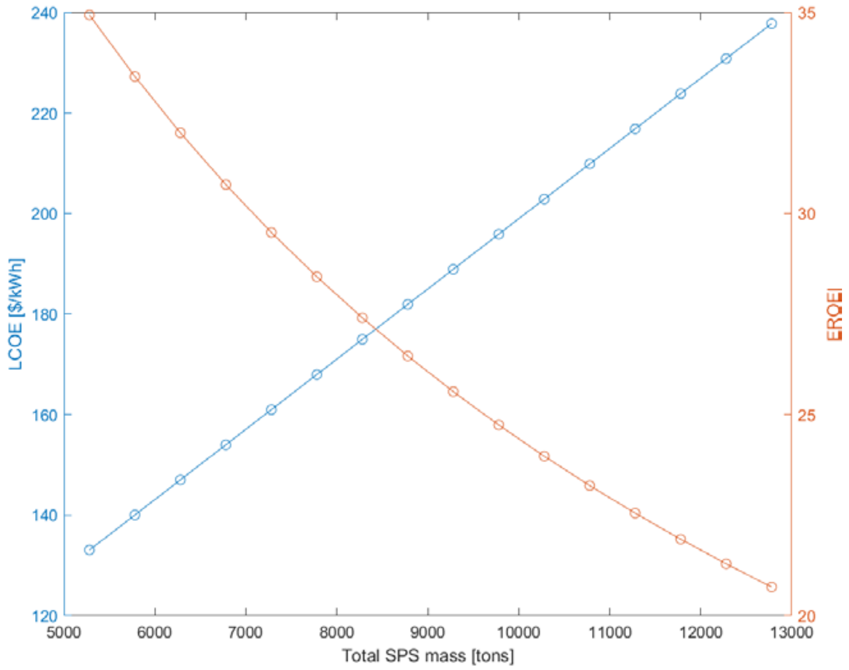

Figure 13-5 LCOE and EROEI as functions of SPS mass

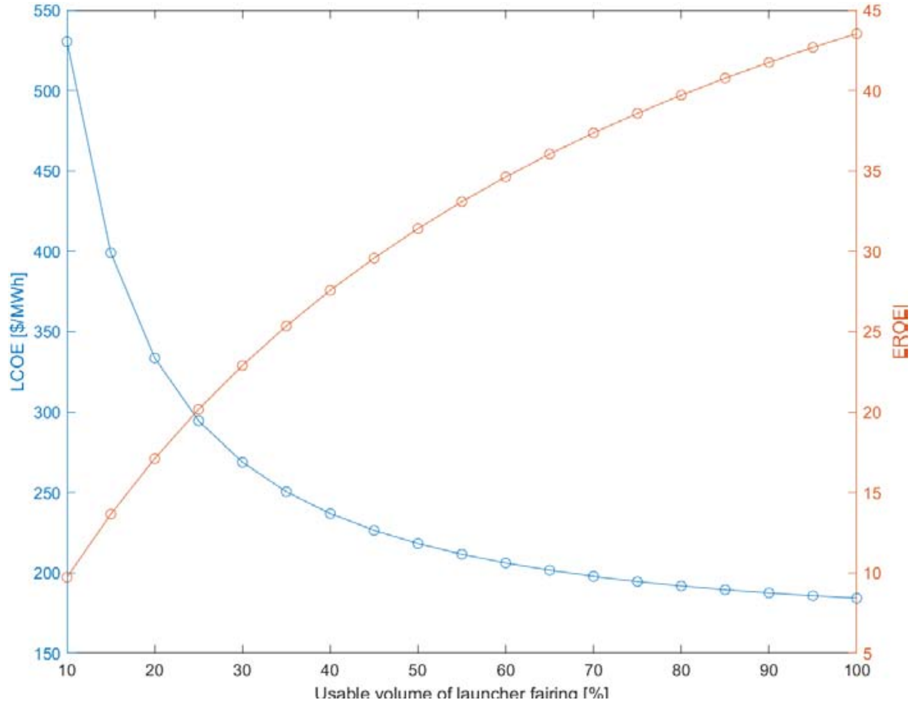

Figure 13-6 LCOE and EROEI as functions of usable volume of the launcher fairing

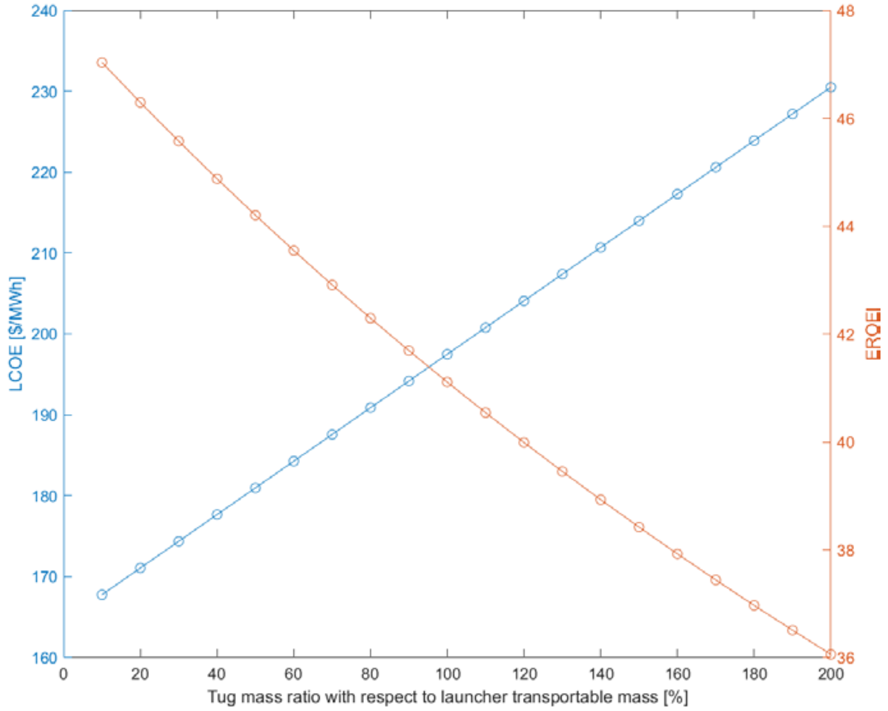

Figure 13-7 LCOE and EROEI as functions of Tug mass ratio with respect to transportable mass

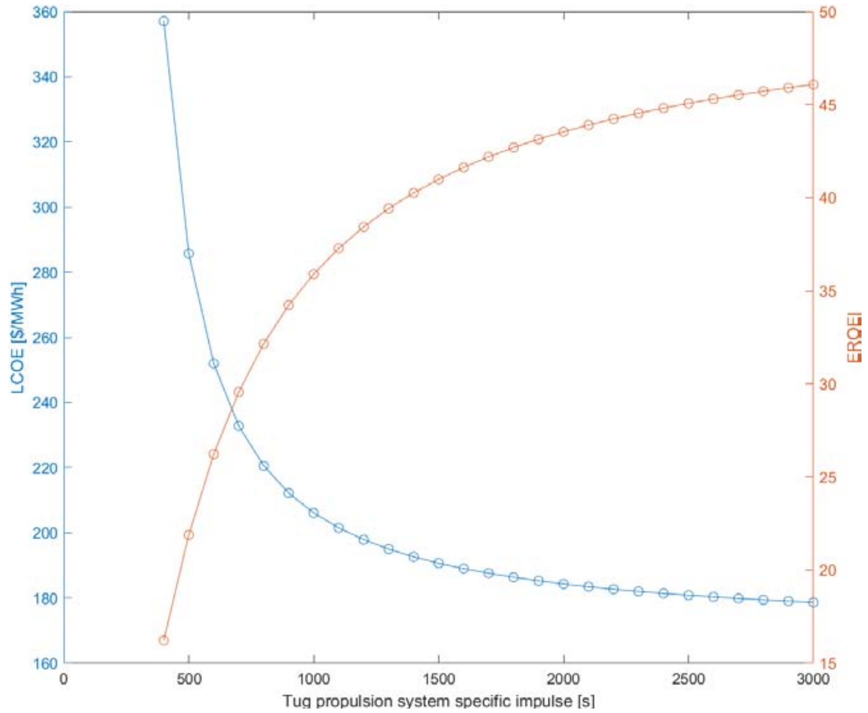

Figure 13-8 LCOE and EROEI as functions of Tug propulsion system specific impulse

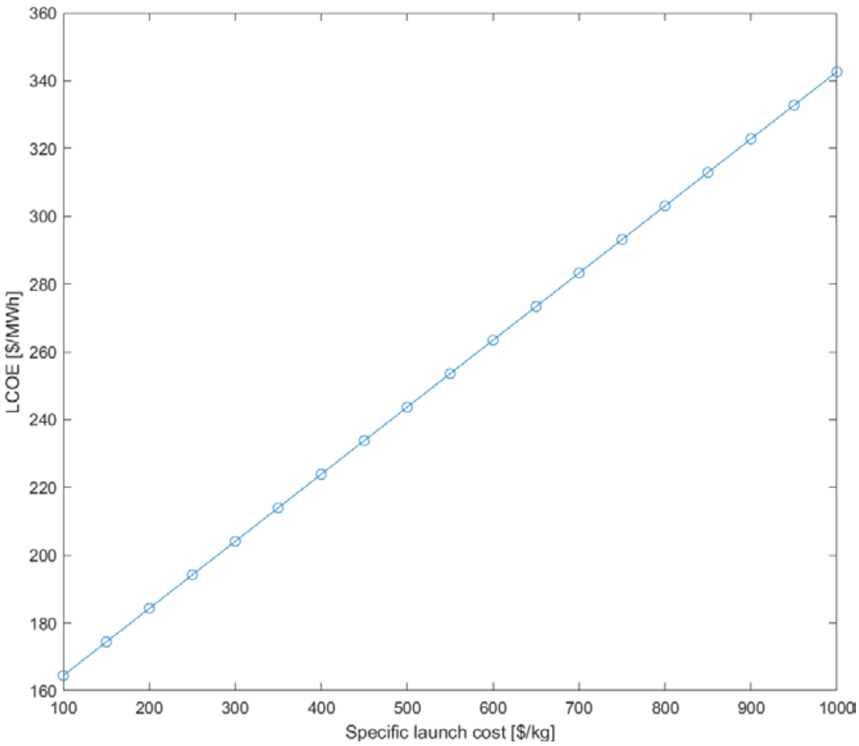

Figure 13-9 LCOE as a function of specific cost per launch (considering launch cost to LEO)

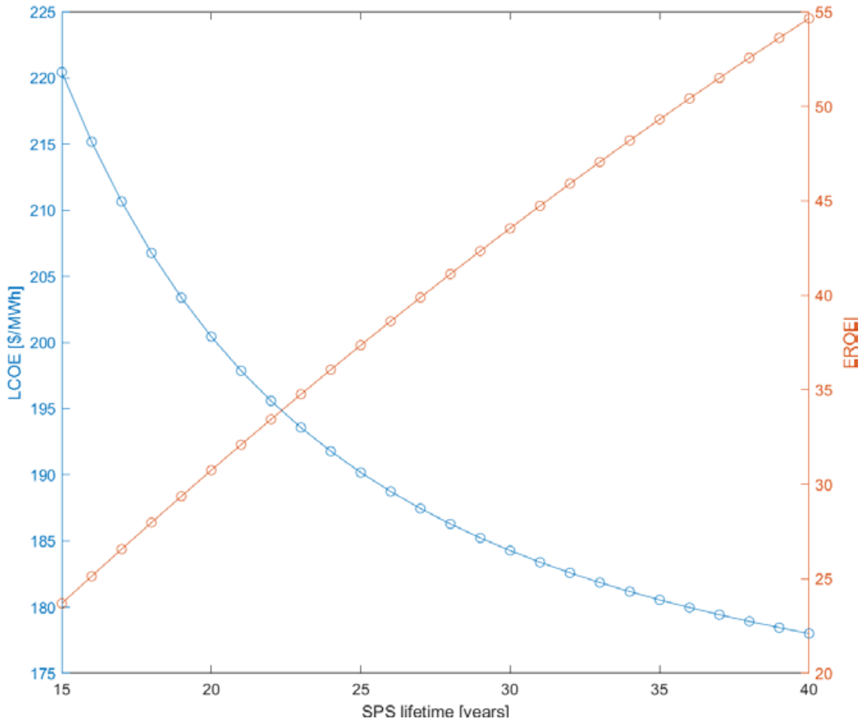

Figure 13-10 LCOE and EROEI as functions of SPS lifetime

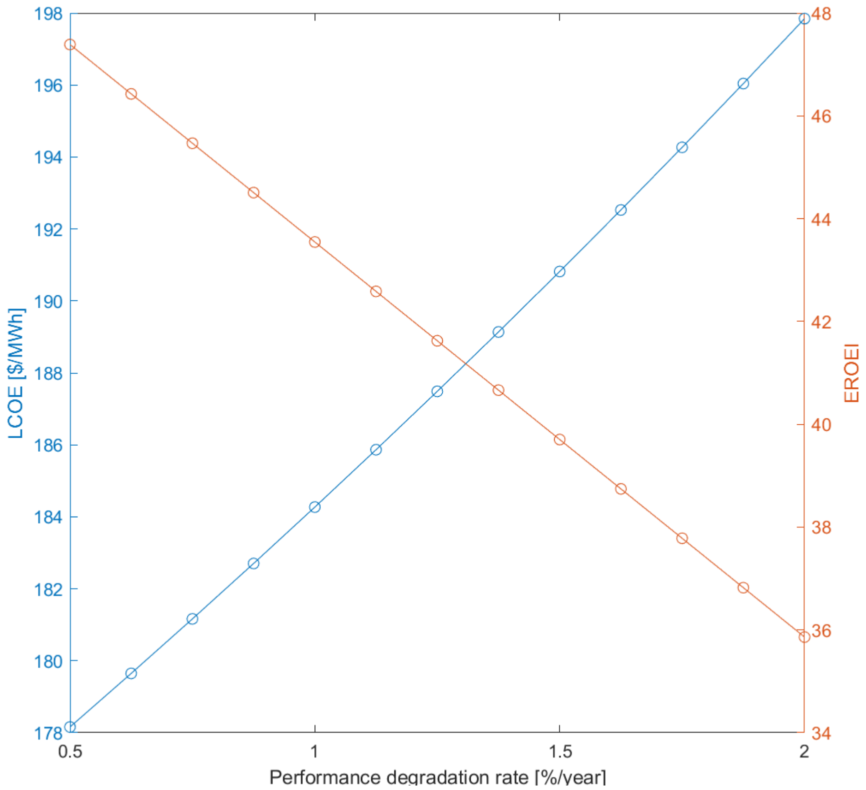

Figure 13-11 LCOE and EROEI as functions of SPS performance degradation rate

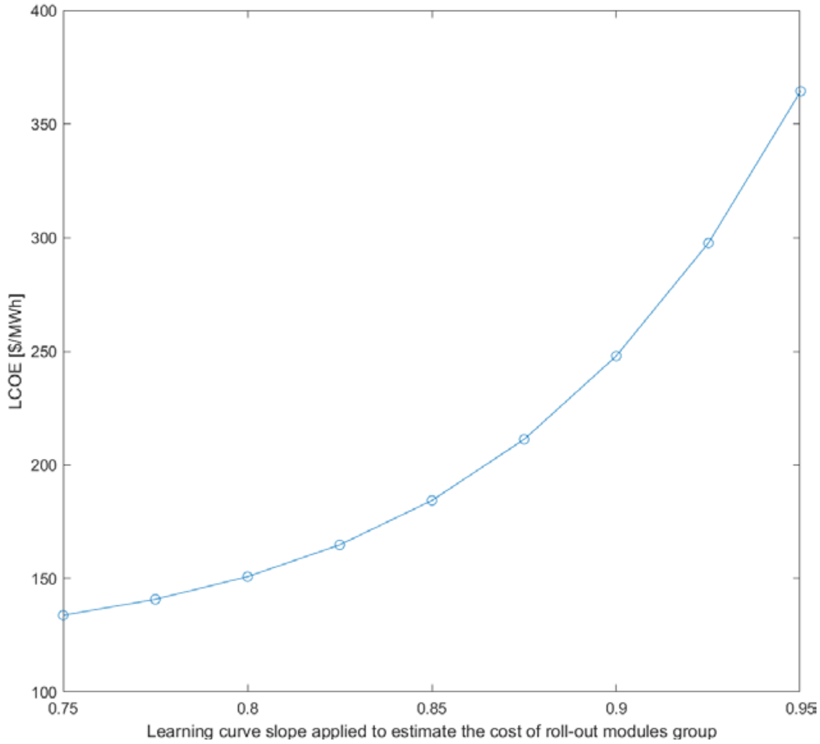

Figure 13-12 LCOE as a function of learning curve slope applied to estimate the cost of roll-out modules group

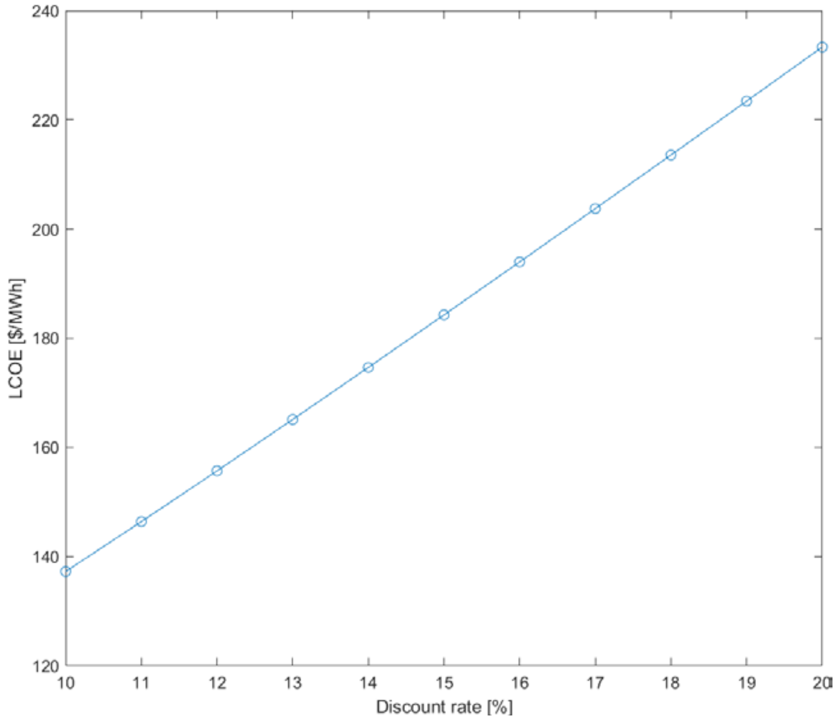

Figure 13-13 LCOE as a function of discount rate

14 Programmatic Aspects

14.1 Business Case Confirmation

The System proposed is compliant with the reference use case as discussed with the stakeholders. Moreover the competitive LCOE proves that the technology can be technically and economically viable in the future energy mix.

14.2 SBSP Roadmap

The SBSP development roadmap towards a commercial scale SBSP system development, including major demonstrators along the way, proposed by our Consortium is shown in Figure 14-1.

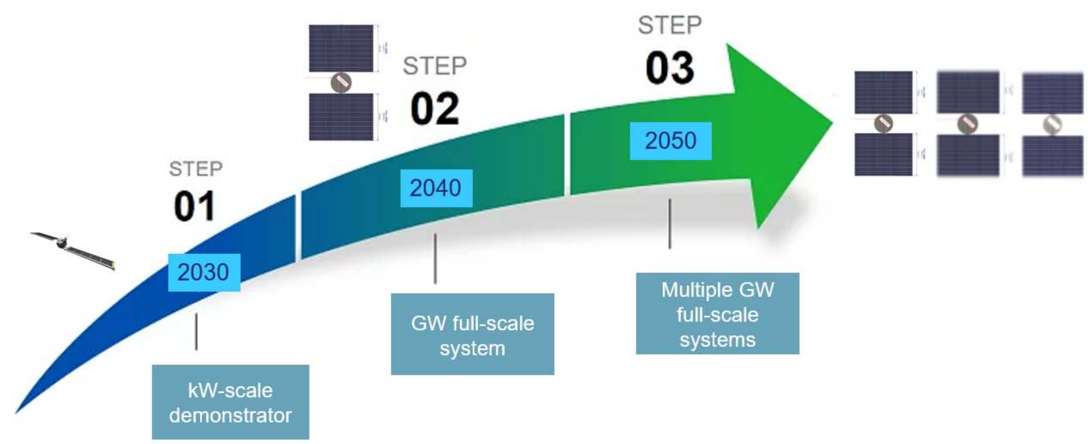

Figure 14-1: SBSP Roadmap

14.3 SBSP Preliminary Risk Analysis

This preliminary risk assessment is based on the SBSP architecture elaboration performed in Chapter 6. The risk register contains the following details for each risk:

- Risk ID/number;
- Risk title and scenario description;
- Risk evaluation in terms of Severity and Likelihood and resulting Risk Index;
- Type of Risk;
- Mitigation/recovery actions (“Pr” when the action is intended for reduction of probability, “Gr” when the action is intended for reduction of gravity/severity).

Additional non technical risks to be considered (not part of the risk register provided in Table 14-1) are the following:

- *The safety of the system and equipment* – for example the effects on other spacecraft (in lower orbits) of passing through the RF power beam and the tolerance of the satellite to debris, including the prevention of debris shedding;

- *Safety of people and wildlife* – agreements on acceptable safe RF beam intensity, both above and outside the rectenna, and strategies to ensure safety if beam lock lost and beam wanders off the rectenna will be required;
- *Environmental* – the effects of microwaves on flora, fauna, and the atmosphere, as well as carbon intensity will need to be better understood;
- *Standards* – a new energy generation technology will require new standards, especially the formation of international standards to allow interoperability between sub-system elements;
- *Security* – to maintain control of the satellite and the beam, ensuring security of a critical national infrastructure;
- *Public acceptability* – There will need to be a properly coordinated information programme to that the public receive the appropriate information so they can make informed decisions rather than be influenced by conspiracy theories.

Risk Number	Risk Title	Risk Scenario	Severity	Likelihood	Index	Type of Risk	Actions
Risk 3	Modular large-scale phased array antenna for highly efficient wireless power transmission	Technology to build large phased array antenna in-orbit not able to be achieved in time.	5	B	10	Technical	Pr: extensive technology development and demontrations required
Risk 1	Perosvkite development and qualification	Perovskite cell technology development delay resulting in schedule impact. So more massive cell techology need to be adopted resulting in mass increase and impact on economic feasibility.	5	B	10	Technical	Pr: extensive technology development and demontrations required Gr: identify alternative design solution
Risk 6	On-orbit robotic assembly technology	Capability to perform large-scale robotic assembly efficiently and affordably is not achieved	5	B	10	Technical	Pr: extensive technology development and demontrations required
Risk 7	Development of flexible structure that can be controlled by AOCS	Controllable lighweight flexible structure cannot be achieved resulting in mass increase for stiffness	5	B	10	Technical	Pr: extensive technology development and demontrations required Gr: identify alternative design solution
Risk 2	Launcher availability	If high cadence heavy-lift low-cost launcher is not available the concept cannot be economically viable.	5	A	5	Technical	Pr: start development of new european launcher as soon as possible
Risk 4	Succeptibility to orbital debris and production of debris	Design solution to protect against orbital debris and production of debris may result in substantial mass cost increase	4	B	8	Technical	Pr: extensive technology development and testing required
Risk 5	Cyberattacks actions	Cyberattack resulting in taking control of the SBSP system inducing off-nominal power beaming or interruptions	4	A	4	Technical	Pr: implement cybersecurity policies in SW/HW design for both space and ground segment Gr: monitor the System and plan contingency operations (e.g. switch-off power beaming) if any attack is detected

Table 14-1 Risk Register

15 Recommendations for Sub-Scale Demonstrator Mission

When dealing with an SBSP demonstrator, it is necessary to reconsider and adapt several key functions and assumptions from the full-scale system to a sub-scale system. The aim of the demonstrator is to prove the feasibility of wireless power transmission from orbit to Earth incorporating and validating as many of the technologies of the full-scale SBSP system.

The following three primary functions of the SBSP energy chain are still valid when addressing sub-scale systems:

- Converting solar power to DC power: accomplished through PV panels;
- Converting DC power to RF power: carried out by an antenna equipped with DC-RF converters;
- Converting RF power to DC power: fulfilled by a Ground Power Station equipped with rectenna (RF-DC converters) mesh.

The first two functions are part of the SPS demonstrator platform, while the third function involves a Ground Power Station that receives the power beaming and converts it into DC power.

The three main system areas that define the SBSP sub-scale system, as for the full-scale system, are:

- PV area;
- On-board antenna area;
- GPS area.

The relationship between the on-board antenna area and the GPS area is influenced by three interrelated factors that necessitate re-evaluation for the sub-scale system:

- Orbit altitude
- Transmission frequency
- Beam collection efficiency (the proportion of the emitted power beam from the antenna that is intended to be captured on ground)

Clearly, the beam collection efficiency, as well as other efficiencies like the RF-DC conversion efficiencies, will affect the total PV area needed.

These aspects will be explored in the following sections in order to highlight the differences between the SBSP demonstrator and the full-scale SBSP system.

15.1 Orbit Selection

In the frame of the demonstrator mission, the key function of the system is to validate technologies trying to scale down each subsystem with the aim to reduce costs as much as possible. Startin from these considerations there are many reasons, listed below, that suggest to transition from a GEO to a LEO operational orbit:

- With no continuous baseload power transmission requirement, the orbit is not bound to the visibility time of the GPS. This allows to take advantage of any orbit with a ground-track that passes on the GPS, so it is possible to pick lower orbits w.r.t. GEO, greatly reducing the energy required to bring the SPS in its operational orbit;
- Considering that antenna area and GPS area are proportional to their reciprocal distance, reducing the orbit's altitude will allow for an overall smaller system;

- As the ground area required to capture the main lobe of the radiated RF beam depends on the elevation angle, transmitting only during the SPS passes on top of the GPS allows to minimize the GPS area.

With these considerations in mind there are two possible options for the operational orbit: a repeating SSO or a LEO orbit.

The main advantage of the repeating SSO is to always have the satellite on top of the GPS when not in eclipse and at the desired time. It is also possible to pick orbital parameters to choose the days between two equal passes. Two examples of orbital parameters are the following:

Altitude [km]	Inclination [deg]	Repeat cycles [days]	Number of revolutions
624	97.7	5	74
485	97.2	4	61

Table 15-1 Examples of repeating SSO orbital parameters

The main disadvantage lies in the higher amount of station-keeping and the higher energy required to bring the spacecraft in orbit w.r.t. a lower inclination orbit.

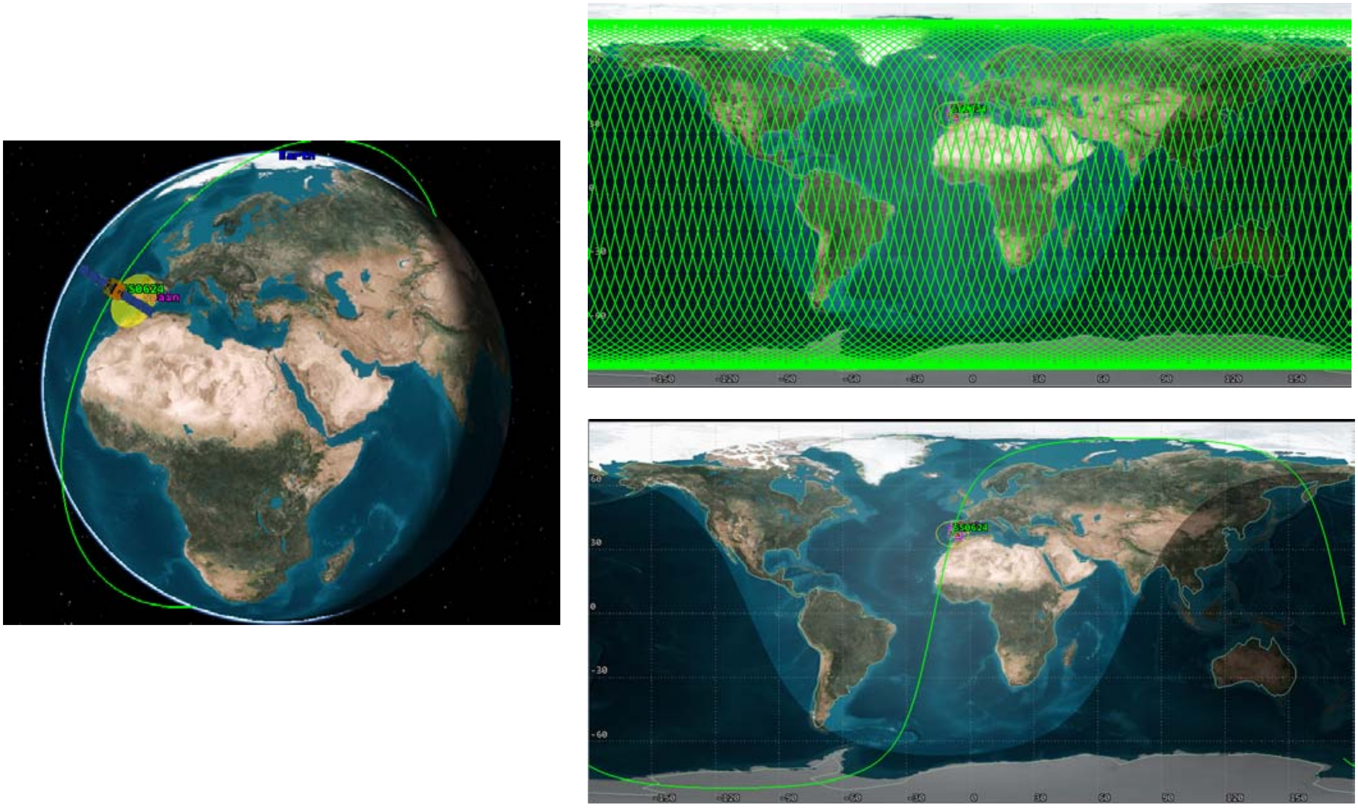

Figure 15-1 Example of repeating SSO orbit

Concerning the LEO orbit, the only requirement is to have an inclination at least equal to the latitude of the GPS. This in order to have the satellite on top of the GPS for at least one orbit. It is suggested to keep the idea of the repeating ground-track to ensure that the satellite will pass on top of the GPS multiple times. The main disadvantage is the possibility to have passes above the GPS during eclipse, thus having unusable passes.

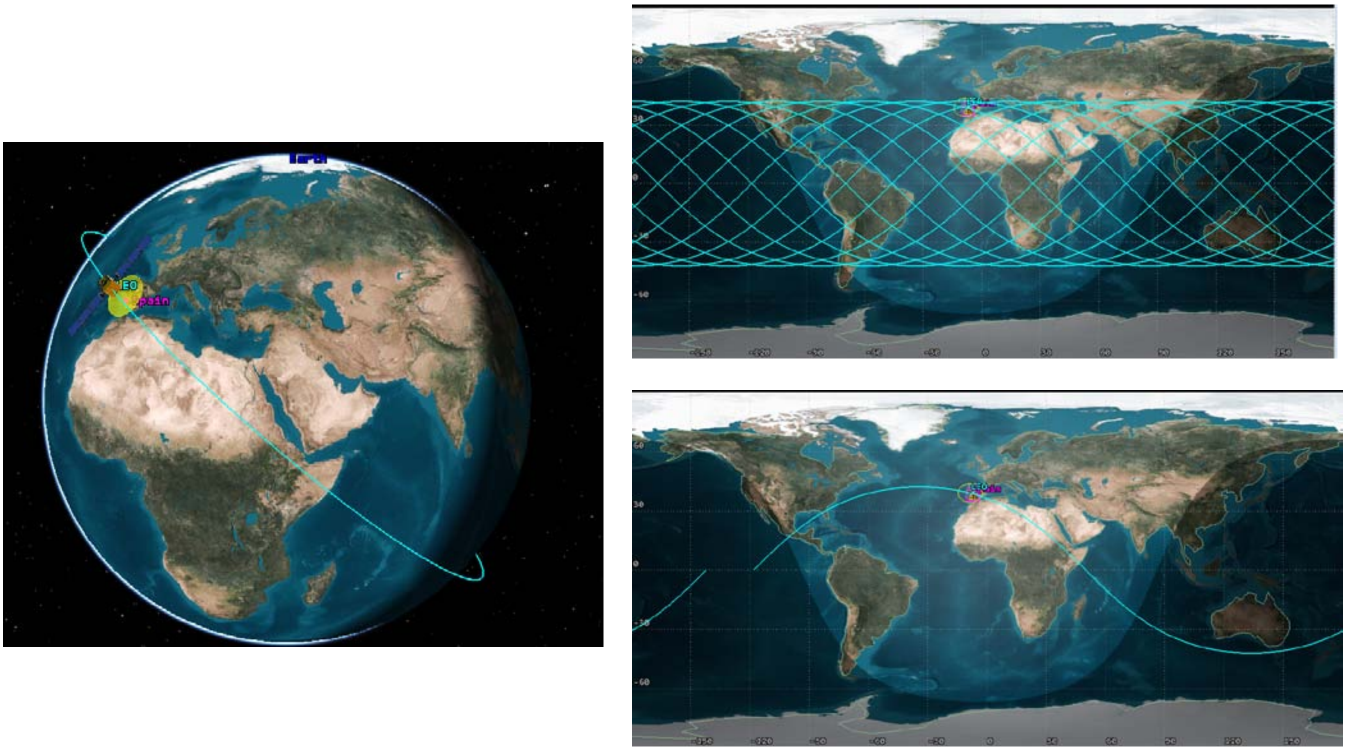

Figure 15-2 Example of repeating LEO orbit

Both options are feasible, so the choice will heavily depend on the demonstrator mission requirements. The orbit's altitude will depend on the required beaming time: the higher the orbit the higher the amount of beaming time per orbit.

15.2 Transmission Frequency

Given the shorter development timeline available for the SBSP demonstrator compared to the full-scale system, the frequency selection of 5.8 GHz adopted for the full-scale system need to be reassessed.

For this assessment the projected curves for DC-RF and RF-DC conversion efficiencies need to be taken into account (e.g., rectenna efficiencies depicted in Figure 2.1). In the context of a shorter-term solution an ad-hoc frequency rationale is necessary.

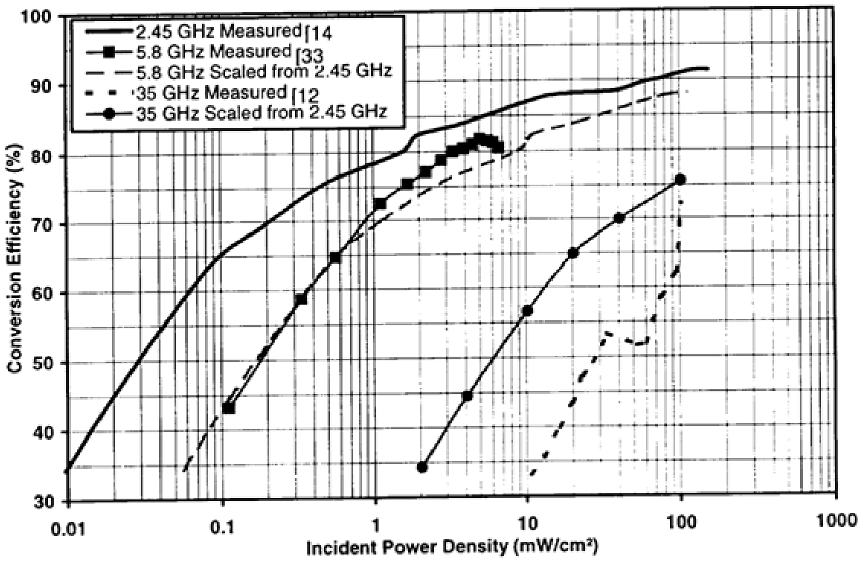

Figure 15-3 Rectenna efficiency curves

From a technological readiness perspective, achieving higher efficiencies is likely to be more attainable when dealing with lower frequencies than 5.8 GHz, such as 2.45 GHz.

This holds particularly true when addressing situations involving very low incident power density. As will be elaborated upon in Section 2.3, the RF-DC efficiency significantly diminishes when dealing with lower power densities, a scenario encountered in a demonstrator where reduced power levels are validated.

Furthermore, this effect becomes more pronounced when working with higher frequencies, as clearly illustrated in Figure 15-3. Hence, it is advisable, especially for an first demonstrator mission, to incorporate DC-RF technologies akin to those in the full-scale system (SSPA converters), while opting for a lower operational transmission frequency of 2.45 GHz.

15.3 Beam Collection Efficiency

The power beam adheres to the principles of the "Airy disk" ray-optical model. The beam's intensity is greatest at its centre and gradually diminishes as we move away from it, ultimately reaching (considering a one-dimensional view) a point where it diminishes to zero; this point is known as the first zero. Subsequently, the intensity oscillates, reaching a second zero and so on (see Figure 15-4).

Consequently, the primary (first) beam contains 83.8% of the total transmitted power, while the second beam accounts for 7.2%. The efficiency of the beam is contingent on the dimensions of the Ground Power Station and the antenna, in addition to the frequency and the distance. The intensity conforms to a diffraction pattern on the Ground Power Station.

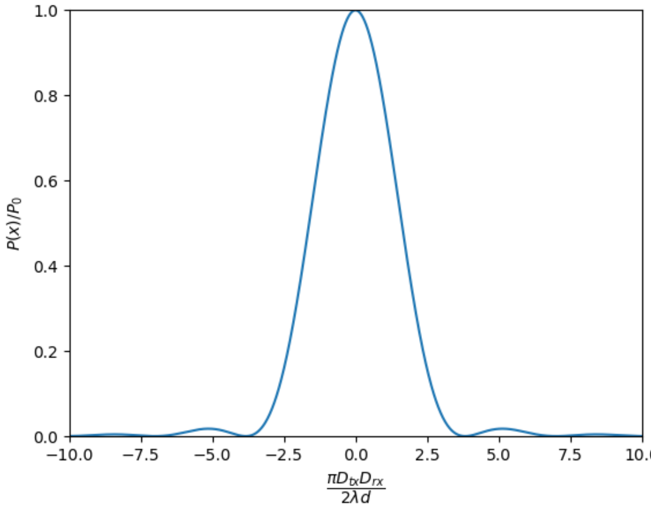

Figure 15-4 Intensity profile due to diffraction

When considering harnessing power up to the first null of the Bessel function (83.8% of the total power), the following formula is applicable:

$$\text{Antenna\_diameter} * \text{GPS\_diameter} = 2.44\ \lambda\ d$$

Where λ is the wavelength (m) and d is the orbit altitude (m).

Nonetheless, the approach of capturing a specific percentage of this power beam on ground shifts slightly when addressing a lower power-level demonstrator mission. In a full-scale system, the objective is to maximize the usable percentage of the beam while adhering to the constraints of maximum (average and peak) W/m2. Conversely, in the case of an initial demonstrator with power arriving on Earth at the kW level, the challenge shifts to ensuring a sufficient average power intensity on the Ground Power Station's rectennas.

Indeed, as illustrated in Figure 15-3, the rectenna efficiency experiences a significant decline as the average incident power density decreases. This is a key factor contributing to the overall energy chain efficiency being lower in comparison to the full system.

To mitigate this effect, it is necessary to strike a balance between this efficiency and the efficiency of the power beam collection.

As depicted in Figure 15-5, when dealing with extremely low power values, having a large GPS area might seem advantageous for collecting a greater portion of the power beam. However, this approach would result in a lower average power density, subsequently leading to a decreased RF-DC conversion efficiency.

Conversely, opting for a smaller GPS area is preferable to achieve a higher average incident power density, thus enhancing the RF-DC conversion efficiency. Nonetheless, this choice implies the collection of a smaller fraction of the overall power beam.

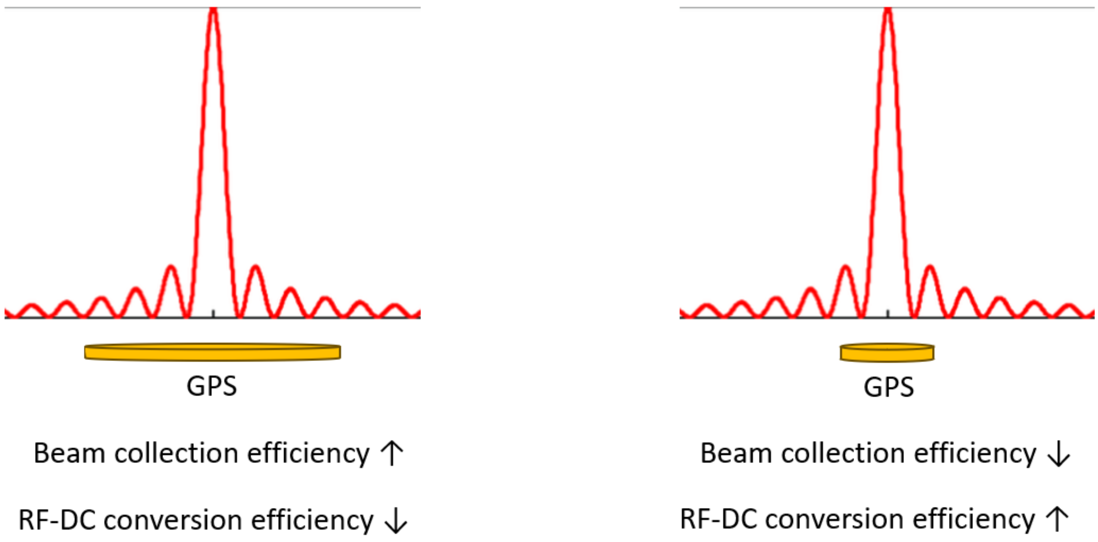

Figure 15-5 Consequences of collecting more or less power on ground

This line of reasoning holds true also in reverse when the Ground Power Station (GPS) area remains constant, and the selection of the on-board antenna area becomes variable. Therefore, in section 15.5, a parametric model is introduced, incorporating all the aforementioned considerations. This model allows to understand how, when we establish a GPS area and a desired power output to be transmitted to the ground, the decision regarding the on-board antenna area impacts the dimensions of the solar panel area. This is explained by accounting of these pivotal efficiencies that influence the overall system.

15.4 Other Aspects

When consideringg the shorter development timeline available for an SBSP demonstrator in comparison to the full-scale system, the following two aspects, incorporated in the parametric model, need to be considered:

- Selection of PV cell technology for the demonstrator: when it comes to a mission closer in time, a more mature technology is essential in contrast to the Perovskite cells chosen as the baseline for the full-scale SBSP system. Consequently, conventional multijunction cells need to be considered for the demonstrator's solar panels, with a corresponding cell efficiency (incorporated into the demonstrator parametric model) of approximately 32%, in accordance with the latest values for space multijunction cell technologies (refer to the Figure 15-6). However, it is worth noting that the demonstrator could also include the option to carry Perovskite cells on board to evaluate key performance parameters and advance this technology for future integration into the full-scale mission.

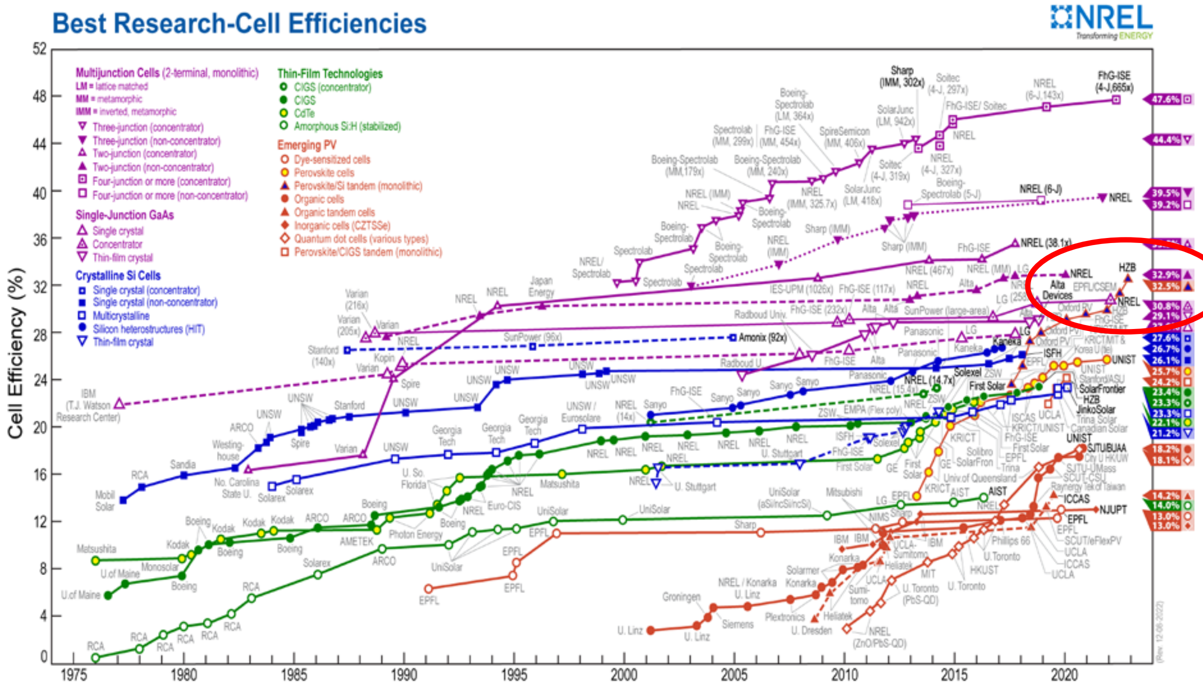

Figure 15-6 State of art of PV cell technologies

- SSPA efficiency: In the context of the full-scale mission, it is reasonable to contemplate expected DC-RF conversion efficiency values. However, the demonstrator mission necessitates a closer examination of the current state-of-the-art converters. Consequently, for the parametric model, it is imperative to take into account more plausible conversion efficiency values of approximately 50% and 60%, which vary depending on the transmission frequency.

15.5 Demonstrator Digital Model Results

A parametric model is established for the SBSP demonstrator mission. This model encompasses a revised efficiency chain and incorporates all the essential formulas and system assumptions. Integrated into the SBSP Analysis Framework, this parametric model takes as input a designated Ground Power Station (GPS) area and a Target Power on ground (either individually or in combination, see Figure 15-7) to generate informative curves that illustrate the relationship between onboard antenna area and solar panel area.

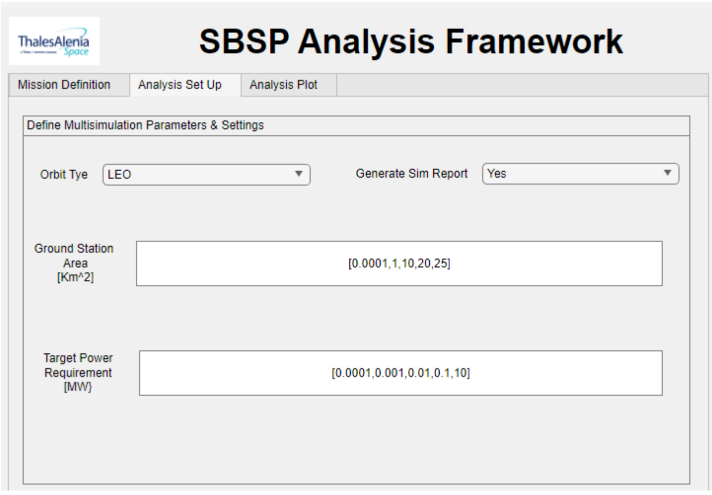

Figure 15-7 SBSP Analysis Framework demonstrator mission scenario GUI

Although the advantages of considering a LEO orbit for the demonstrator have been explained in paragraph 15.1, the graphical user interface allows to select the following orbit:

- LEO orbit (500 km)
- MEO orbit (20 000 km)
- GEO orbit (35 786 km)

The objective here is to gain a practical understanding of the drawbacks associated with opting for an higher altitude orbit for an first demonstration mission.

Among the analyses performed, the one reported below is for LEO orbit, a target power ranging from 1kW to 1MW and a GPS area of 10km^2.

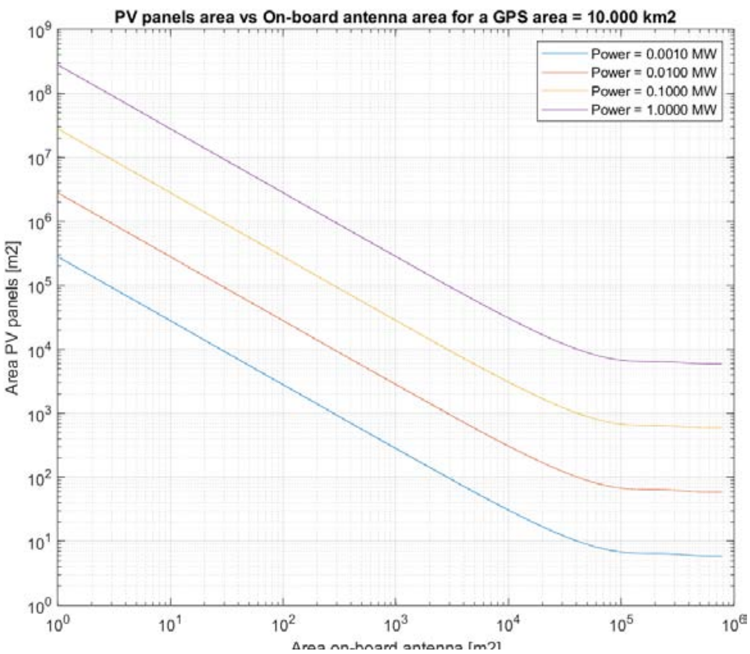

Figure 15-8 Analysis results

Additional analyses are possible by means of the parametric model implemented into the SBSP Framework Analysis.

For our first SBSP demonstrator, some viable solutions have been identified considering a ground power generation capability of maximum 1 kW. The following configurations are proposed:

Area GPS [km2]	Power on ground [kW]	Power generated in orbit [kW]	Area solar array [m2]	Area on-board antenna [m2]	On-board antenna diameter [m]
10	1	200	560	500	25.2
5	0.5	200	560	500	25.2
1	0.5	480	1400	1000	35.7
1	0.01	72	230	100	11.3

Table 15-2 Four possible demonstrator configurations

These combinations are just examples and represent a subset of potential configurations for achieving this values of output power. The proposed solutions arise from an initial compromise involving the three primary SBSP domains: the GPS area, the PV area, and the on-board antenna area. In future studies, these values may be subject to adjustments and are presented here solely to illustrate the scale of the systems that must be considered for a demonstrator mission.

15.6 Preliminary Recommendations For The Demonstrator Mission

The demonstrator allows to test various aspects of SBSP technologies, in order to assess the feasibility of their use in the full-scale system. In particular it allows to test and validate:

- emerging cell technologies, such as Perovskite, in space environment
- the power conversion performances
- the effectiveness of wireless power transmission
- the reliability of the SPS components (such as roll-out deployment mechanisms)

All of these steps are considered crucial to allow the full-scale system to be constructed and operated.

The requirements defined for the full-scale SBSP system are considered valid with the exceptions of the following that are not considered applicable to the demonstrator, given the objectives mentioned above:

- UR-REQ-0010 (Commercial Utilisation) which is valid only for the SBSP full-scale system;
- UR-REQ-0060 (Target SBSP Capability) which is valid for multiple SBSP full-scale systems;
- UR-REQ-0070 (System Lifetime) which is valid only for the SBSP full-scale system;
- UR-REQ-0110 (Constant power provision) as there will be no need to demonstrate, at this stage, a baseload power provision;

- UR-REQ-0150 (SBSP fluctuation planning) considering that fluctuations are relevant only for the SBSP full-scale system;
- UR-REQ-0160 (SBSP service interruptions) considering that service interruptions are relevant only for the SBSP full-scale system.

Due to the nature of the system, many critical technologies will not be available in the timeframe of the first demonstrator satellite. One of these is probably going to be the In-Orbit assembly technologies although many studies are developing these capabilities, like TAS IOS mission. In order to be independent from other satellites, a one-launch mission is suggested for the first demonstrator mission. Using as reference the values from the 0.01 kW on ground proposed satellite in Table 3-1, it would be possible to use deployable solar panels and a foldable/inflatable phased array antenna to fit the satellite inside a single launcher fairing. The ISS ROSA demonstrates the capability to deploy large solar panels from a compact container, while many studies are tackling the concept of foldable phased array antennas, which may allow to insert a 100 m^2 antenna in a 5 m diameter fairing (like the Ariane 6 or Falcon 9 ones). Other promising papers regarding foldable phased array sheets, like Caltech's one, may allow to reduce the volume required furthermore in the near future.

The satellite's design shall prioritize the maximization of both solar array and antenna areas in order to reduce the required GPS area. Considerations on the beam collection efficiency, as showed in Figure 15-5, will also help in reducing the GPS area, for example by collecting only the peak of the intensity profile, increasing the mean rectenna efficiency.

In line with the considerations reported in this chapter, a demonstrator mission will play a pivotal role in assessing the viability of a full-scale Space-Based Solar Power (SBSP) mission.

16 Conclusions

The space-based solar power (SBSP) solution proposed presents a promising perspective for addressing our growing energy needs.

- **Technical Feasibility**: the technical analysis reveals that the concept of harnessing solar power in space is scientifically grounded. Advances in solar panel efficiency, wireless power transmission, and space-based construction techniques make the overall feasibility of the project realistic.
- **Economic Viability**: on the basis of our study, although the initial investment for space-based solar power infrastructure is substantial, the long-term economic benefits are foreseen to overweigh the costs in virtue of the expected energy production. Continued technological advancements and economies of scale could further enhance the economic viability of SBSP.
- **Programmatic Feasibility**: implementing a space-based solar power program requires international collaboration, regulatory frameworks, and strategic planning. Our study underscores the importance of robust international partnerships and comprehensive policies to tackle the complexities of space-based energy generation.

In essence, the technical, economic, and programmatic aspects collectively suggest that the space-based solar power holds promise as a sustainable and potentially transformative energy solution. Further research, development, and international cooperation will be key in realizing the full potential of this innovative approach.

END OF DOCUMENT